

ELODIE KIENLEN



**ROLE OF THE PEROXISOME PROLIFERATOR-
ACTIVATED RECEPTOR-ALPHA IN HEART FAILURE
RELATED MYOCARDIAL REMODELLING**

INAUGURAL-DISSERTATION

zur Erlangung des Grades eines

Dr. med. vet.

beim Fachbereich Veterinärmedizin
der Justus-Liebig-Universität Gießen



édition scientifique
VVB LAUFFERSWEILER VERLAG

Das Werk ist in allen seinen Teilen urheberrechtlich geschützt.

Jede Verwertung ist ohne schriftliche Zustimmung des Autors oder des Verlages unzulässig. Das gilt insbesondere für Vervielfältigungen, Übersetzungen, Mikroverfilmungen und die Einspeicherung in und Verarbeitung durch elektronische Systeme.

1. Auflage 2009

All rights reserved. No part of this publication may be reproduced, stored in a retrieval system, or transmitted, in any form or by any means, electronic, mechanical, photocopying, recording, or otherwise, without the prior written permission of the Author or the Publishers.

1st Edition 2009

© 2009 by VVB LAUFERSWEILER VERLAG, Giessen
Printed in Germany



édition scientifique
VVB LAUFERSWEILER VERLAG

STAUFENBERGRING 15, D-35396 GIESSEN
Tel: 0641-5599888 Fax: 0641-5599890
email: redaktion@doktorverlag.de

www.doktorverlag.de

Aus dem Institut für Pharmakologie und Toxikologie
Fachbereich Veterinärmedizin
der Justus-Liebig-Universität Gießen
Betreuer: Prof. Dr. Ernst Petzinger

und

Bayer HealthCare AG, Wuppertal
Betreuer: PD Dr. Stefan Schäfer

**Role of the peroxisome proliferator-activated
receptor-alpha in heart failure related
myocardial remodelling**

INAUGURAL-DISSERTATION

zur Erlangung des Grades eines

Dr. med.vet.

beim Fachbereich Veterinärmedizin
der Justus-Liebig-Universität Gießen

eingereicht von

Elodie Kienlen

Tierärztin aus Colmar / Frankreich

Gießen, 2009

Mit Genehmigung des Fachbereiches Veterinärmedizin
der Justus-Liebig-Universität Gießen

Dekan: Prof. Dr. Dr. habil. Georg Baljer

Gutachter: Prof. Dr. Ernst Petzinger
PD Dr. Stefan Schäfer

Tag der Disputation: 26. Juni 2009

To my parents

Content

Abbreviations	8
1. Introduction	11
1.1 Heart failure	11
1.2 Peroxisome proliferator-activated receptors (PPARs)	12
1.3 Peroxisome proliferator-activated receptor alpha (PPAR)	14
1.4 Aim of the study	18
2. Material	20
2.1 Animals	20
2.2 Drugs	20
2.3 Chemicals	21
2.4 Material	22
2.4.1 Equipment	22
2.4.2 Surgical instruments and threads	23
2.4.3 Computer and software	23
2.5 Solutions	23
3. Methods	24
3.1 PPAR KO mice	24
3.2 Chronic myocardial infarction: Ischemia induced heart failure	25
3.3 DOCA: Hypertension induced heart failure	26
3.4 Medication	28
3.4.1 Vehicle (Placebo)	28
3.4.2 Fenofibrate	29
3.4.3 Ramipril	29
3.5 Metabolic cages / Diuresis	29
3.6 Haemodynamic measurements	30
3.7 Blood samples	32
3.8 Necropsy	32
3.8.1 Organs	32
3.8.2 Morphometric analysis	33
3.8.3 Scoring of infarct sizes	33
3.9 Biomarker analyses	33
3.9.1 RNA extraction	33

3.9.2 cDNA synthesis	34
3.9.3 Real time polymerase chain reaction (RT PCR) analysis	35
3.10 Statistics	36
4. Results	37
4.1 cMI model	37
4.1.1 Mortality and morphology in WT and KO mice	37
4.1.2 Haemodynamics in WT and KO mice	42
4.1.3 Biomarker analysis / RT-PCR analysis	47
4.1.4 Blood analysis	54
4.2 DOCA model	58
4.2.1 Morphology in WT and KO mice	58
4.2.2 Haemodynamics in WT and KO mice	62
4.2.3 Diuresis in WT and KO mice	66
4.2.4 Biomarker analysis / RT-PCR analysis	69
4.2.5 Blood analysis	74
5. Discussion	79
5.1 Heart failure in PPAR α WT and KO mice	80
5.2 Heart failure development under treatment with a PPAR α agonist in WT and KO mice	83
5.3 Cardiorenal syndrome	86
5.4 Mechanisms for the protective effects of PPAR α activity	87
5.5 Conclusion	92
6. Summary	94
7. Zusammenfassung	96
8. Reference list	98
9. Own abstracts	111
10. Declaration	112
11. Acknowledgments	113
12. Appendix	114

Abbreviations

µg	microgram
ACE	angiotensin converting enzyme
ACS	acyl Co A synthase
am	ante meridian
ANP	atrial natriuretic peptide
AP-1	activator protein 1
Apo-A-1	apolipoprotein A-1
Apo-A-2	apolipoprotein A-2
Apo-A-5	apolipoprotein A-5
Apo-C-3	apolipoprotein C-3
AU	arbitrary units
B2M	-2-microglobulin
bpm	beats per minute
cMI	chronic myocardial infarction
COL1A1	collagen 1A1
CPT-1	carnitine palmitoyl transferase 1
d	day
DNA	deoxyribonucleic acid
DOCA	deoxycorticosterone acetate
ET-1	endothelin-1
EtOH	Ethanol
FA	fatty acids
FABP	fatty acid binding protein
FATP	fatty acid transport protein
FA- ox / FAO	fatty acid oxidation
FBG	fibrinogen gene
Feno	Fenofibrate
FFA	free fatty acids
GLUT-1	glucose transporter-1
HDL	high density lipoprotein
HF	heart failure
HPRT	Hypoxanthin-guanin-phosphoribosyltransferase

HR	heart rate
ICAM	intercellular adhesion molecule
IL-6	interleukin-6
JNK	c-Jun N-terminal kinases
kg	kilogram
KO	knock out
L32	mitochondrial ribosomal protein L32
LAD	left anterior descending coronary artery
LDL	low density lipoprotein
LPL	lipoprotein lipase
LV	left ventricular
LV dP/dt_{max}	left ventricular maximum delta pressure / delta time
LV dP/dt_{min}	left ventricular minimum delta pressure / delta time
LVEDP	left ventricular end-diastolic pressure
LVPs	left ventricular maximum systolic pressure
MCAD	medium chain acyl-coenzyme A dehydrogenase
mg	milligram
MHC-PPAR mice	mice with cardiac-restricted overexpression of PPAR
mM	millimolar
mmol	millimol
mRNA	messenger ribonucleic acid
MyHC	myosin heavy chain
MyHC	myosin heavy chain
NaCl	Sodium chloride
NF- B	nuclear factor kappa-light-chain-enhancer of activated B cells
ng	nanogram
OPN	osteoontin
p.o.	per os
PBS	phosphate buffered saline
PDK-4	pyruvate dehydrogenase kinase, isozyme-4
pm	post meridian
PPARs	peroxisome proliferator-activated receptors

PPAR	peroxisome proliferator-activated receptor alpha
PPRE	peroxisome proliferator response elements
RNA	ribonucleic acid
rpm	rotations per minute
RT-PCR	real time polymerase chain reaction
RV	right ventricular
RXR	retinoid X receptor
s	second
TIMP1	tissue inhibitor of metalloproteinase 1
TNF	tumor necrosis factor-alpha
VCAM-1	vascular cell adhesion molecule 1
VLDL	very low density lipoprotein
WHO	World Health Organization
WT	wild type

1. Introduction

1.1 Heart failure

Heart failure is a progressive clinical syndrome which is characterized by the inability of the heart to pump or fill with a sufficient amount of blood through the systemic circulation. This condition can result from any structural or functional disorder of the heart (Mann et al. 2005). The symptoms of heart failure vary depending on the affected ventricle, but are most frequently characterized by shortness of breath upon exertion and peripheral or lung oedema. Heart failure is usually chronic, it deteriorates progressively, leading to loss of exercise capacity, dyspnoea, and ultimately, death.

In epidemiological studies, heart failure accounts for almost 30 % of the mortality in the world (WHO, World health report 2006). Despite important progress made in its management using β -blockers, ACE inhibitors, AT1 antagonists and diuretics in the last decades, heart failure remains associated with a long-term prognosis of 50% mortality within 5 years of diagnosis (Halapas et al. 2008, Frigerio et al. 2005, Cohn et al. 2000).

The main cause for the development of heart failure is coronary heart disease, accounting for approximately 60 % of cases. In the majority of cases the triggering event is an initial myocardial infarction. About 30% of heart failure patients develop heart failure due to long-term hypertension (Lloyd-Jones et al. 2002). Other causes for heart failure include valvular diseases and genetic or toxic cardiomyopathies (ESC 2008).

Besides the functional abnormalities, heart failure is characterized by accompanying alterations in cardiac morphology at the organ, tissue and cellular level. These alterations include left ventricular and cardiomyocyte hypertrophy, interstitial fibrosis and a dysregulation of the composition of interstitial matrix.

Together, these features comprise a phenomenon which is frequently referred to as “cardiac remodelling”. Alone and in combination, myocardial remodelling contributes to the functional decline of the heart.

In the beginning of the disease, the heart can compensate remodelling processes by increasing contractility, frequency and end-diastolic volume (Kempf et al. 2007). Those changes are also accompanied by an early activation of the adrenergic nervous system and salt- and water-retaining systems (renin-angiotensin-aldosterone-system) in order to preserve cardiac output (Eichhorn et al. 1996, Eisenhofer et al. 1996, Hasking et al. 1986). In the short term, these systems are able to restore cardiovascular function to a normal range, with the result that the patient remains asymptomatic. However, with time the sustained activation of these systems can lead to secondary end-organ damage within the ventricle, with enhanced left ventricular remodelling and subsequent cardiac decompensation (Mann et al. 2005). Therefore, counteracting the adrenergic system and the renin-angiotensin-aldosterone-system are, nowadays, the two most important treatment options for heart failure patients. In fact, the introduction of ACE inhibitors and β -blockers has largely contributed to the amelioration in mortality and morbidity, due to improvement of cardiac remodelling and subsequent cardiac function (Cohn et al. 2000).

Nevertheless, despite the enormous progress in the treatment of heart failure, its prognosis remains poor and the need for new therapeutic options to improve cardiac remodelling continues to be great. Huge efforts are therefore being undertaken in academic as well as industry based research, to understand better the mechanisms underlying the pathogenesis of heart failure, and to identify novel targets for the prevention of cardiac remodelling.

1.2 Peroxisome proliferator-activated receptors (PPARs)

One receptor, which seems to be involved in those remodelling processes and in the modulation of the progression of heart failure, is the peroxisome proliferator-activated receptor alpha (PPAR α), which belongs to the family of the peroxisome proliferator-activated receptors (PPARs).

PPARs were first described in 1976 by Lazarow and de Duve. As nuclear hormone receptors (Isseman and Green 1990), PPARs regulate a multitude of genes involved,

among others, in lipid and glucose homeostasis and in the remodelling processes seen in the heart.

The PPAR family includes three members: PPAR α , PPAR β/δ and PPAR γ . All PPAR receptors subtypes have similar structures and mode of actions but bind to different target genes and are activated by different compounds.

The exact structure of the PPARs was described by Zoete et al. (2007), Gearing et al. (1994), Motojima (1993) and Dreyer et al. (1992).

PPAR receptors contain an N-terminal domain that regulates PPAR activity, a DNA-binding domain that binds to a peroxisome proliferator response element, a domain for a cofactor, and a C-terminal ligand-binding domain which determines ligand specificity (Ferré 2004, Tugwood et al. 1992).

PPAR receptors regulate the transcription of target genes by forming heterodimers with the retinoid X receptor (RXR) and by binding to specific peroxisome proliferator response elements in the promoter region of target genes (Kliwer et al. 2001, Wan et al. 2000, Ijpenberg et al. 1997) (Figure 1.1).

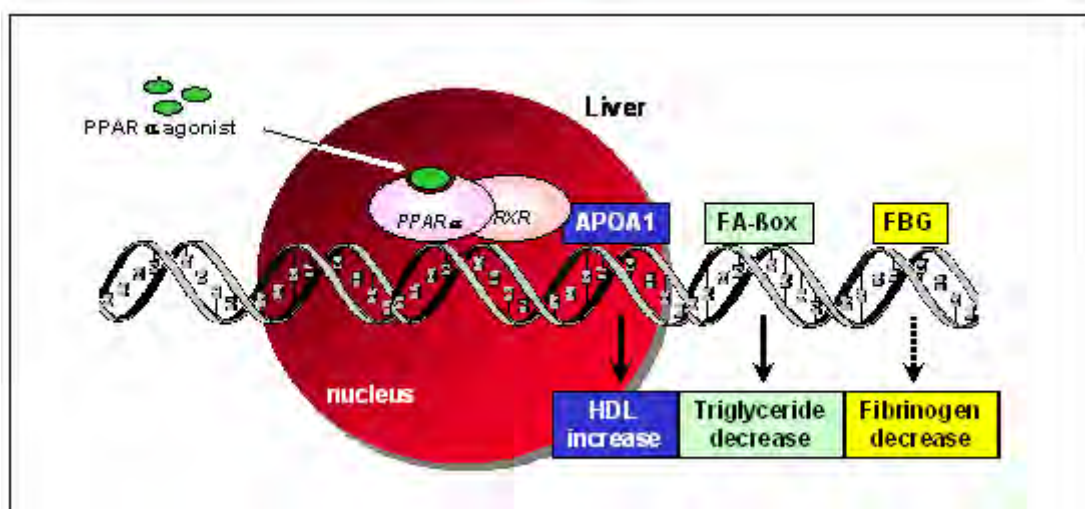


Figure 1.1: Binding of PPAR α agonist on target genes in the liver; RXR: retinoid-X-receptor, APOA1: apolipoprotein A1, HDL: high density lipoprotein, FA-ox: fatty acid oxidation, FBG: fibrinogen gene

In the inactivated state, PPARs are bound to corepressor proteins. Upon binding to their ligands, PPARs dissociate from their corepressors and recruit coactivators, including a PPAR-binding protein and the steroid receptor coactivator-1 (Llopis et al.

2000). Thereafter, the PPAR/RXR heterodimer activates the transcription of target genes or antagonize their activity.

Agonists of the PPAR α subtype (thiazolidinediones) are currently used for the treatment of diabetes mellitus (Raji et al. 2002, Kudzma 2002). However, use of those compounds is associated with an increased risk to develop heart failure. This phenomenon is related to the potential of the thiazolidinediones to induce weight gain and fluid retention (Nesto et al. 2003).

PPAR γ agonists are not commercialized at present, but they are supposed to have a role in cell differentiation and lipid metabolism.

The present study focuses on the PPAR α subtype because this subtype seems to be the most promising in the therapy of heart failure, due to its prominent role in myocardial remodelling (see below).

1.3 Peroxisome proliferator-activated receptor (PPAR α)

PPAR α is ubiquitously expressed. In the heart, PPAR α modulates glucose and lipid homeostasis and also has remodelling functions (Mukherjee et al. 1997, Braissant et al. 1996, Kliewer et al. 1995) (Figure 1.2). But PPAR α is also highly expressed in tissues with high lipid β -oxidation rates, such as liver, muscle and adipose tissues, where this receptor has an important regulating function in lipid and glucose metabolism (Mukherjee et al. 1997, Braissant et al. 1996, Kliewer et al. 1995).

Endogenous PPAR α agonists are fatty acids, lipid metabolites (Kliewer et al. 2001) and eicosanoids such as leukotriene B₄, 8-(S)-hydroxyeicosatetraenoic acid and 15-deoxy- $\Delta^{12,14}$ -prostaglandin J₂ (15d-PGJ₂) (Kliewer et al. 1997, Devchand et al. 1996, Kliewer et al. 1995, Forman et al. 1994).

Exogenous PPAR α agonists are the fibrates, a class of drugs which are used to treat hyperlipidaemia (Fruchart et al. 2006, Staels et al. 1998, Issemann and Green 1990). On the one hand, effects of the fibrates, such as clofibrate and fenofibrate, on lipid

metabolism of patients have been convincingly established in randomized clinical trials (e.g.: DAIS, FIELD and ACCORD trials) where they decreased triglycerides and LDL cholesterol and increase HDL cholesterol.

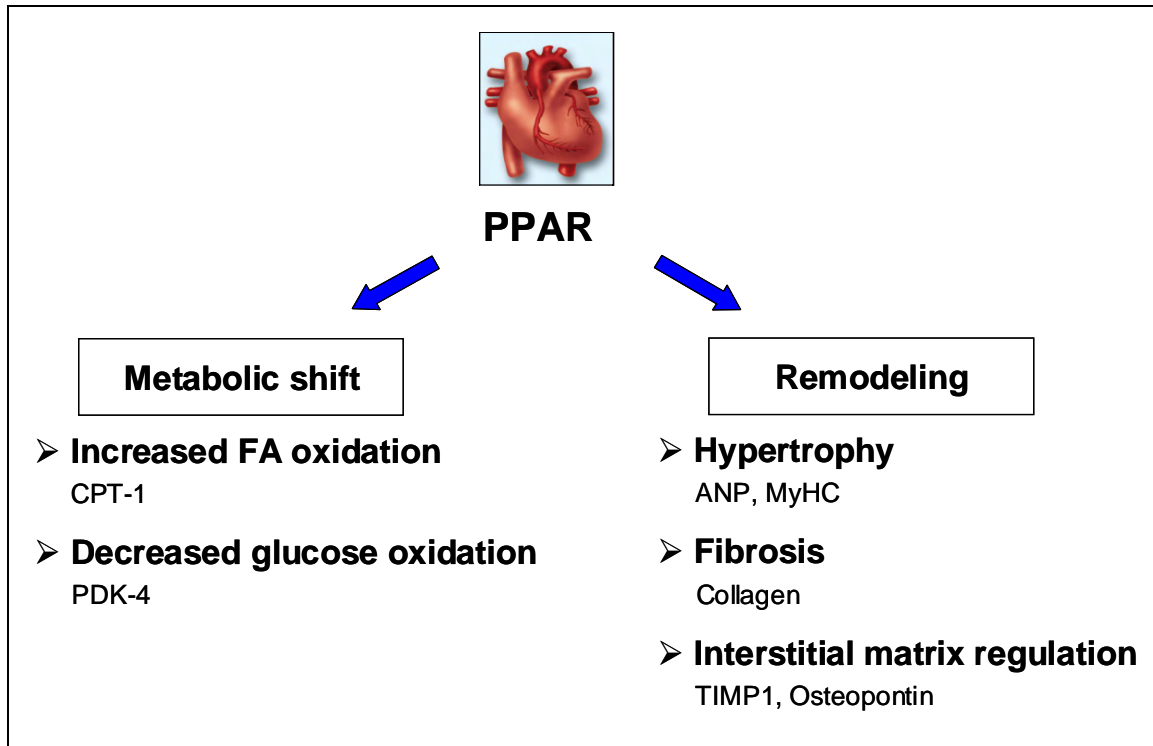


Figure 1.2: Effects of PPAR on the heart; ANP: atrial natriuretic peptide, CPT-1: carnitine palmitoyl transferase 1, MyHC: myosin heavy chain, PDK-4: pyruvate dehydrogenase kinase, isozyme-4, TIMP1: tissue inhibitor of matrix metalloproteinase 1

PPAR is highly expressed in tissues with elevated capacity for fatty acid oxidation (FAO) and is an important transcriptional regulator of myocardial energy and lipid homeostasis, through modulation of key enzymes of the FAO (Finck et al. 2002, Watanabe et al. 2000). Indeed, PPAR directly regulates different genes involved in fatty acids uptake and oxidation as well as lipoprotein metabolism through peroxisome proliferator response elements (PPRE). Free fatty acids (FFA) uptake is increased through fatty acid transport protein (FATP). Once in the cell, fatty acids are esterified and activated by acyl Co A synthase (ACS) or bind to fatty acid binding protein (FABP). Finally free fatty acids are catabolized through fatty acid oxidation where the majority of enzymes, such as medium chain acyl-coenzyme A dehydrogenase (MCAD) or carnitine palmitoyl transferase 1 (CPT-1), are directly regulated by PPAR (van Raalte et al. 2004). PPAR agonists lower triglyceride

plasma levels by directly increasing activity of lipoprotein lipase (LPL) or indirectly increasing LPL activity by decreasing apolipoprotein C-3 (Apo-C-3, inhibitor of LPL) and increasing apolipoprotein A-5 (Apo-A-5, activator of LPL). Furthermore by reducing triglyceride stores, PPAR agonists are able to reduce very low density lipoprotein (VLDL) levels. Finally, PPAR agonists increase high density lipoprotein (HDL) cholesterol, by increasing activity of apolipoprotein A-1 (Apo-A-1) and A-2 (Apo-A-2) in the liver (Kersten 2008, Staels et al. 1998). But PPAR is also supposed to indirectly regulate lipid homeostasis by regulating glucose homeostasis. Indeed, it has been described that PPAR is able to bind to glucose and glucose metabolite and so may decrease FAO (Hostetler et al. 2008). But this effect could also be due to the direct regulation of enzymes involved in the glucose pathway, such as pyruvate dehydrogenase kinase, isozyme-4 (PDK-4) and the glucose transporter 1 (GLUT-1) (Panagia et al. 2005).

On the other hand, effects on heart failure by fibrate compounds have yet not been studied in patients. In fact, heart failure was an exclusion criterion in patients for the clinical trials. However, the available non-clinical data collected in animal studies indicate promising effects of PPAR in heart failure.

In experiments, PPAR has been described to have a lipid independent anti-inflammatory effect through direct and indirect inhibition of genes induced by the nuclear factor kappa-light-chain-enhancer of activated B cells (NF- κ B) including vascular cell adhesion molecule 1 (VCAM-1), intercellular adhesion molecule (ICAM), cyclooxygenase 2 (COX-2), interleukin-6 (IL-6) and tumor necrosis factor-alpha (TNF α) (Schiffrin 2005) (Figure 1.2). Furthermore PPAR activation can reduce fibrosis via reducing the expression of activator protein 1 (AP-1), and inhibition of endothelin-1 (ET-1) and the expression of collagen I and III, (Ogata et al. 2002). Endothelin-1 is also an important mediator of hypertrophy development. PPAR agonists negatively modulate the ET-1 pathway by regulation of AP-1 binding activity and inhibition of the c-Jun N-terminal kinases (JNK) pathway and the formation of c-Fos / c-Jun heterodimers (Li et al. 2008, Irukayama-Tomobe et al. 2004).

Furthermore, the expression of PPAR seems to be reduced in patients with hypertensive heart disease (Goikoetxea et al. 2005) or in diabetic patients with non

ischaemic heart failure (Razeghi et al. 2002). Accordingly, a decrease of PPAR mRNA expression is found in preclinical heart failure models, such as mice and rats with aortic banding (Young et al. 2001, Barger et al. 2000, Sack et al. 1997) and rats with chronic myocardial infarction (Morgan et al. 2006).

However, conflicting data exist in some forms of heart disease regarding the protection by PPAR. Schupp et al. (2005) reported that in patients with dilated cardiomyopathy PPAR expression is increased. There are several literary sources which suggest that the overexpression of PPAR in heart results in the development of cardiomyopathy. It has been reported that hearts of mice with cardiac-restricted overexpression of PPAR (MHC-PPAR) exhibit signs of diabetic cardiomyopathy including ventricular hypertrophy and systolic dysfunction subsequent to increased myocardial fatty acids -oxidation rates and decreased glucose oxidation rates (Finck et al. 2002). Furthermore, it seems that treatment of healthy WT mice with PPAR agonists induces cardiomyocyte degeneration and necrosis, due to increased fatty acid oxidation and subsequent accumulation of oxidative stress intermediates, an effect not observed in PPAR KO mice (Pruimboom-Brees et al. 2006). Sambandam et al. (2006) also showed a deterioration of cardiac recovery after ischaemia / reperfusion in isolated hearts from MHC-PPAR mice.

Finally, it has been reported that reactivation of PPAR in early stages of heart failure development could be deleterious by accumulating lipids in the myocardium and worsening cardiac dysfunction. Young et al. (2001) showed that reactivation of PPAR with a PPAR agonist, resulted in severe depression of cardiac power and efficiency in the hypertrophied heart because of the prevention of substrate switching in an aortic banding study in rats. To maintain its contractile function, the hypertrophied heart decreases its reliance on fatty acids as a major substrate for ATP generation while increasing its reliance on glucose as a fuel, mainly through regulation of PPAR. However, long term down regulation of PPAR and FAO may contribute to energy starvation (lower ATP production through Glucose oxidation) of the myocardium and cardiac lipotoxicity (storage of lipid in the myocyte followed by apoptosis). The process which at first appears to be adaptive may turn out maladaptive in the longer term (Balakumar et al. 2007, Ogata et al. 2004).

In summary, the literary sources show that PPAR α is downregulated in heart failure development and that overexpression of PPAR α could be detrimental in the recovery after an initial event. However, there are no data yet available concerning the differentiation between PPAR α activity levels and protection in ischaemia or long-term hypertension induced heart failure in animal models, nor in clinical studies. Furthermore, several publications described a number of pathways, in which PPAR α is involved and beneficial, but its effects on the main features of myocardial remodelling, hypertrophy, fibrosis and interstitial matrix regulation, and the subsequent cardiac dysfunction have not been clearly established, as yet, in long term models of ischaemia and hypertension induced heart failure.

The availability of both specific exogenous PPAR α activators and PPAR α KO mice (see 3.1) represent a suitable tool box to study the biological roles of PPAR α in health and disease. PPAR α agonists allow an activation of PPAR α , PPAR α KO mice permit to study effects correlated to a lack of PPAR α protein and a lack of activation of the PPAR α induced target genes.

1.4 Aim of the study

The aim of this study was to investigate the role of PPAR α in the remodelling processes related to heart failure, in models of ischaemia and hypertension induced heart failure, the two most important causes of heart failure development in patients.

To reflect the ischaemia induced heart failure, the model of chronic myocardial infarction in mice was used. This model, induced by permanent ligation of the left anterior descending coronary artery (LAD), resembles the pathophysiological changes of remodelling and deterioration of systolic and diastolic cardiac function in patients with ischaemia induced heart failure.

To mimic hypertension induced heart failure, the deoxycorticosterone acetate (DOCA) salt model was used. DOCA mimics hyperaldosteronism and induces hypertension with pronounced end-organ damage in heart with hypertrophy, fibrosis and cardiac dysfunction, reflecting the pathophysiological changes observed in patients with hypertension.

If the presence of PPAR is protective in heart failure, the following effects can be expected: 1./ Lack of PPAR is detrimental in heart failure development and 2./ Activation of PPAR ameliorates heart failure development.

To investigate these, the effects of abrogation of PPAR activity in KO mice were compared to normal activity in WT mice and activation of PPAR by the PPAR agonist fenofibrate in the two aforementioned models.

2. Materials

2.1 Animals

PPAR α wild-type mice (129S1/SvImJ) were purchased from Charles River, Sultzfled, Germany.

PPAR α knock-out mice (129S4/Sv Jae-Ppara-tm1 Gonz) were bred in the breeding station of Bayer HealthCare AG, Wuppertal, Germany.

All mice were 6-8 weeks old, weighed 20-22 g and were male.

Mice were held in single cages (Type II) on chipped wood, regular pellet chow for mice and rats (Provimi Kiba AG, Kaiseraugst, Germany), with free access to tapwater.

Animal rooms had a constant temperature and humidity and a 12 hours day (light) / night (dark) rhythm (from 6.30 am to 6.30 pm).

2.2 Drugs

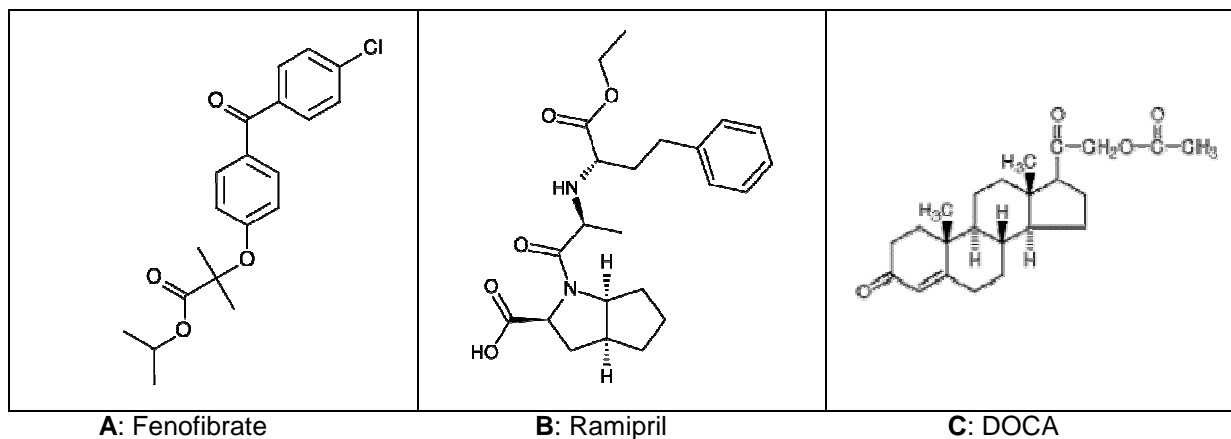


Figure 2.1: Structure of chemicals

- **Fenofibrate**

Fenofibrate (Figure 2.1, A) is a specific agonist of the PPAR α subtype. It is approved for the treatment of hyperlipidaemia and is marketed under the brand name of “Fenobeta®” in Germany.

Fenofibrate was purchased from Sigma-Aldrich, Munich, Germany.

- **Ramipril**

Ramipril (Figure 2.1, B) is an inhibitor of the angiotensin converting enzyme (ACE). It is approved for the treatment of hypertension and chronic heart failure and is marketed under the brand name of “Delix®” in Germany.

Ramipril was purchased from Sigma-Aldrich, Munich, Germany.

- **DOCA (deoxycorticosterone acetate)**

DOCA (Figure 2.1, C) is an aldosterone agonist and as such binds to the mineralocorticoid receptor. This chemical is used in animal experiments to increase blood pressure.

DOCA was purchased from Innovative Research of America, Sarasota, FL, USA.

- **Carprofen (Rimadyl®)**

Carprofen (Rimadyl®) is a non steroidal anti-inflammatory drug (inhibitor of cyclooxygenase-2) and was administered post-operationally at a dose of 5µg / g body weight after appropriate dissolution.

Carprofen was purchased from Pfizer, Karlsruhe, Germany.

2.3 Chemicals

The following chemicals were used for the biomarker analysis:

Chloroform	Merck, Darmstadt, Germany
DNase RNase free	Gibco by Invitrogen, Heidelberg, Germany
ImProm-II Reverse Transcription System	Promega, Mannheim, Germany
Isopropanol	Merck, Darmstadt, Germany
Superscript-II RT-PCR Kit	Invitrogen, Heidleberg, Germany
TaqMan Universal Master Mix	Eurogentec, Brussels, Belgium
TRIZol reagent	Invitrogen, Carlsbad, CA, USA

All other chemicals were of the highest quality available and purchased from commercial suppliers (see Appendix 12.1.1).

2.4 Material

2.4.1 Equipment

- **Equipment for the biomarker analysis**

ABI Prism 7700 sequence detection facility	Applied Biosystems, Framingham, MA, USA
Centrifuge 5417R	Eppendorf, Wesseling-Berzdorf, Germany
Centrifuge, Minifuge 2	Heraeus Christ GmbH, Osterode, Germany
FastPrep FP120 cell disrupter	Bio 101 Thermo Savant, Illkirch, France
Lysing matrix D tubes	MP biomedicals, Solon, OH, USA
MS1 minishaker	IKA®, Staufen, Germany
NanoDrop ND-1000 spectrophotometer	NanoDrop Technologies Wilmington, DE, USA

- **Equipment for the haemodynamic measurements**

Animal Bio Amp	ML136 (EKG)
Micro - Tip ® catheter transducer, SPF 621, 1.4F, 65cm	Millar instruments Inc., Houston, TX, USA
Powerlab System 4/25	ADI Instruments by Föhr Medical Instruments GmbH, Seeheim-Ober-Beerbach, Germany
Pressure control unit PCU 2000	Millar instruments Inc., Houston, TX, USA

All other used equipments are part of the standard laboratory equipment and listed in the Appendix 12.1.2.

2.4.2 Surgical instruments and threads

Surgical instruments were purchased from Aesculap and Martin GmbH, Tuttlingen, Germany. Surgical threads were purchased from Ethicon, St.-Stevens-Woluwe, Belgium (Appendix 12.1.3).

2.4.3 Computer and software

For data analysis and processing, a conventional personal computer system was used with Windows XP using following softwares: Genedata Expressionist software, Chart 5 for windows, GraphPad Prism 4.02, Microsoft Office Excel and Microsoft Office Word.

2.5 Solutions

The active compounds, Fenofibrate and Ramipril, were dissolved in a vehicle solution, composed of 10 % Ethanol, 40 % Solutol and 50 % water. The vehicle and all active compounds were prepared as stock solution, without water and frozen away as aliquots. Aliquots were weekly supplied with water, to treat the animals.

3. Methods

All experiments conformed to the German federal animal protection law and were approved by the legal district authority.

3.1 PPAR KO mice

PPAR KO mice were purchased from Jackson Laboratories, Maine, USA and the breed was kept by crossing the progenies in the Bayer Healthcare breeding station, Germany, laboratory of Dr. Hagelschuer.

Engineering of the PPAR KO mouse was first described by Lee et al. in 1995. Briefly, a targeting plasmid containing a neomycin resistance and a herpes simplex virus thymidine kinase was constructed and inserted between the *Pst*I and *Sph*I sites in exon 8 of the ligand-binding domain of the PPAR gene. This targeting construct was introduced in Sv/129 mouse embryonic stem cells via electroporation. Embryonic stem cell clones were injected in C57BL/6N blastocysts. Male chimeras were mated to C57BL/6N female, and germ line transmission was scored by the presence of agouti offspring in the F₁ litter.

PPAR KO mice show complete transcription of mRNA for PPAR, but the resulting protein contains a non-sense mutation and is not functional. KO mice do not respond to PPAR agonists. Furthermore, these mice do not show phenotypical changes compared to WT littermates (Gonzalez 1997), but they do show age dependent lipid accumulation and fibrosis in liver and heart (Howroyd et al. 2004). Those changes appear commonly after the 6th month of age. To circumvent interactions between these changes and the development of heart failure in the cMI and DOCA models, mice at the starting age of six to eight weeks were used in these studies.

3.2 Chronic myocardial infarction (cMI): Ischaemia induced heart failure

The chronic myocardial infarction model was first described in rats by Pfeffer et al. in 1979. It resembles the pathophysiological changes of remodelling and deterioration of systolic and diastolic cardiac function in patients with ischaemia induced heart failure.

In this study, 140 male WT and 104 male KO mice were subjected to pre-anaesthesia by 5 % Isofluran in a mix of oxygen/pressurized air (2/1) and intubated. Thereafter mice were intubated and anaesthesia was continued with 1.2 – 1.5 % Isofluran with 140-150 strokes/min and 10 µl strokes volume/g mouse.

Mice were fixed in a slight dorso-lateral position and left leg stretched out cranial on a heating panel (40 °C). Before start of the surgery, the surgery field was shaved and disinfected with Cutasept F skin disinfectant, mice were injected with 5 mg/kg/sc Carprofen in the popliteal fold and their eyes were covered with Panthenol.

Incision was placed at the level of the left elbow. With two micro suture tying forceps the M. pectoralis profundus was separated from the M. pectoralis superficialis. The chest was opened between the 3rd and the 4th rib and spread with an eyelid spreader. The pericardium was opened with two micro suture tying forceps and the LAD visualized.

With a Prolene 6/0 thread (0.7 metric, TF-6, EH7814H), the permanent occlusion was settled in the proximal 3rd of the LAD with 3 single knots.

After occlusion, the myocardium distal the knots became pale, due to the interrupted blood supply.

After inflation of the lung, the ribs and pectoralis muscles were adapted separately using Vicryl 6/0 (0.7 metric, TF1, V234H). Finally the skin was sutured using Ethibone 5/0 (1 metric, V-18, 6913H).

After surgery, Isofluran was turned off, the wound was cleaned with NaCl and coated with Nebacetin powder spray.

Mice were kept ventilated until they showed spontaneous respiration.

After awakening, mice were replaced in cages on heating panels to avoid hypothermia.

▪ Treatment groups

After surgery, mice were examined daily to supervise their general condition.

Fenofibrate was used as a specific PPAR agonist.

Treatment with Ramipril, an ACE inhibitor, was used as a standard reference.

Mice were randomly divided into 8 groups:

Sham WT (n=12) and KO (n=7)

Placebo WT (n=19) and KO (n=9)

Fenofibrate WT (n=16) and KO (n=8)

Ramipril WT (n=16) and KO (n=10)

All mice received treatment with either Vehicle, Fenofibrate (80 mg/kg/d) or Ramipril (10 mg/kg/d).

Treatment was initiated one week after surgery and lasted for 8 weeks (Figure 3.1).

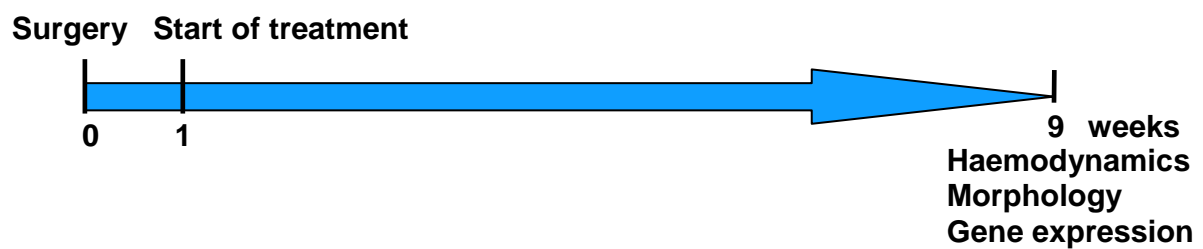


Figure 3.1: chronic myocardial infarction study plan

3.3 DOCA: Hypertension induced heart failure

The DOCA model was first described by Friedman et al. in 1948 in rats. It is used to mimic the pathophysiological changes in hypertension induced heart failure. DOCA treated rats develop pronounced heart and kidney damage with increased heart hypertrophy and fibrosis and kidney dysfunction.

In this study, 70 male WT and 70 male KO mice were subjected to pre-anaesthesia by 5 % Isofluran in a mix of oxygen/pressurized air (2/1). Thereafter they were placed on the right side on an heating panel (40 °C) and hung by the upper incisive in a narcosis mask, where they continuously were ventilated with 1.2 – 1.5 % Isofluran and allowed to breath spontaneously. Before start of the surgery, the surgery field

was shaved and disinfected with Cutasept F skin disinfectant, mice were injected 5 mg/kg/sc Carprofen in the neck and their eyes covered with Panthenol.

- **Nephrectomy of the left kidney**

A 7-10 mm horizontal skin cut was placed behind the last rib and 3 mm beneath the lombal musculature. Vertical incision of the musculature was placed above the left kidney. Thereafter, the kidney was cautiously pushed out of the abdomen with help of a curved anatomical forceps. Fatty tissue was separated from the kidney and the blood vessels were freed. A ligature was placed below the left kidney with an Ethibone 5/0 thread (1 metric, V-18, 6913H) and kidney was removed. Finally the abdominal muscles were sutured with a continuous suture and a Vicryl 6/0 thread (0.7 metric, TF1, V234H).

- **DOCA pellet implantation**

DOCA pellets (150 mg DOCA, 60 days release) were placed subcutaneously in the popliteal fold of the anaesthetized, nephrectomised mice.

From the cut, skin was released from the musculature with dissecting forceps toward the left knee. After obtaining a vast pocket, a DOCA pellet was placed and skin was sutured using Ethibone 5/0 thread (1 metric, V-18, 6913H).

After surgery, Isofluran was turned off, wound was cleaned with NaCl and coated with Nebacetin powder spray.

After awakening mice were replaced in cages, on heating panels to avoid hypothermia.

- **Treatment groups**

After surgery, mice were examined daily to supervise their general condition.

Mice were randomly divided into 8 groups:

Sham WT (n=10) and KO (n=10)

Placebo WT (n=15) and KO (n=15)

Fenofibrate WT (n=14) and KO (n=15)

Ramipril WT (n=13) and KO (n=13)

All mice received a treatment with either Vehicle, Fenofibrate (80 mg/kg/d) or Ramipril (10 mg/kg/d).

Furthermore, DOCA mice received 1 % NaCl in the drinking water. Only sham operated mice received normal drinking water.

Treatment was initiated one day after surgery and lasted for 42 days (6 weeks) (Figure 3.2).

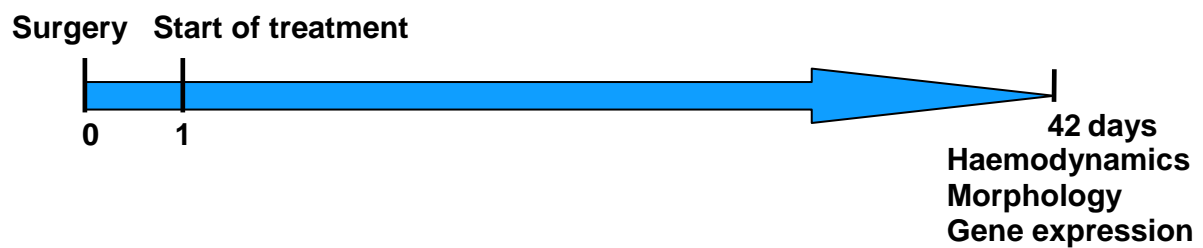


Figure 3.2: DOCA study plan

3.4 Medication

For both experiments, mice were treated with the following compounds.

Vehicle, Fenofibrate or Ramipril in the following concentrations: Fenofibrate: 80 mg/kg/d and Ramipril: 10 mg/kg/d.

All substances were given orally dissolved in 10 ml/kg/d of vehicle.

3.4.1 Vehicle (Placebo)

Sham and Placebo groups were given Vehicle medication.

Vehicle was composed of 10 % Ethanol, 40 % Solutol and 50 % water.

The mix of Solutol and Ethanol without water was portioned in 50 mL Falcon tubes, for a weekly use and frozen by -20 °C.

Every week a new Falcon tube was thawed and 20 mL water was added.

3.4.2 Fenofibrate

Fenofibrate groups were treated with 80 mg/kg/d p.o. Fenofibrate in 10 % Ethanol, 40 % Solutol and 50 % water.

3.696 g Fenofibrate was dissolved in 184.8 ml Solutol and 46.2 ml Ethanol before start of treatment and then portioned without water in 50 mL Falcon tubes, for a weekly use and frozen by -20 °C.

Every week a new Falcon tube was thawed and 20 mL water was added.

3.4.3 Ramipril

Ramipril groups were treated with 10 mg/kg/d p.o. Ramipril in 10 % Ethanol, 40 % Solutol and 50 % water.

462 mg Ramipril was dissolved in 184.8 ml Solutol and 46.2 ml Ethanol before start of treatment and then portioned without water in 50 mL Falcon tubes, for a weekly use and frozen by -20 °C.

Every week a new Falcon tube was thawed and 20 mL water was added.

3.5 Metabolic cages / Diuresis

In the DOCA model, diuresis experiments were performed in PPAR WT and KO mice.

Baseline (0-Diuresis) levels were measured one week before surgery.

Final-Diuresis levels were measured one week before haemodynamic measurements (in the 5th week after surgery).

- **Metabolic cages**

Mice were placed in metabolic cages for 24 hours. During this time they received water and food ad libitum.

At 0-diuresis, all animals received normal drinking water.

At final-diuresis, DOCA mice received 1 % NaCl in drinking water, whereas Sham mice received normal drinking water.

Urine and faeces were collected in two separated containers.

After 24 hours, each urine sample was separately collected, weighed and finally frozen by -20 °C until analysis.

- **Analysis of urine samples**

Urine samples were analyzed by the department of clinical chemistry, Bayer HealthCare AG, Wuppertal, Germany, laboratory of Dr. Ingo Loof.

Investigated parameters were: Urine volume, protein content, urea content, creatinine content, Na⁺ content and K⁺ content.

Urine volume was evaluated by weighing with a balance.

Other urine parameters were evaluated using commercial kits from Roche diagnostics and Eppendorf-Netheler-Hinz GmbH (Appendix 12.2.1).

3.6 Haemodynamic measurements

Mice of the chronic myocardial infarction model were subjected to haemodynamic measurements 9 weeks after surgery.

Mice of the DOCA model were subjected to haemodynamic measurements 6 weeks after surgery.

After the measurements organs and blood samples were collected.

- **Computer program**

To monitor left ventricular pressure, the Chart 5 program for windows was used.

A Micro - Tip® catheter transducer, 1.4 F was used as a pressure sensor and connected to an amplifying box to allow the computer assisted monitoring of blood pressure.

The pressure tip catheter was calibrated before each measurement. For the calibration, the electrical 0, 25 and 100 mV points were tested.

- **Haemodynamics**

Mice were pre-anaesthetized with 5 % Isofluran in a mix of oxygen/pressurized air (2/1) and placed in ventilation masks on heating panels (40°C). Thereafter, mice

were exposed to 1.2 – 1.5 % Isofluran, allowed to breath spontaneously and were collocated on the back and the throat was shaved and disinfected with Cutasept F (skin disinfectant).

A cut of one cm length was done on the median line of the throat.

After blunt preparation of the sub cutaneous fatty tissue the two salivary glands were visualized and separated in the median line to free the trachea.

Subsequently the A. carotis dextra was prepared. For this purpose the M. sternocleidomastoideus was released, the A. carotis dextra was separated from the N. vagus and finally released from the surrounding tissue.

Three ligation threads were placed underneath the A. carotis dextra.

The cranial thread was ligated as cranial as possible to impair blood flow.

The distal thread was fastened with a mosquito clamp and the vessel subjected to traction, as far as the blood supply was impaired.

With a curved 26G needle a hole was punched as proximal as possible, underneath the ligature, in the vessel. Thereafter the pressure tip catheter (1.4F) was introduced in this hole and pushed until the distal thread.

With the middle thread, a knot was placed above the pressure tip catheter and the distal thread was released, to allow the catheter to be pushed into the left ventricle.

Once the pressure tip catheter placed in the A. carotis dextra, the blood pressure was monitored.

After one minute, the pressure tip catheter was pushed forward into the left ventricle.

Mice were allowed to stabilize for two minutes, until the monitoring started.

Finally, after the systolic and diastolic pressure had been monitored for two minutes, the pressure tip catheter was removed from the left ventricle.

After measurements, blood samples were taken and mice killed by cervical dislocation. Finally organ samples were collected.

▪ **Analysis**

Measurements were analyzed by the Chart 5 program for Windows.

Systolic and diastolic ventricular pressures were measured, and from those parameters heart rate, LVEDP, dP/dt_{max} , dP/dt_{min} and tau were calculated.

From each mouse a set of data was analyzed and mean and standard deviations were calculated.

3.7 Blood samples

Venous blood samples from all mice were taken in 1.2 mL lithium heparin tubes. Blood was collected after haemodynamic measurements under anaesthesia. The abdominal wall was opened from caudal to cranial on both side. The obtained skin and muscle lab was then held on the cranial side to discover the abdominal cavity. Intestines were pushed on the left side of the mice to get to the right V. iliaca interna. The vein was then punctured with a Monovette 20 G needle and the blood collected.

After blood collection, lithium heparin tubes were centrifuged by 6000 rpm for 10 minutes by 4 ° C. Plasma was collected / pipetted and conserved in 1.5 mL eppendorf tubes at -20 ° C for further analysis.

- **Lipid profile**

To determine lipid plasma profiles of mice, plasma samples were analyzed in the Cobas integra 400 plus analyzer, using photometry (enzymatic colour test) in specific commercial kits, purchased from Roche Diagnostics GmbH (Appendix 12.2.2).

Lipid profiles were composed out of triglycerides, total cholesterol, LDL cholesterol and HDL cholesterol.

3.8 Necropsy

3.8.1 Organs

Mice were killed by cervical dislocation.

Heart, without atrium and divided into left and right ventricle, lung, liver and right kidney were collected, washed in PBS, weighed and shock frozen on carbohydrate ice.

All organs were conserved at -80 °C.

3.8.2 Morphometric analysis

In cMI and DOCA models, morphometric analyses of the organs were performed. For this analysis mice and organs were separately weighed.

Afterward a quotient between organ weight and body weight was calculated.

$\frac{\text{Organ weight (g)}}{\text{Body weight (g)}} \times 1000 = \text{quotient (mg/g)}$

Body weight (g)

3.8.3 Scoring of infarct sizes

For the cMI model, infarct sizes were scored.

All left ventricles from the cMI mice were visually classified in 5 categories according to the infarct sizes.

1: no infarct (all sham operated mice)

2: small infarct

3: medium infarct

4: big infarct

5: huge infarct

3.9 Biomarker analyses

Biomarker analyses were performed with help of the department of target discovery, Bayer HealthCare AG, Wuppertal, under supervision of Dr. Peter Ellinghaus and collaborators. Analyses were done by real time polymerase chain reaction (RT PCR) with mRNA samples extracted from collected tissues.

3.9.1 RNA extraction

RNA was extracted from the frozen (-80 °C) left ventricle of all mice to perform RT PCR analysis.

Left ventricles were crushed in precooled mortars on dry ice.

After crushing, the samples were given in Lysing matrix D tubes and hold on dry ice until further handling.

Samples were first denatured with 600 µl TRIzol reagent and shaken for 20 s at 4 m/s in the FastPrep FP120 cell disrupter.

Thereafter samples were precipitated with 120 µl chloroform and shaken for 10 s on a MS1 minishaker.

They were centrifuged for 15 min and 4 ° C at 1400 rpm (Eppendorf, Centrifuge 5417R).

After centrifugation the clear supernatant was removed from samples and pipetted in new tubes, and 210 µl Isopropanol were added before vortexing.

Mixes were placed for 10 min on ice and afterwards centrifuged for 15 min and 4 ° C by 1400 rpm (Eppendorf, Centrifuge 5417R). Finally supernatants were removed.

The pellets were washed twice with 150 µl 80 % EtOH and allowed to dry for 15 min at room temperature.

Pellets were re suspended in 50 µl Ultrapure distilled water DNase RNase free and stored at -80 ° C.

3.9.2 cDNA synthesis

RNA samples were quantified by a NanoDrop ND-1000 spectrophotometer before further processing.

The ImProm-II Reverse Transcription System was used for the DNA digestion and for the reverse transcription of the mRNA.

In brief, 1 µg RNA were dissolved in 1 µl ImProm-II 5x reaction buffer 10x (200 mM Tris-HCl (pH8.4)), 1 µl Amplification Grade DNase I and DEPC-water (q.s.p. 10 µl). Mixes were then incubated for 15 min at room temperature and stopped by adding 1 µl 25 mM EDTA.

Samples were incubated for further 15 min at 65° C on a thermomixer 5436 and finally for 1 min on ice.

For the reverse transcription, 2.2 µl Oligo dT Primer were added and samples were incubated 5 min at 70 ° C and 5 min on ice.

During incubation time Master Mix was composed with Nuclease free water (38.6 %), ImProm-II 5x reaction buffer 10x (27.1 %), MgCl₂ 25 mM (20.4 %), 10 mM dNTPs

(6.6 %), Recombinant RNAsin Ribonuclease inhibitor, 20-40 U/μl (3.3 %) and ImProm-II Reverse Transcriptase, 50 U/μl (3.8 %).

From the master mix 39.6 μl were added to the samples, which were then incubated for 5 min at 25 ° C and 60 min at 42 ° C.

Finally 147 μl nuclease free water were added and samples stored by -20 ° C until the RT PCR analysis.

3.9.3 Real time polymerase chain reaction (RT PCR) analysis

The method of RT PCR was described in the paper by Uckert et al. (2007).

2.5 % (approximately 40 ng) of cDNA were submitted to amplification with the TaqMan Universal Master Mix using the following protocol: denaturation during 15 seconds by 94 ° C and annealing / extension during 1 minute by 60 ° C for 40 cycles. DNA sequences of PCR primers and labeled probes were designed using Primer Express, version 1.5 software (Applied Biosystems). The concentration of primers and labeled probes was 300 nmol/L and 150 nmol/L respectively. Fluorescence signals were measured using an ABI Prism 7700 sequence detection facility (Applied Biosystems).

All measurements were normalized to the expression of transcripts encoding for the housekeeping gene hypoxanthin-guanin-phosphoribosyltransferase (HPRT) (Table 3.1).

Table 3.1: RT-PCR analysis: sequences of forward and reverse primers and probes used to amplify mRNA transcripts. In the studies, HPRT served as a housekeeping gene.

Gene	Forward primer (5'-3')	Reverse primer (5'-3')	Probe (5'-FAM-3'TAMRA)
HPRT	GTTGCAAGCTTGCTGGTGAA	GATTCAAATCCCTGAAGTACTCA	CCTCTCGAAGTGTGGATACAGGCCA
L32	ACTGGAGGAAACCCAGAGGC	CATCAGGATCTGGCCCTTGA	TCGACAACAGGGTGCGGAGAAGG
B2M	GAAGCCGAACATACTGAACTGCTA	CCCGTTCTTCAGCATTTGGAT	CACAGTTCCACCCGCCTCACATTG
ANP	AGGAGAAGATGCCGGTAGAAGA	GCTTCCTCAGTCTGCTCACTCA	AGGTGATGCCCCCGCAGGC
MYHC	CAGCCATGCCAACCCTATG	TCCACGATGGCGATGTTCT	ATGCTGTCCGTGCCAATGACGACC
TIMP1	GTCCCAGAACCAGCAGTGAAG	CTGATGTGCAAATTTCCGTT	TTTCTCCATCACGGGCCGCCTAA
COL1A1	CAACCTGGACGCCATCAAG	GAGGCACAGACGGCTGAGTAG	TGCAACATGGAGACAGGTGAGACCTGTG
PPAR	TTGCCACTGTTCCAGGGACCT	TGTGCAAATCCCTGCTCTCC	CGAGGCCTGCGGCCCCAT
PDK-4	TGCTTTTCTGCGCAAGAG	TAAGCGGTGAGGCAGGATGT	CGTCCGCCTGGCCAATATCCTGA
OPN	GCGGTGAGTCTAAGGAGTCCC	TGATCAGAGGGCATGCTCAG	CGATGTCATCCCTGTTGCCAGCT

3.10 Statistics

The statistical analysis was performed using the GraphPad Prism program. For every analyzed parameter and for each group mean and standard deviation (SEM) were calculated. Differences between groups were analyzed using a one-way ANOVA, followed by the student Newmann-Keuls post hoc analysis or using an unpaired t-test.

All results are represented as mean \pm SEM. For all graphs statistical significances were represented as asteriks: * $p < 0.05$; ** $p < 0.01$; *** $p < 0.001$.

In the chronic myocardial infarction study one outlier was taken off the study after use of the outlier test of Nalimov.

Admission criteria for the DOCA study were a systolic blood pressure higher than 100 mmHg at the end of the study. No outliers were taken off the DOCA study.

4. Results

4.1 cMI model

4.1.1 Mortality and morphology in WT and KO mice

- Mortality

128 WT mice and 93 KO mice were subjected to permanent ligation of the LAD and 12 WT and 11 KO mice were subjected to Sham operation. In the first week after surgery, mortality of the ligated KO mice was almost twice as high as in ligated WT mice, with 40.9 % (n= 38) compared to 22.6 % (n= 29), respectively (Figure 4.1.1). All Sham WT (n= 12) and KO (n= 11) mice survived.

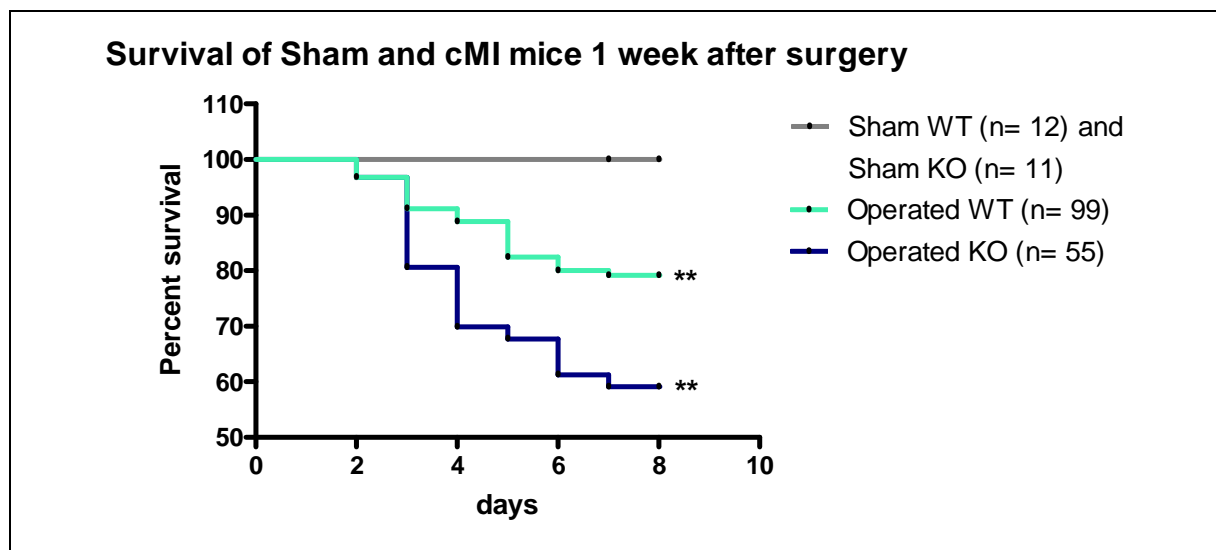


Figure 4.1.1: Survival curves of Sham and cMI PPAR^{-/-} WT and KO mice one week after surgery, ** p<0.01, Logrank test

In the following weeks, no further WT mice died in contrary to the KO mice. At the end of the study, 72.7 % of Sham (n= 8), 64.3 % of Placebo (n= 9), 53.3 % of Fenofibrate (n= 8) and 76.9 % of Ramipril (n= 10) KO mice survived.

- **Infarct sizes**

Infarct sizes were measured semi quantitatively using arbitrary scores.

As expected, WT and KO Sham mice had an infarct score of 0 (no sign of infarcts) after nine weeks (Figure 4.1.2 and Appendix table 1). The WT groups had similar infarct sizes with 3.2, 3.4 and 3.0 in the Placebo, Fenofibrate and Ramipril groups, respectively. As well, the KO groups had comparable infarct sizes with 3.6, 3.1 and 4 in the Placebo, Fenofibrate and Ramipril groups, respectively. The infarct scores were also comparable between the WT and KO groups, where all mice had medium to big size infarcts.

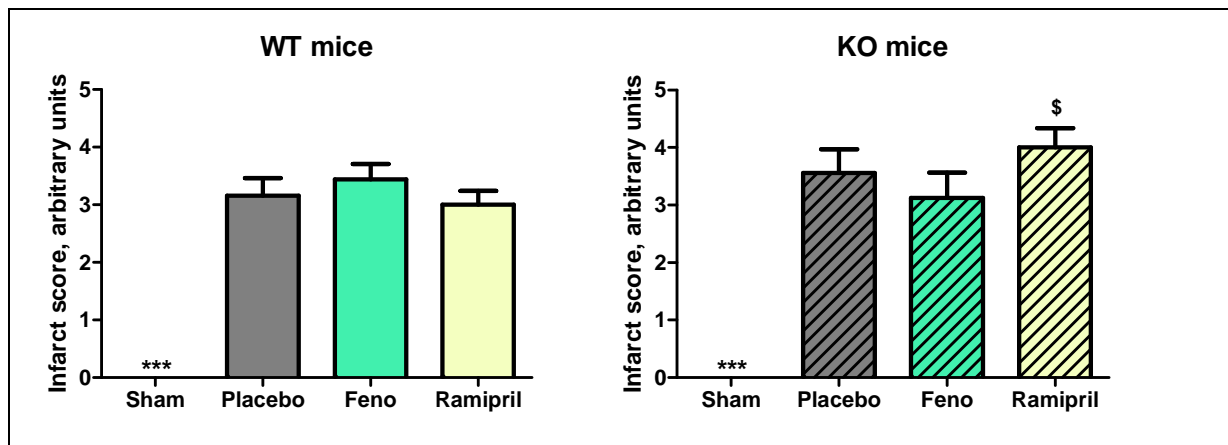


Figure 4.1.2: Infarct sizes of Sham and cMI PPAR WT and KO mice after eight weeks of treatment; n= 16 (WT), 8 (KO); mean \pm SEM; *** p<0.001 vs respective Placebo; ANOVA, followed by Student-Newmann-Keuls post hoc analysis; \$ p<0.05 vs respective WT group; unpaired t-test

- **Body weight**

At the end of the study, body weights were comparable within WT and KO groups (Appendix table 2). However, KO mice, with 25 g in average, were significantly smaller than WT mice, with 30g in average (Sham p<0.01 and Placebo p<0.001), although they were the same age and the same weight before surgery.

- **Heart weight**

As an important parameter of cardiac hypertrophy, relative heart weights were comparable between WT and KO Sham mice, with 4.2 and 4.3 mg/g, respectively

(Figure 4.1.3 and Appendix table 3). A significant increase of 14 % and 12 % of the relative heart weight was seen in WT and KO mice, respectively, after nine weeks of permanent LAD ligation ($p < 0.001$ and $p < 0.01$ respectively in unpaired t-test). Treatment with Ramipril significantly reduced relative heart weight increase to Sham levels ($p < 0.001$) in WT animals. Treatment with Fenofibrate had no significant effect compared to Placebo mice. In KO animals, no amelioration of the relative heart weight was observed after eight weeks of treatment with Fenofibrate or Ramipril.

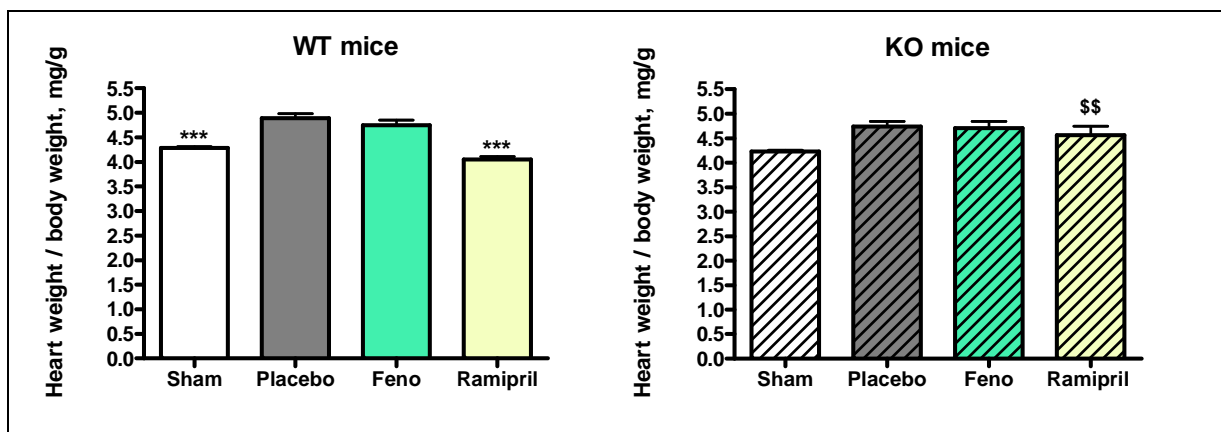


Figure 4.1.3: Relative heart weights of Sham and cMI PPAR WT and KO mice after eight weeks of treatment; $n = 16$ (WT), 8 (KO); mean \pm SEM; *** $p < 0.001$ vs respective Placebo; ANOVA, followed by Student-Newmann-Keuls post hoc analysis; \$\$ $p < 0.01$ vs respective WT group; unpaired t-test; Note the absence of an effect of ramipril in the KO mice.

- **Ventricular weight**

Increase of the heart weight is due to an increase of one or both ventricle weight. Therefore weights of the left ventricle + septum and of the right ventricle were separately investigated.

- Left ventricular weight

Relative left ventricular weight of Sham KO mice was significantly lower compared to Sham WT mice ($p < 0.05$ in unpaired t-test) (Figure 4.1.4 and Appendix table 4).

An increase of 0.6 and 0.5 mg/g in the relative left ventricular weight was seen in Placebo WT and KO mice, respectively, compared to their Sham groups ($p < 0.001$ in WT mice).

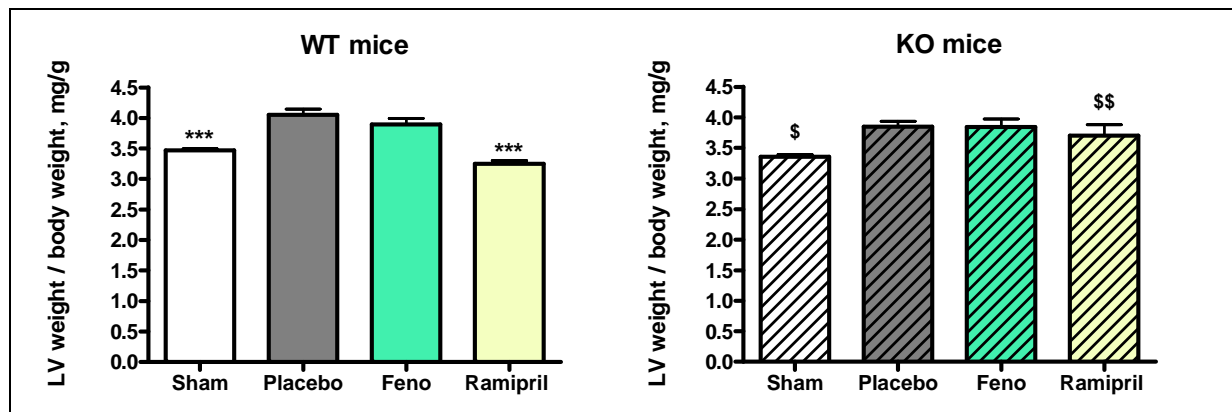


Figure 4.1.4: Relative left ventricular weights of Sham and cMI PPAR α WT and KO mice after eight weeks of treatment; n= 16 (WT), 8 (KO); mean \pm SEM; *** p<0.001 vs respective Placebo; ANOVA, followed by Student-Newmann-Keuls post hoc analysis; \$ p<0.05, \$\$ p<0.01 vs respective WT group; unpaired t-test;

Note the absence of an effect of ramipril in the KO mice.

Similar to the relative heart weight, treatment with Ramipril significantly reduced the relative left ventricular weight increase to Sham levels (p<0.001) in WT animals.

Treatment with Fenofibrate had no significant effect on this weight.

In KO mice, treatment with Fenofibrate or Rampril had no significant effect on the left ventricular hypertrophy after eight weeks.

- Right ventricular weight

In WT as well as in KO mice relative right ventricular weights were comparable with an average of 0.81 – 0.86 mg/g in all groups (Appendix table 5).

- **Organ weights: lung, liver, right kidney**

Heart failure may induce congestion in the body circulation. To evaluate this possibility, organ weights were measured. Furthermore, PPAR α agonists are known to induce a peroxisome proliferation, which induces an increase of the liver weight (Kliwer et al. 2001).

- Lung weight

Relative lung weights were comparable between all WT groups with values of 4.9 – 5.0 mg/g, but slightly inferior to the KO groups with values of 5.3 -5.5 mg/g (Appendix table 6).

- Liver weight

In WT mice, relative liver weights of Sham and Placebo groups were comparable with 42.2 and 42.3 mg/g, respectively (Figure 4.1.5 and Appendix table 7).

Treatment with Ramipril induced a significant increase of 8 % of the relative liver weight compared to Placebo mice ($p < 0.01$). Furthermore, treatment with Fenofibrate induced, as expected, an increase of almost 68 % of the relative liver weight compared to Placebo mice ($p < 0.001$).

On the contrary, liver weights were similar in all KO groups with values of 45.2 – 49.2 mg/g.

No congestion of the liver was observed after chronic myocardial infarction.

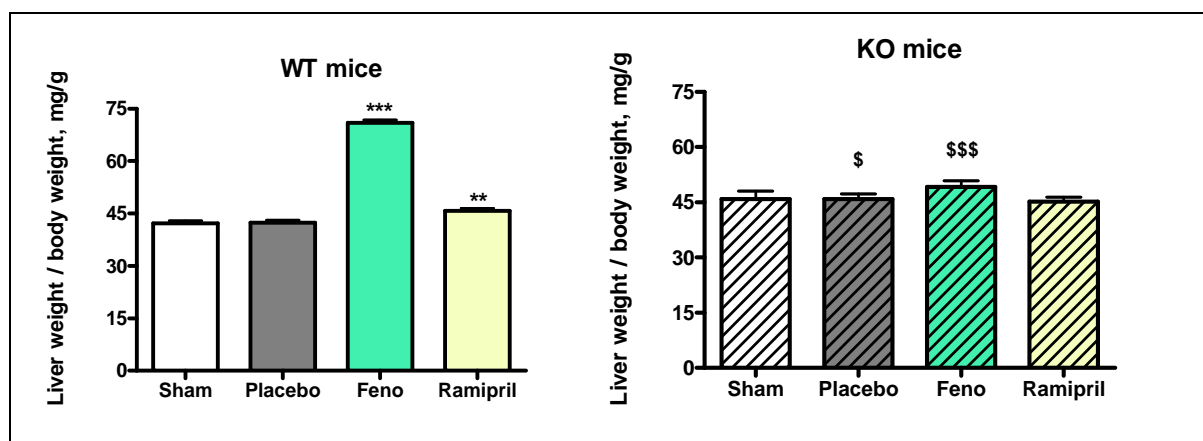


Figure 4.1.5: Relative liver weights of Sham and cMI PPAR WT and KO mice after eight weeks of treatment; $n = 16$ (WT), 8 (KO); mean \pm SEM; ** $p < 0.01$, *** $p < 0.001$ vs respective Placebo; ANOVA, followed by Student-Newmann-Keuls post hoc analysis; \$ $p < 0.05$, \$\$\$ $p < 0.001$ vs respective WT group; unpaired t-test;

Note that fenofibrate had no effect on the liver weight in KO mice.

- Right kidney weight

All WT groups had similar relative right kidney weights of 7.0 – 7.1 mg/g, apart from the Fenofibrate group (Appendix table 8). Eight weeks of treatment with Fenofibrate induced a significant increase of 0.6 mg/g of the relative right kidney weight compared to Placebo mice ($p < 0.001$).

In the KO groups, all mice had similar relative right kidney weights of 6.7 – 7.0 mg/g.

4.1.2 Haemodynamics in WT and KO mice

The morphological changes induced by a heart failure are often reflected in impairments of the haemodynamic functions of the myocardium.

- **Heart rate**

Heart rate was similar between all groups in the WT mice with values between 437 and 454 bpm (Figure 4.1.6 and Appendix table 9). Whereas in the KO mice heart rate was higher in the Sham groups than in all other treatment groups with 382 bpm compared to values between 337 and 343 bpm. Furthermore, Sham and Placebo KO mice had decreased heart rates compared to their respective WT groups ($p < 0.01$ and $p < 0.001$, respectively).

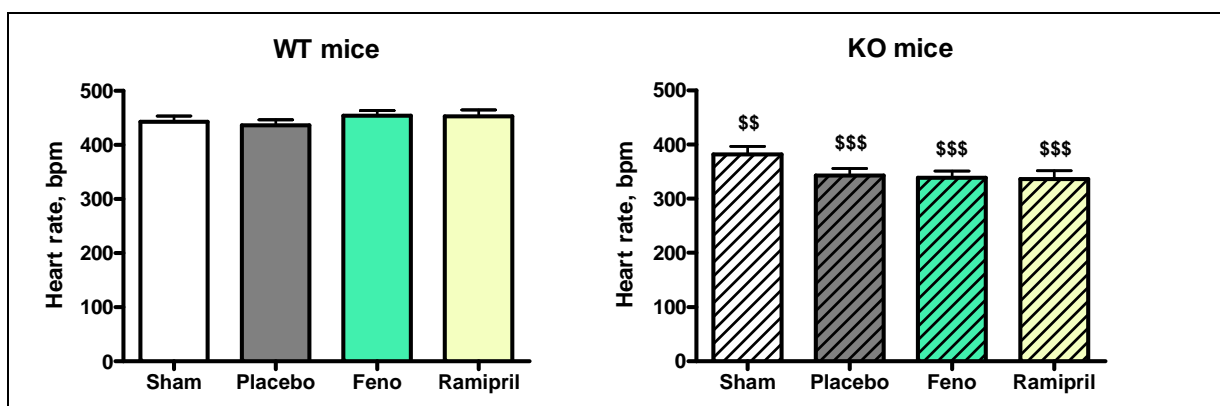


Figure 4.1.6: Heart rate of Sham and cMI PPAR WT and KO mice after eight weeks of treatment; $n = 16$ (WT), 8 (KO); mean \pm SEM; \$\$ $p < 0.01$, \$\$\$ $p < 0.001$ vs respective WT group; unpaired t-test; Note the lower heart rate in KO mice compared to WT mice.

- **Left ventricular systolic pressure (LVP)**

Permanent ligation of the LAD induced a slight decrease of the left ventricular systolic pressure in Placebo WT compared to Sham WT and a significant decrease of pressure in Placebo KO compared to Sham KO mice ($p < 0.001$) (Figure 4.1.7 and Appendix table 10). Furthermore, LVP of Placebo KO mice was significantly reduced compared to Placebo WT mice ($p < 0.001$ in unpaired t-test), although it was similar in Sham groups.

In both WT and KO mice, left ventricular systolic pressures were comparable after treatment with Placebo and Fenofibrate but significantly reduced by 20 mmHg in WT mice and by 16 mmHg in KO mice after treatment with Ramipril (both $p < 0.001$).

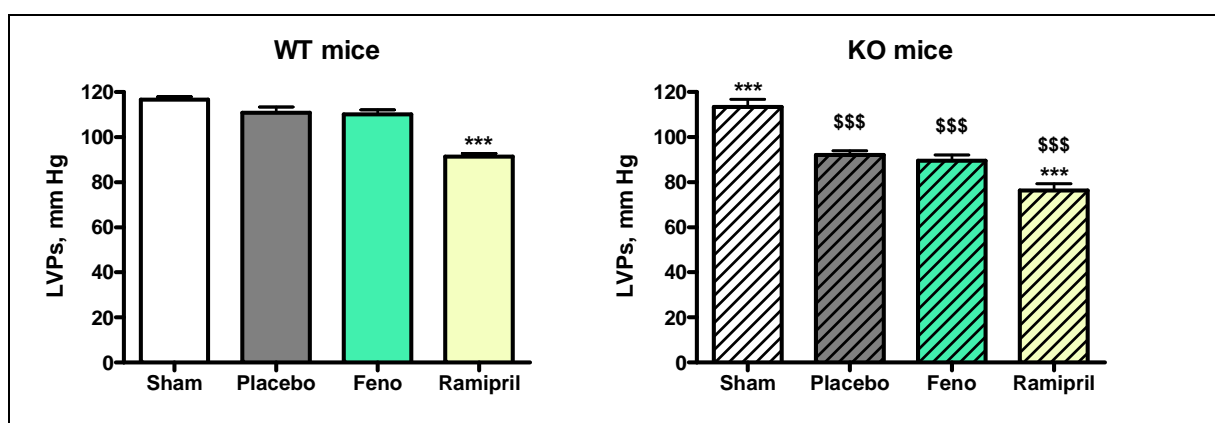


Figure 4.1.7: Left ventricular systolic pressure of Sham and cMI PPAR^{-/-} WT and KO mice after eight weeks of treatment; $n = 16$ (WT), 8 (KO); mean \pm SEM; ** $p < 0.01$, *** $p < 0.001$ vs respective Placebo; ANOVA, followed by Student-Newmann-Keuls post hoc analysis; \$\$\$ $p < 0.001$ vs respective WT group; unpaired t-test;

Note the lower systolic pressure in KO mice with heart failure compared to WT mice.

- **Left ventricular end-diastolic pressure (LVEDP)**

LVEDP is an important parameter for the diastolic function and relaxation of the heart and increases by heart failure.

In both WT and KO mice, permanent ligation of the LAD resulted in a significant increase of LVEDP by 3.3 and 4.8 mmHg, respectively in Placebo compared to their respective Sham groups ($p < 0.01$ in WT and $p < 0.05$ in KO in unpaired t-test) (Figure 4.1.8 and Appendix table 11).

Sham KO mice had a significant lower left ventricular end-diastolic pressure than Sham WT mice with 6.0 mmHg compared to 10.2 mmHg, respectively ($p < 0.01$).

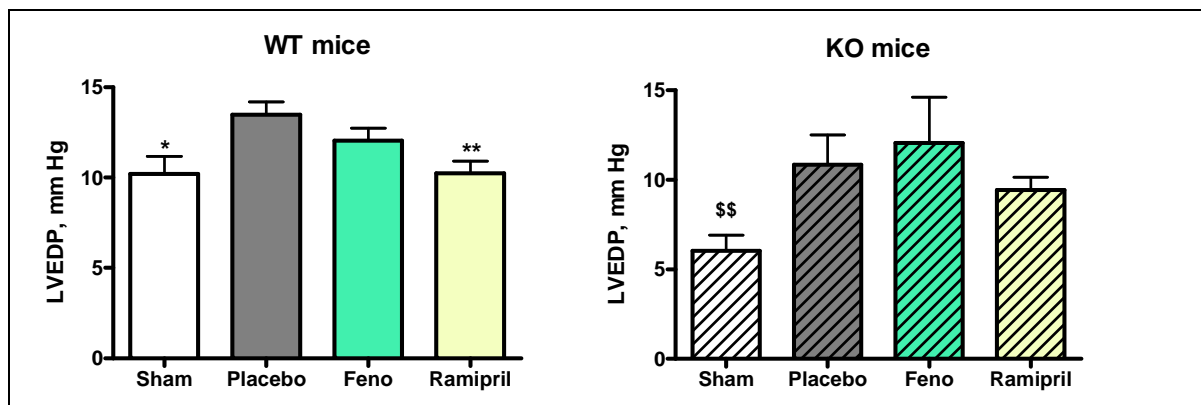


Figure 4.1.8: Left ventricular end diastolic pressure of Sham and cMI PPAR WT and KO mice after eight weeks of treatment; $n = 16$ (WT), 8 (KO); mean \pm SEM; * $p < 0.05$, ** $p < 0.01$ vs respective Placebo; ANOVA, followed by Student-Newmann-Keuls post hoc analysis; \$\$ $p < 0.01$ vs respective WT group; unpaired t-test;

Note the lower LVEDP in Sham KO mice compared to Sham WT mice.

In WT animals, eight weeks of treatment with Fenofibrate tend to decrease left ventricular end-diastolic pressure by 1.5 mmHg compared to Placebo mice, whereas treatment with Ramipril significantly decreased LVEDP to levels similar to Sham (10.2 mmHg, $p < 0.01$).

Whereas in KO mice, treatments with Fenofibrate or Ramipril had no effect on the left ventricular end-diastolic pressure compared to Placebo mice.

- **Contractility (left ventricular dP/dt_{max})**

The left ventricular dP/dt_{max} is a parameter for the systolic function and contractility of the heart. It is usually decreased in heart failure.

The dP/dt_{max} was comparable in Sham WT and KO with values of 7685 and 7613 mmHg/s, respectively (Figure 4.1.9 and Appendix table 12). In both WT and KO mice, permanent ligation of the LAD induced a significant decrease of the contractility in Placebo compared to Sham mice (both $p < 0.001$). However, this decrease was significantly more pronounced in the Placebo KO mice compared to the Placebo WT mice with values of 4630 mmHg/s compared to 6574 mmHg/s, respectively ($p < 0.001$ in unpaired t-test).

Treatment of WT animals with the PPAR agonist Fenofibrate significantly improved ($p < 0.05$) contractility after eight weeks compared to Placebo. Treatment with Ramipril had no effect.

On the contrary, treatment with Fenofibrate in the KO mice had no effect on left ventricular dP/dt_{max} , nor had the treatment with Ramipril.

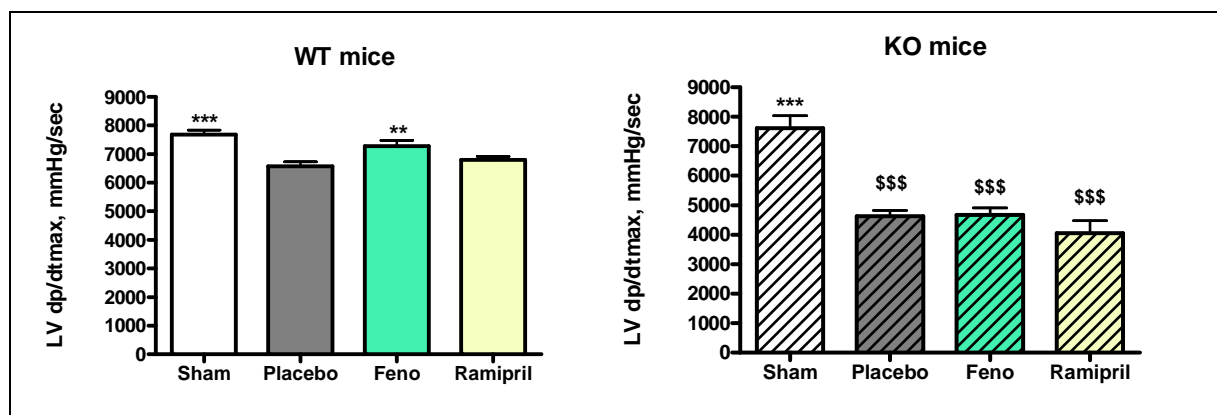


Figure 4.1.9: Left ventricular contractility (dP/dt_{max}) of Sham and cMI PPAR WT and KO mice after eight weeks of treatment; $n = 16$ (WT), 8 (KO); mean \pm SEM; * $p < 0.05$, ** $p < 0.01$, *** $p < 0.001$ vs respective Placebo; ANOVA, followed by Student-Newmann-Keuls post hoc analysis; \$\$\$ $p < 0.001$ vs respective WT group; unpaired t-test;

Note the further decreased contractility in operated KO mice compared to their respective WT mice.

- **Relaxation (left ventricular dP/dt_{min})**

As a parameter for relaxation, left ventricular dP/dt_{min} increases in heart failure.

Left ventricular dP/dt_{min} values were slightly higher in Sham KO compared to Sham WT mice with -7714 mmHg/s compared to -8986 mmHg/s, respectively (Figure 4.1.10 and Appendix table 13).

In both WT and KO mice permanent ligation of the LAD resulted in a significant increase (both $p < 0.001$) of the relaxation in the Placebo groups compared to their respective Sham groups, but this increase was significantly higher in Placebo KO compared to Placebo WT mice, with increases of 45 % and 28 % respectively ($p < 0.001$ in unpaired t-test).

In WT mice, both treatment with Fenofibrate and Ramipril showed a significant improvement of the relaxation (both $p < 0.05$).

On the contrary, PPAR KO mice showed worsened values of left ventricular dP/dt_{min} and none of the treatments could improve the relaxation after eight weeks.

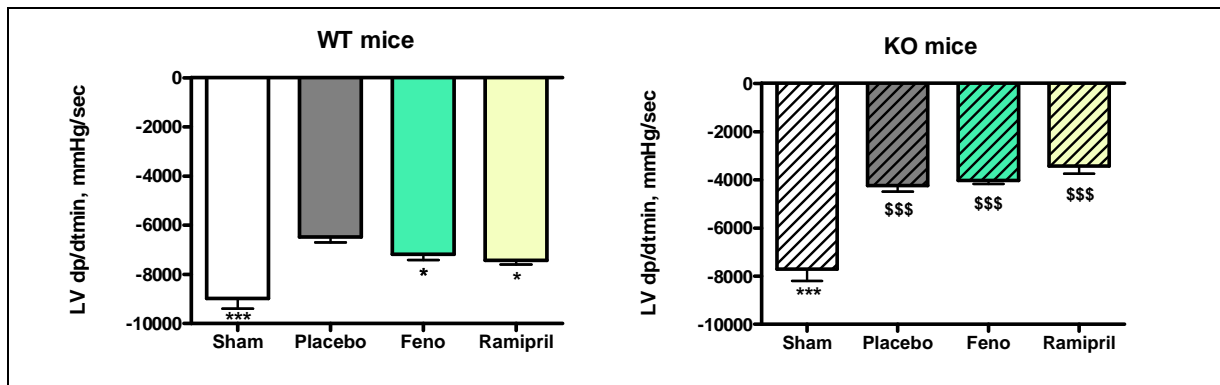


Figure 4.1.10: Left ventricular relaxation (dP/dt_{min}) of Sham and cMI PPAR WT and KO mice after eight weeks of treatment; n= 16 (WT), 8 (KO); mean ± SEM; ** p<0.01, *** p<0.001 vs respective Placebo; ANOVA, followed by Student-Newmann-Keuls post hoc analysis; \$\$\$ p<0.001 vs respective WT group; unpaired t-test;

Note the further increased dP/dt_{min} in operated KO mice compared to operated WT mice.

- **Left ventricular relaxation constant tau**

A further parameter for the diastolic function and the relaxation of the heart is the left ventricular relaxation constant tau. It is usually increased in heart failure.

Tau was comparable in Sham WT and KO mice with values of 12.4 and 14 ms, respectively (Figure 4.1.11 and Appendix table 14). In both WT and KO mice, ligation induced a significant increase of tau in Placebo mice compared to their Sham mice (both p<0.001). However, this increase was much higher in Placebo KO compared to Placebo WT mice with an increase of 19.3 ms compared to an increase of 7 ms, respectively (p<0.001 in unpaired t-test).

In WT mice, treatment with Fenofibrate and Ramipril significantly reduced tau by 15 % and 30 %, respectively (p<0.05 and p<0.001, respectively).

However in the KO mice, none of the treatments affected tau.

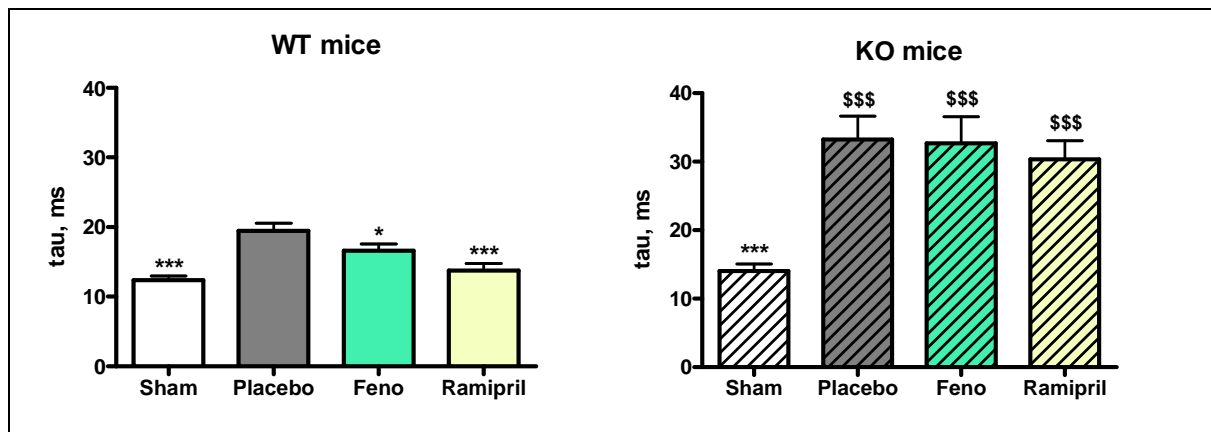


Figure 4.1.11: Left ventricular relaxation constant tau of Sham and cMI PPAR α WT and KO mice after eight weeks of treatment; n= 16 (WT), 8 (KO); mean \pm SEM; ** p<0.01, *** p<0.001 vs respective Placebo; ANOVA, followed by Student-Newmann-Keuls post hoc analysis; \$\$\$ p<0.001 vs respective WT group; unpaired t-test;

Note the increased tau in operated KO mice compared to their respective WT mice.

4.1.3 Biomarker analysis / RT-PCR analysis

- **Expression of PPAR α and PPAR β regulated genes**

- PPAR α

PPAR α expression was similar in Sham WT and KO groups with expression of 1724 and 1808 arbitrary units (AU), respectively, but significantly increased in Placebo KO compared to Placebo WT mice (p<0.01) (Figure 4.1.12 and Appendix table 15).

PPAR α gene expression can be detected in PPAR α KO mice due to the design of the KO expression plasmid (see methods 3.1) (full mRNA transcript containing a non sense mutation resulting in a non functional protein).

Furthermore, in WT and KO mice, ligation of the LAD resulted in a decrease of the PPAR α mRNA expression by 54 % and 26 %, respectively, in Placebo compared to Sham mice (p<0.01 in WT and p<0.05 in KO).

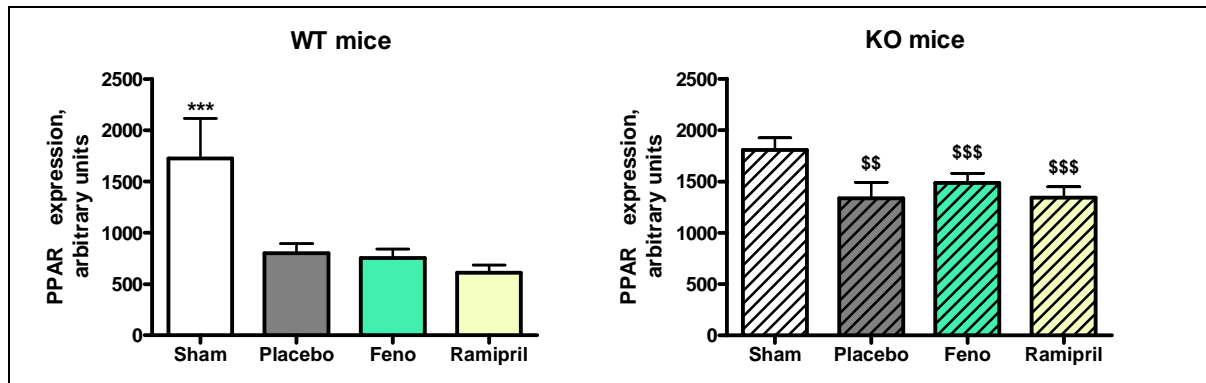


Figure 4.1.12: mRNA expression of PPAR of Sham and cMI PPAR WT and KO mice after eight weeks of treatment; n= 16 (WT), 8 (KO); mean \pm SEM; *** p<0.001 vs respective Placebo; ANOVA, followed by Student-Newmann-Keuls post hoc analysis; \$\$ p<0.01, \$\$\$ p<0.001 vs respective WT group; unpaired t-test;

In WT mice, treatment with Fenofibrate or Ramipril could not preserve decrease of PPAR mRNA expression.

In KO mice, Fenofibrate and Ramipril groups showed less reduction of PPAR mRNA expression compared to WT mice.

- PPAR regulated genes: Pyruvate dehydrogenase kinase, isozyme-4 (PDK-4)

PDK-4 is a mitochondrial enzyme playing a role in the glucose metabolism and is partly regulated by PPAR.

PDK-4 mRNA expression was tendentially decreased in Sham KO compared to Sham WT mice and significantly decreased in Placebo KO compared to Placebo WT mice (p<0.05) with values of 3426 AU compared to 5041 AU and 1785 AU compared to 4083 AU, respectively (Figure 4.1.13 and Appendix table 16).

In both WT and KO mice, ligation of the LAD resulted in a tendencial decrease of the PDK-4 mRNA expression in Placebo mice compared to their respective Sham littermates.

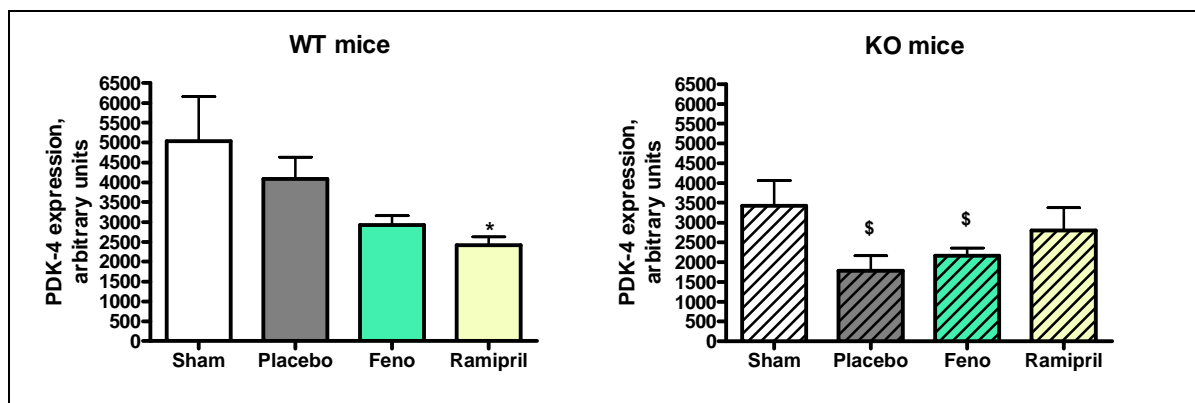


Figure 4.1.13: mRNA expression of PDK-4 of Sham and cMI PPAR WT and KO mice after eight weeks of treatment; n= 16 (WT), 8 (KO); mean \pm SEM; * p<0.05 vs respective Placebo; ANOVA, followed by Student-Newmann-Keuls post hoc analysis; \$ p<0.05 vs respective WT group; unpaired t-test;

Note the further decreased PDK-4 mRNA expression in KO mice compared to WT mice.

In WT mice and KO mice, mRNA expression of PDK-4 was similar between all groups. However, expression levels were lower in KO mice compared to WT mice.

▪ **Markers of hypertrophy**

As markers of hypertrophy, the expression of atrial natriuretic peptide (ANP) and myosin heavy chain- (MyHC) were analyzed.

○ Atrial natriuretic peptide (ANP)

Permanent ligation of the LAD resulted in a significant 2.8 fold and 3 fold increase of the ANP mRNA expression in Placebo groups compared to their respective Sham in WT and KO mice (both p<0.01) (Figure 4.1.14 and Appendix table 17).

However, there was a tendency towards reduced ANP mRNA expression in KO groups compared to their respective WT groups.

In WT mice, treatment with Fenofibrate and Ramipril decreased the ANP mRNA expression compared to Placebo by 30 % and 47 %, respectively (p<0.01 in Ramipril).

In KO mice, treatment with Fenofibrate or Ramipril did not ameliorate ANP mRNA expression compared to Placebo mice.

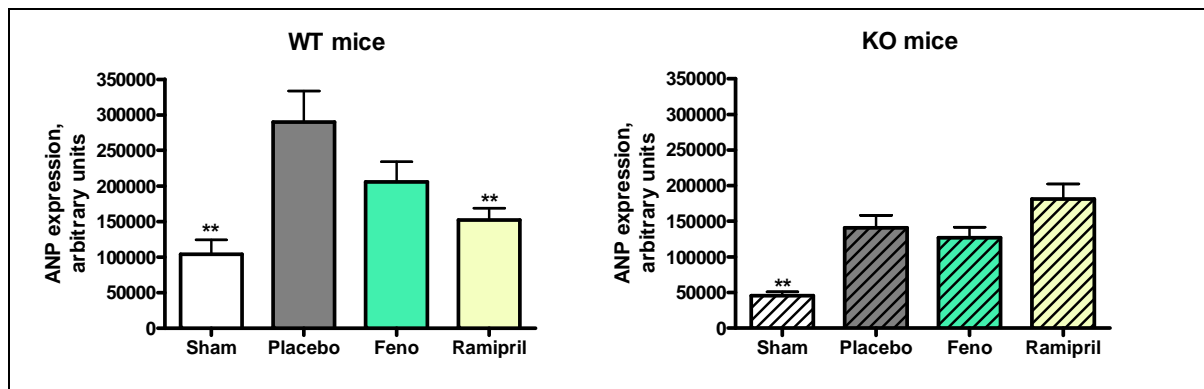


Figure 4.1.14: mRNA expression of ANP of Sham and cMI PPAR WT and KO mice after eight weeks of treatment; n= 16 (WT), 8 (KO); mean \pm SEM; ** $p < 0.01$ vs respective Placebo; ANOVA, followed by Student-Newmann-Keuls post hoc analysis

- Myosin heavy chain- (MyHC)

In WT and KO Placebo mice, permanent ligation of the LAD induced a 2.7 fold and 3.8 fold increase of MyHC mRNA expression, respectively, compared to their Sham mice ($p < 0.05$ in WT and $p < 0.001$ in KO) (Figure 4.1.15 and Appendix table 18).

However, MyHC mRNA expression in KO mice was significantly higher as in WT mice ($p < 0.001$ in Sham and Placebo). Indeed the MyHC mRNA expression was almost seven times as high in Sham KO as in Sham WT mice and almost ten times as high in Placebo KO compared to Placebo WT mice.

Furthermore, in WT mice, treatment with Fenofibrate or Ramipril significantly decreased the MyHC mRNA expression by 50 % and 70 %, respectively, compared to Placebo ($p < 0.01$ in Fenofibrate and $p < 0.001$ in Ramipril).

In KO mice, on the contrary, treatment with Fenofibrate or Ramipril did not ameliorate MyHC mRNA expression compared to Placebo.

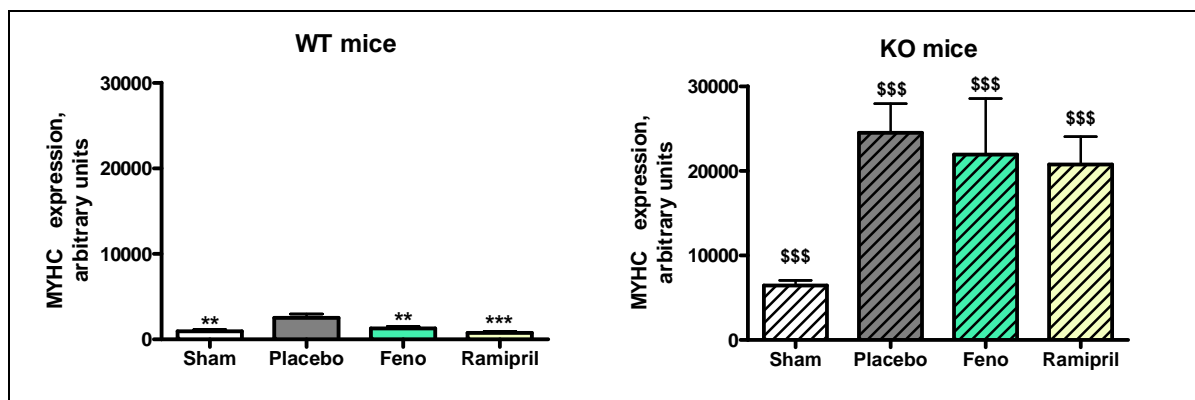


Figure 4.1.15: mRNA expression of MyHC of Sham and cMI PPAR WT and KO mice after eight weeks of treatment; n= 16 (WT), 8 (KO); mean \pm SEM; ** p<0.01, *** p<0.001 vs respective Placebo; ANOVA, followed by Student-Newmann-Keuls post hoc analysis; \$\$\$ p<0.001 vs respective WT group; unpaired t-test;

Note the higher expression of MyHC in KO mice compared to WT mice.

- **Markers of fibrosis and interstitial matrix remodelling**

As a marker of fibrosis, collagen 1A1 (COL1A1) was analyzed and as markers of interstitial matrix remodelling, tissue inhibitor of metalloproteinase 1 (TIMP1) and osteopontin were analyzed.

- Collagen 1A1 (COL1A1)

Permanent ligation of the LAD tended to increase the collagen mRNA expression in Placebo WT compared to Sham WT and a significant increase in Placebo KO compared to Sham KO mice (p<0.001) (Figure 4.1.16 and Appendix table 19). Furthermore, collagen mRNA expression in KO mice was significantly higher than in WT mice (p<0.05 in Sham and p<0.001 in Placebo). Indeed collagen mRNA expression was almost four times as high in Placebo KO as in Placebo WT mice and almost twice as high in Sham KO as in Sham WT mice.

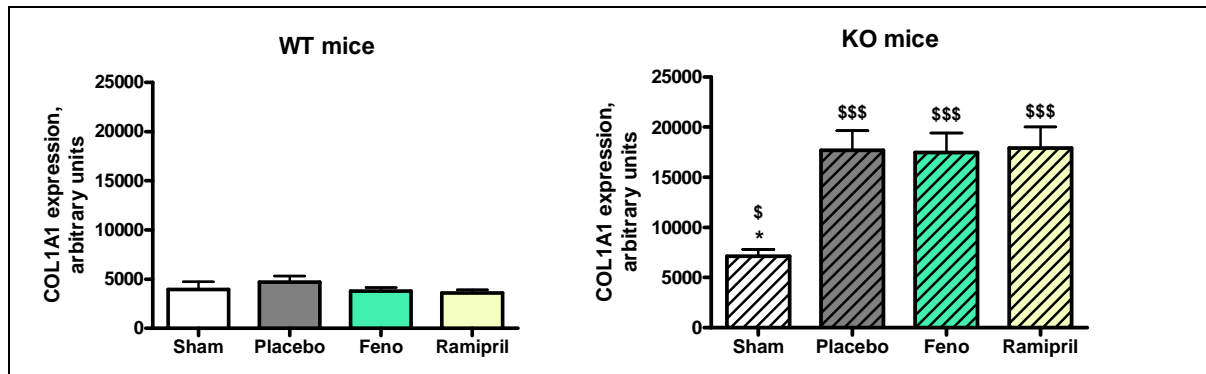


Figure 4.1.16: mRNA expression of collagen 1A1 of Sham and cMI PPAR WT and KO mice after eight weeks of treatment; n= 16 (WT), 8 (KO); mean \pm SEM; * p<0.05, vs respective Placebo; ANOVA, followed by Student-Newmann-Keuls post hoc analysis; \$ p<0.05, \$\$\$ p<0.001 vs respective WT group; unpaired t-test;

Note the higher expression of collagen 1A1 in KO mice compared to WT mice.

In WT mice, treatment with Fenofibrate and Ramipril tended to decrease collagen mRNA expression by 20 % and 24 %, respectively, compared to Placebo mice.

On the contrary, treatment with Fenofibrate or Ramipril in KO mice could not influence collagen mRNA expression compared to Placebo mice.

- Tissue inhibitor of metalloproteinase 1 (TIMP1)

In WT and KO Placebo mice, permanent ligation of the LAD induced a 3 and 4.9 fold increase of TIMP1 mRNA expression compared to their respective Sham mice (p<0.01 in WT and p<0.05 in KO) (Figure 4.1.17 and Appendix table 20).

Furthermore, TIMP1 mRNA expression was almost four and six times higher in Sham and Placebo KO mice as in their respective WT groups (both p<0.001 in unpaired t-test).

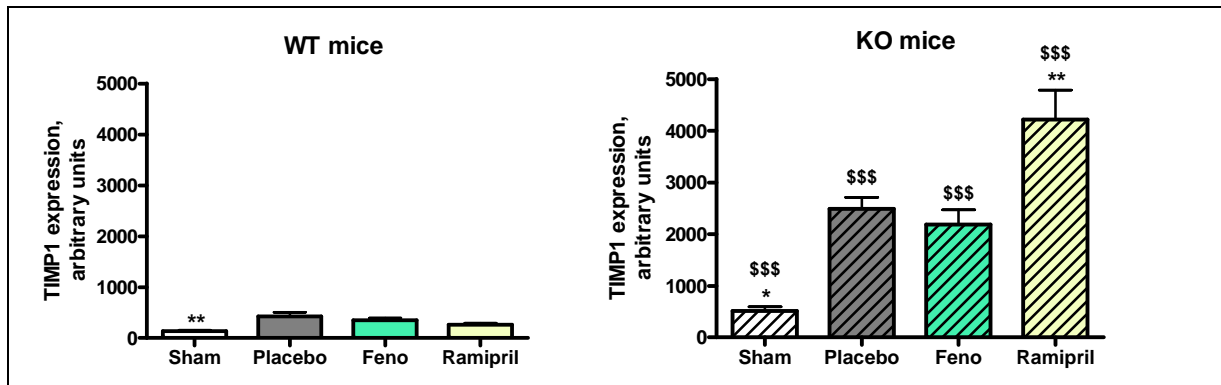


Figure 4.1.17: mRNA expression of TIMP1 of Sham and cMI PPAR WT and KO mice after eight weeks of treatment; n= 16 (WT), 8 (KO); mean \pm SEM; * p<0.05, ** p<0.01 vs respective Placebo; ANOVA, followed by Student-Newmann-Keuls post hoc analysis; \$\$\$ p<0.001 vs respective WT group; unpaired t-test;

Note the higher expression of TIMP1 in KO mice compared to WT mice.

Furthermore, treatment with Fenofibrate and Ramipril in WT mice decreased TIMP1 mRNA expression by 29 % and 39 %, respectively, compared to Placebo mice. In KO mice, treatment with Fenofibrate had no effect any more on TIMP1 mRNA expression and treatment with Ramipril significantly increased by almost 70 % TIMP1 mRNA expression compared to Placebo mice (p<0.01).

- Osteopontin (OPN)

Permanent ligation of the LAD resulted in a three fold and 18 fold increase of the osteopontin mRNA expression in Placebo groups compared to their respective Sham in WT and KO mice, respectively (p<0.01 in WT and p<0.001 in KO) (Figure 4.1.18 and Appendix table 21).

However, OPN mRNA expression in KO groups was on average 5 – 10 fold lower as in WT groups.

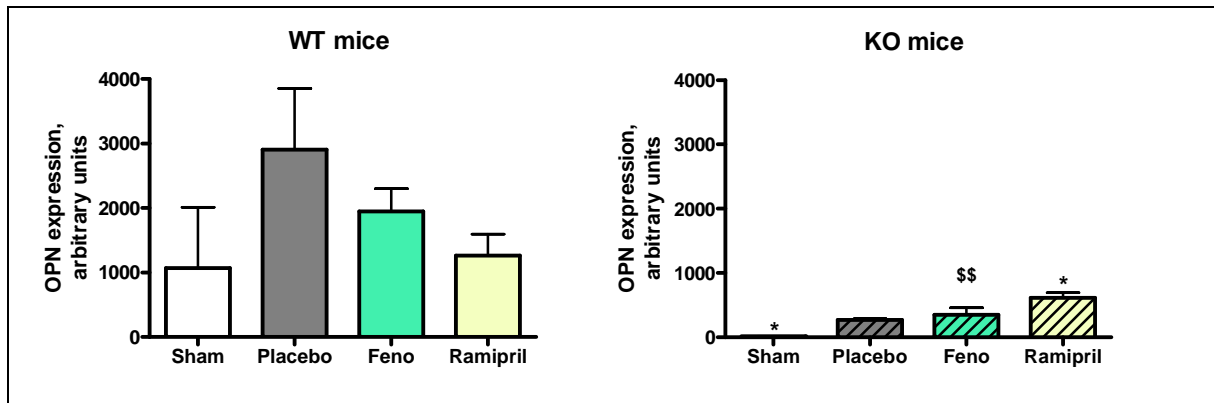


Figure 4.1.18: mRNA expression of osteopontin of Sham and cMI PPAR α WT and KO mice after eight weeks of treatment; n= 16 (WT), 8 (KO); mean \pm SEM; * p<0.05 vs respective Placebo; ANOVA, followed by Student-Newmann-Keuls post hoc analysis; \$\$ p<0.01 vs respective WT group; unpaired t-test;

Note the lower expression of osteopontin in KO mice compared to WT mice.

In WT mice, treatment with Fenofibrate and Ramipril decreased osteopontin mRNA expression by 33 % and 57 %, respectively, compared to Placebo mice.

On the contrary, in KO mice, treatment with Fenofibrate did not influence osteopontin mRNA expression compared to Placebo mice. However, KO mice receiving Ramipril treatment had almost twice as high osteopontin levels compared to Placebo mice.

4.1.4 Blood analysis

PPAR α is an important regulator of lipid metabolism. Therefore, lipid profiles of the mice were determined in their plasma.

- **Triglycerides**

Triglycerides levels were similar in WT groups, with a tendency towards decreased triglycerides in the Fenofibrate group compared to Placebo mice with values of 99 mg/dL and 108 mg/dL, respectively (Appendix table 22).

Triglycerides levels were equivalent in KO groups.

- **Total cholesterol**

In WT mice, total cholesterol levels were similar in Sham, Placebo and Ramipril groups with values of 105, 113 and 122 mg/dL, respectively (Figure 4.1.19 and Appendix table 23). However, treatment with Fenofibrate significantly increased those levels by 40 %, compared to Placebo mice ($p < 0.001$).

In KO mice, total cholesterol levels were comparable in Sham, Placebo and Ramipril mice with values of 128, 120 and 132 mg/dL, respectively, but were significantly increased by 13 % after treatment with Fenofibrate ($p < 0.05$).

Furthermore, cholesterol levels of KO mice were higher as WT mice, with statistical significance in the Sham groups ($p < 0.001$ in unpaired t-test).

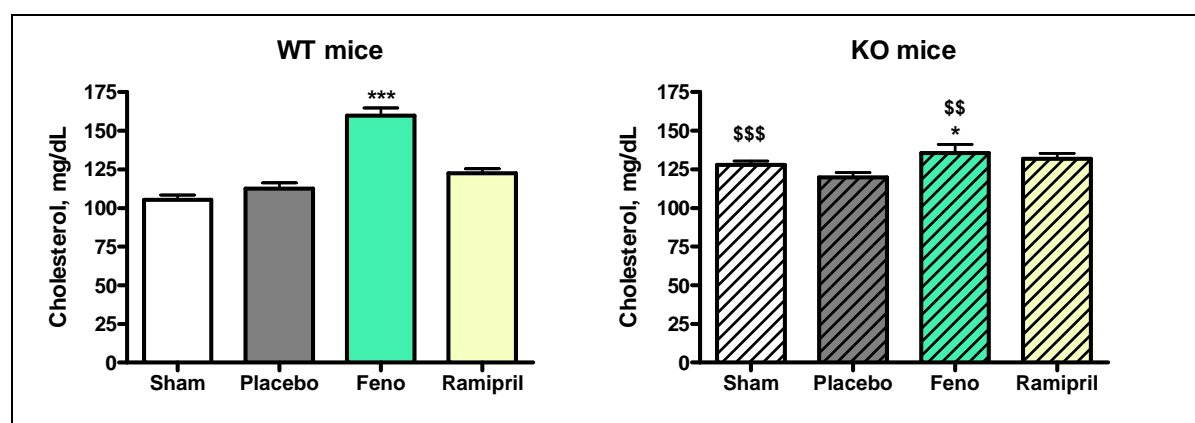


Figure 4.1.19: Total cholesterol plasma levels of Sham and cMI PPAR WT and KO mice after eight weeks of treatment; $n = 16$ (WT), 8 (KO); mean \pm SEM; * $p < 0.05$, *** $p < 0.001$ vs respective Placebo; ANOVA, followed by Student-Newmann-Keuls post hoc analysis; \$\$ $p < 0.01$ vs respective WT group; unpaired t-test;

Note the higher cholesterol plasma levels in KO mice compared to WT mice and the lack of effect of fenofibrate in KO mice.

- **HDL cholesterol**

No differences were seen between Sham and Placebo groups of WT and KO mice (Figure 4.1.20 and Appendix table 24). However, plasma levels of HDL cholesterol were 33 % and 17 % higher in Sham and Placebo KO mice compared to their respective WT mice ($p < 0.001$ in Sham and $p < 0.01$ in Placebo).

Furthermore, in WT mice, high density lipoprotein levels were similar in Sham, Placebo and Ramipril groups with values of 95, 102 and 108 mg/dL, respectively.

However, treatment with Fenofibrate significantly increased HDL cholesterol levels by 48 % compared to Placebo mice (both $p < 0.001$).

In KO mice, HDL cholesterol levels were comparable in all groups with values between 119 and 136 mg/dL.

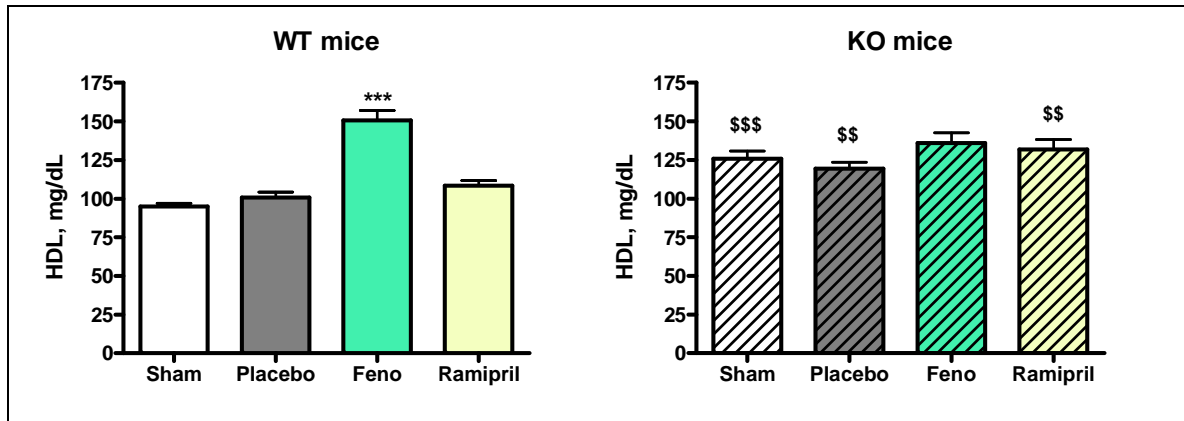


Figure 4.1.20: HDL cholesterol plasma levels of Sham and cMI PPAR WT and KO mice after eight weeks of treatment; $n = 16$ (WT), 8 (KO); mean \pm SEM; *** $p < 0.001$ vs respective Placebo; ANOVA, followed by Student-Newmann-Keuls post hoc analysis; ; \$\$ $p < 0.01$ vs respective WT group; unpaired t-test;

Note the higher HDL cholesterol plasma levels in KO mice compared to WT mice and the lack of effect of fenofibrate in these mice.

▪ LDL cholesterol

In WT mice, low density lipoprotein levels were similar in Sham, Placebo and Ramipril groups with values of 3, 5 and 5 mg/dL, respectively (Figure 4.1.21 and Appendix table 25). However, treatment with Fenofibrate induced a significant almost 3 fold increase of those levels compared to Placebo mice ($p < 0.001$).

In KO mice, LDL levels were comparable in Sham, Placebo, Fenofibrate and Ramipril mice with values of 7, 6, 7 and 8 mg/dL, respectively.

Furthermore, LDL levels of KO mice were higher as WT mice, with statistical significance in the Sham groups ($p < 0.001$ in unpaired t-test).

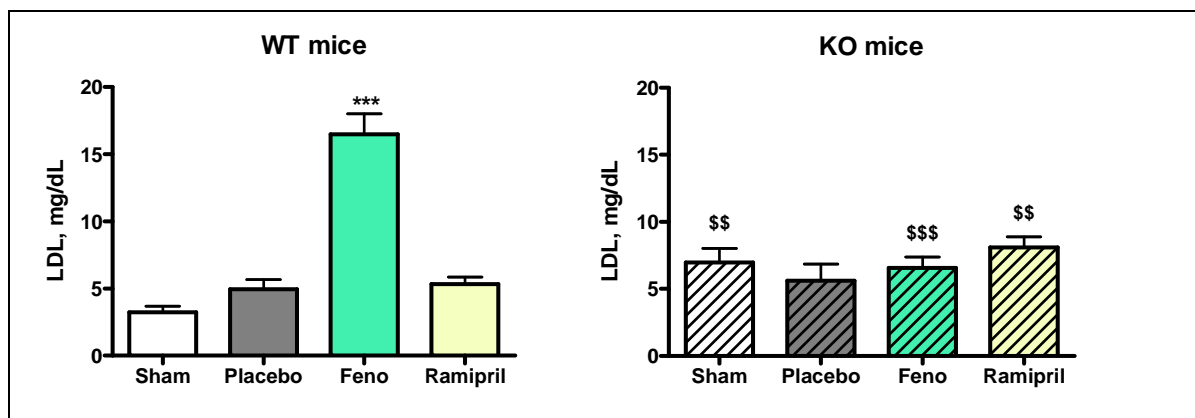


Figure 4.1.21: LDL cholesterol plasma levels of Sham and cMI PPAR WT and KO mice after eight weeks of treatment; n= 16 (WT), 8 (KO); mean \pm SEM; *** p<0.001 vs respective Placebo; ANOVA, followed by Student-Newmann-Keuls post hoc analysis; \$\$ p<0.01, \$\$\$ p<0.001 vs respective WT group; unpaired t-test;

Note the higher LDL cholesterol plasma levels in KO mice compared to WT mice and the lack of effect of fenofibrate on this level in KO mice compared to WT mice.

4.2 DOCA model

For the DOCA model, the same morphological, haemodynamic and biomarker analysis as for the cMI model were performed.

4.2.1 Morphology in WT and KO mice

- **Body weight**

Placebo and Ramipril WT groups were significantly smaller than Sham and Fenofibrate WT groups after six weeks of treatment, with weights of 26.8, 27.0, 30.2 and 28.8g, respectively (Appendix table 26).

In KO groups, all mice had comparable body weights of 25g in average.

However, groups of Sham and Placebo KO mice were significantly smaller than respective WT groups (Sham $p < 0.01$, Placebo $p < 0.05$), although they were the same size and age at the time of the surgery.

- **Heart weight**

Relative heart weights were similar between Sham WT and KO mice, with 4.4 and 4.3 mg/g and between Placebo WT and KO mice, with 5.1 and 5.6 mg/g (Figure 4.2.1 and Appendix table 27).

DOCA treatment induced a significant increase of the relative heart weight in Placebo groups compared to their respective Sham groups of WT and KO mice by 16 and 30 %, respectively (both $p < 0.001$).

In WT mice, treatment with Fenofibrate and Ramipril significantly reduced the relative heart weight compared to Placebo (both $p < 0.05$).

In KO mice, no differences between Placebo and Fenofibrate treated mice were seen. However, treatment with Ramipril significantly reduced relative heart weight compared to the Placebo group ($p < 0.01$).

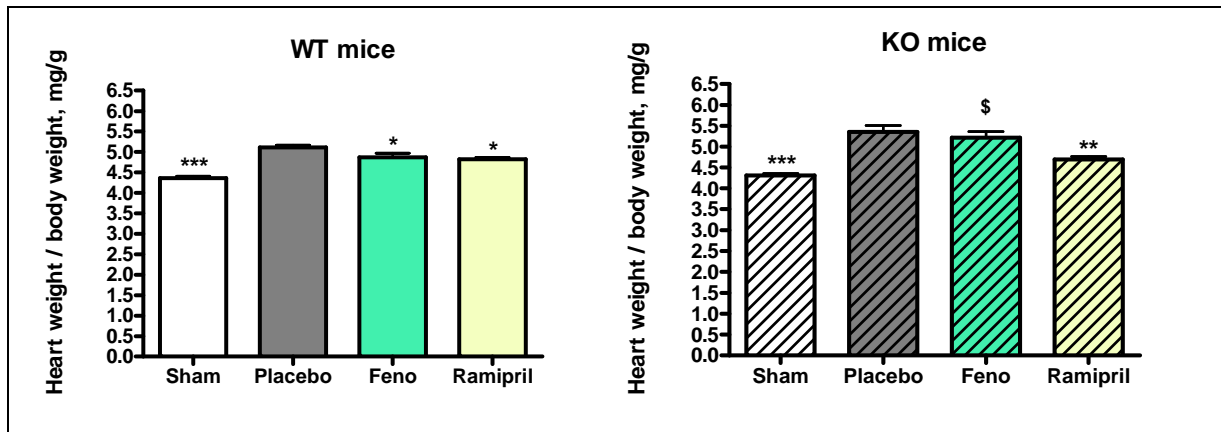


Figure 4.2.1: Relative heart weights of WT and KO mice after six weeks of treatment; n= 15; mean \pm SEM; * p<0.05, ** p<0.01, *** p<0.001 vs respective Placebo; ANOVA, followed by Student-Newmann-Keuls post hoc analysis; \$ p<0.05 vs respective WT group; unpaired t-test; Note the lack of effect of fenofibrate in KO mice compared to WT mice.

- **Ventricular weights**

- Left ventricular weight

Relative left ventricular weights were comparable between Sham WT and KO mice, with values of approximately 3.5 mg/g (Figure 4.2.2 and Appendix table 28).

In WT and KO mice, a significant increase of the relative left ventricular weight by 23 and 34 %, respectively, was seen in Placebo groups compared to their respective Sham groups (p<0.001).

In WT mice, treatment with Fenofibrate and Ramipril significantly reduced the relative left ventricular weight by 7 % compared to Placebo (both p<0.01).

In KO mice, no differences between Placebo and Fenofibrate treated mice were seen. However, treatment with Ramipril significantly reduced relative left ventricular weight by 17 % compared to Placebo mice (p<0.01).

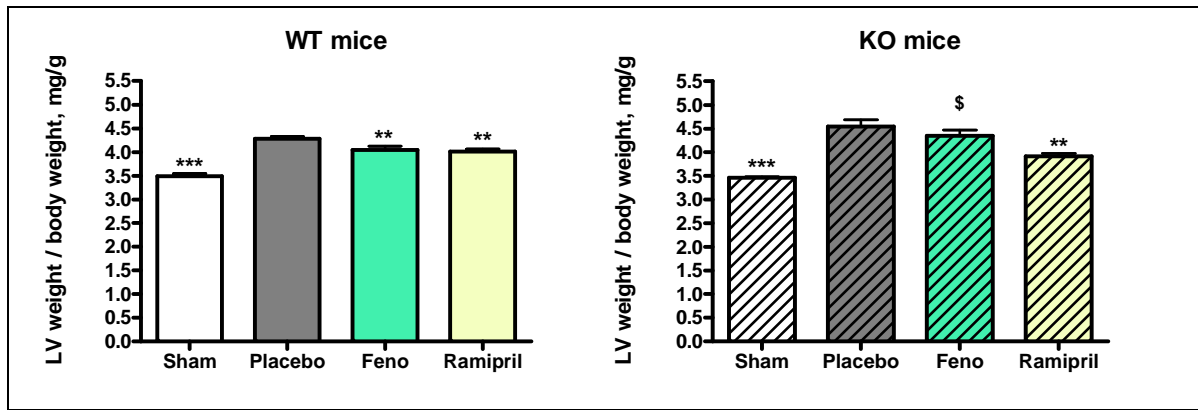


Figure 4.2.2: Relative left ventricular weights of WT and KO mice after six weeks of treatment; n= 15; mean \pm SEM; * $p < 0.05$, ** $p < 0.01$, *** $p < 0.001$ vs respective Placebo; ANOVA, followed by Student-Newmann-Keuls post hoc analysis; § $p < 0.05$ vs respective WT group; unpaired t-test; Note the lack of effect of fenofibrate in KO mice compared to WT mice.

- Right ventricular weight

Relative right ventricular weights were comparable in WT as well as in KO groups with values between 0.76 and 0.92 mg/g (Appendix table 29).

- **Organ weights: lung, liver, right kidney**

- Lung

Relative lung weights of Sham groups were similar in WT and KO mice with values of 5.1 and 5.3 mg/g, respectively (Appendix table 30).

In Placebo WT and KO mice, DOCA treatment induced a significant increase of the relative lung weight compared to their respective Sham groups (both $p < 0.05$ in unpaired t-test).

In WT as well as in KO treatment groups, relative lung weights were comparable to their respective Placebo groups. However, KO mice showed higher lung weights as WT mice, with statistical significance in Placebo groups ($p < 0.05$).

- Liver

Relative liver weights were comparable in Sham WT and KO mice, but significantly increased by 31 and 53 %, respectively, in Placebo WT and KO mice compared to their respective Sham groups ($p < 0.001$) (Figure 4.2.3 and Appendix table 31).

Furthermore, Placebo KO mice showed a significant increased relative liver weight compared to Placebo WT mice ($p < 0.01$).

In WT mice, relative liver weights of Placebo and Ramipril treated mice were comparable. However, treatment with Fenofibrate induced an increase by 71 % of the relative liver weight compared to Placebo mice ($p < 0.001$).

In KO mice, relative liver weights were comparable in Placebo, Fenofibrate and Ramipril treated groups.

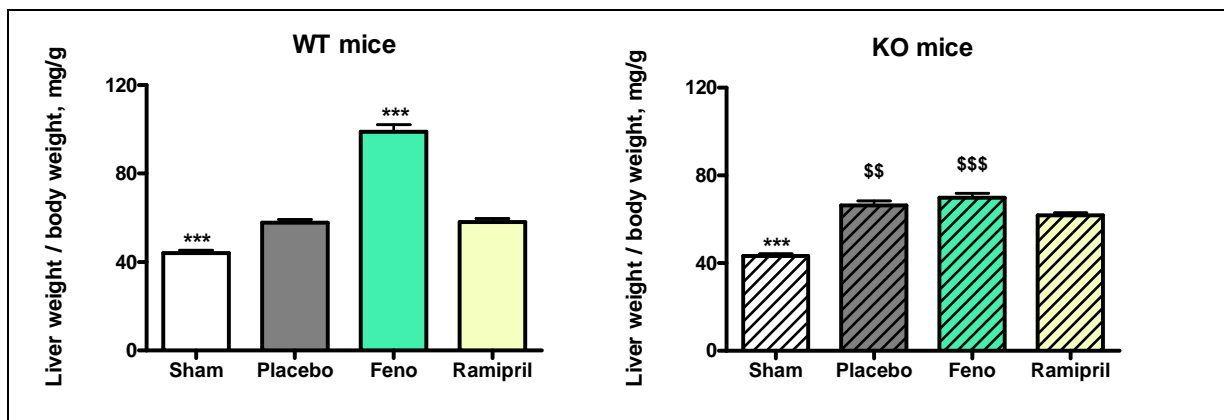


Figure 4.2.3: Relative liver weights of WT and KO mice after six weeks of treatment; $n = 15$; mean \pm SEM; *** $p < 0.001$ vs respective Placebo; ANOVA, followed by Student-Newmann-Keuls post hoc analysis; \$\$ $p < 0.01$, \$\$\$ $p < 0.001$ vs respective WT group; unpaired t-test; Note the lack of effect of fenofibrate on the liver weight in KO mice compared to WT mice.

- Right kidney

Relative right kidney weights were comparable in Sham WT and KO mice with values of 6.9 and 7.2 mg/g, but significantly increased by 81 % in Placebo WT mice and by 107 % in Placebo KO mice compared to their respective Sham groups after six weeks (both $p < 0.001$) (Figure 4.2.4 and Appendix table 32).

Furthermore, Placebo KO mice showed a significantly increased relative right kidney weight compared to Placebo WT mice ($p < 0.001$).

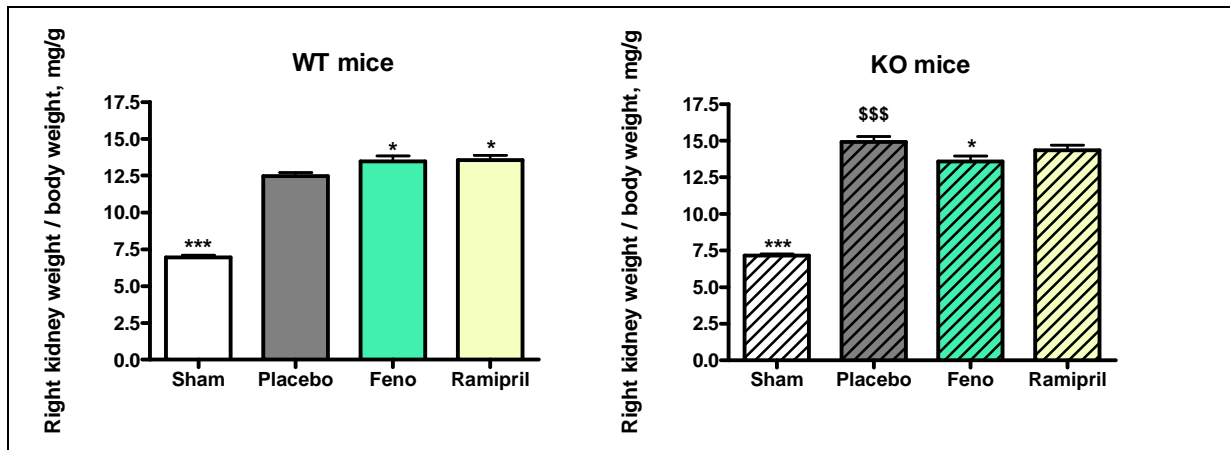


Figure 4.2.4: Right kidney weights of WT and KO mice after six weeks of treatment; n = 15; mean \pm SEM; * $p < 0.05$, *** $p < 0.001$ vs respective Placebo; ANOVA, followed by Student-Newmann-Keuls post hoc analysis; \$\$\$ $p < 0.001$ vs respective WT group; unpaired t-test; Note the higher increase of the right kidney weight in placebo KO mice compared to placebo WT mice.

In WT mice, relative right kidney weights were significantly increased after treatment with Fenofibrate and Ramipril compared to Placebo mice (both $p < 0.05$).

In KO mice, relative right kidney weights were similar in Placebo and Ramipril treated mice, but significantly decreased in Fenofibrate treated mice compared to Placebo mice ($p < 0.05$).

4.2.2 Haemodynamics in WT and KO mice

▪ Heart rate

In WT and KO mice, Sham and Placebo groups had comparable heart rates of 442, 425, 474 and 504 bpm (Figure 4.2.5 and Appendix table 33). However, heart rates were significantly increased in KO mice compared to the respective WT mice ($p < 0.05$ in Sham and $p < 0.001$ in Placebo).

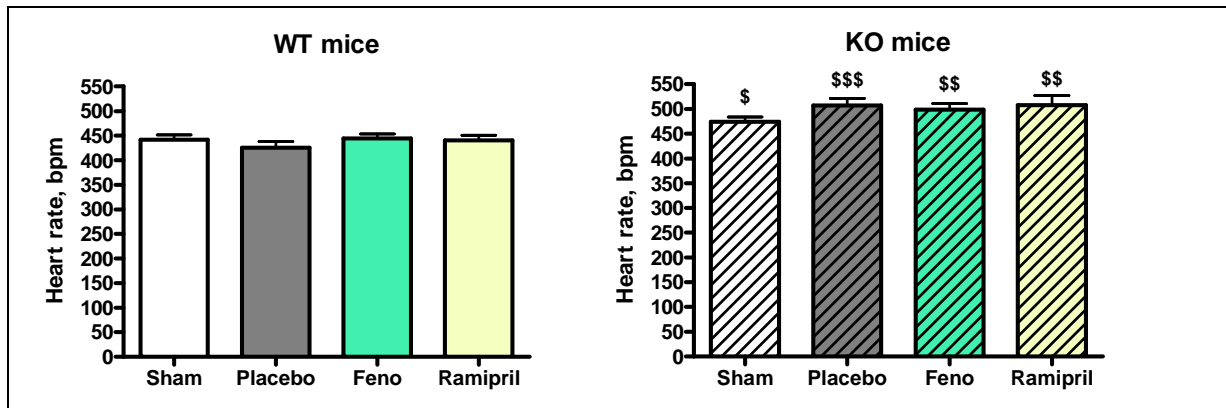


Figure 4.2.5: Heart rate of WT and KO mice after six weeks of treatment; n= 15; mean ± SEM; \$ p<0.05, \$\$ p<0.01, \$\$\$ p<0.001 vs respective WT group; unpaired t-test; Note the higher heart rate in KO mice compared to WT mice.

In WT mice, heart rates were comparable between Sham, Placebo, Fenofibrate and Ramipril treated groups. As well, in KO mice heart rates were similar in all groups.

- **Left ventricular systolic pressure**

In WT and KO mice, Sham groups had comparable left ventricular systolic pressures of 120 and 115 mmHg (Figure 4.2.6 and Appendix table 34).

Furthermore, DOCA treatment resulted in a significant increase of the left ventricular systolic pressure by 23 mmHg in Placebo WT mice and by 18 mmHg in Placebo KO mice compared to their respective Sham groups (both p<0.001).

In WT mice, left ventricular systolic pressures were comparable in Placebo and Fenofibrate treated groups, but significantly reduced by 10 mmHg after treatment with Ramipril compared to Placebo groups (p<0.01).

In KO mice, left ventricular systolic pressures were similar in Placebo, Fenofibrate and Ramipril treated groups.

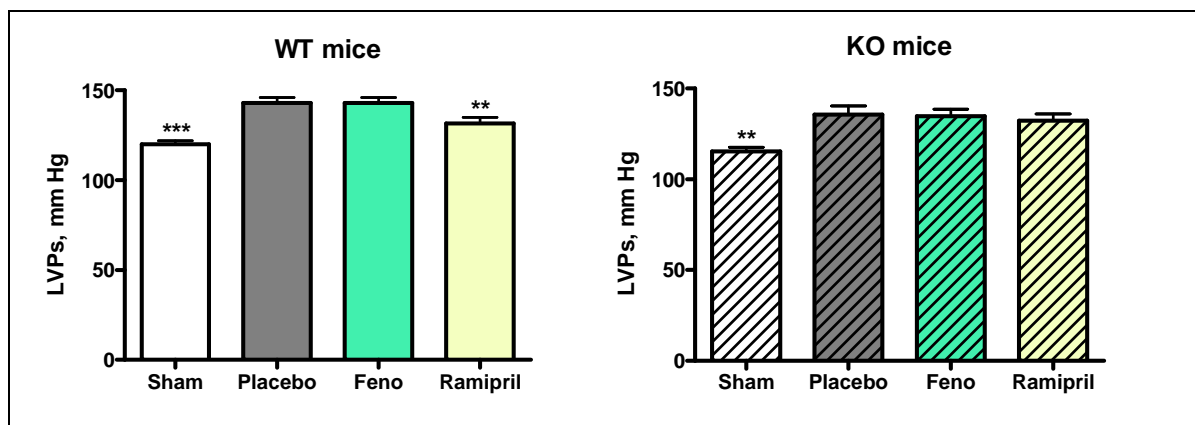


Figure 4.2.6: Left ventricular systolic pressure of WT and KO mice after six weeks of treatment; n= 15; mean \pm SEM; ** p<0.01, *** p<0.001 vs respective Placebo; ANOVA, followed by Student-Newmann-Keuls post hoc analysis

- **Left ventricular end-diastolic pressure**

No significant differences of left ventricular end-diastolic pressure were observed between Sham and Placebo WT mice, although there was a tendency towards a decrease of LVEDP in Placebo mice by 31 % (Figure 4.2.7 and Appendix table 35). In KO mice, no significant differences were seen between Sham and Placebo groups, although there was a tendency towards increased LVEDP in Placebo mice by 26 %. However, left ventricular end-diastolic pressure was significantly lower in Sham KO mice compared to Sham WT mice (p<0.01).

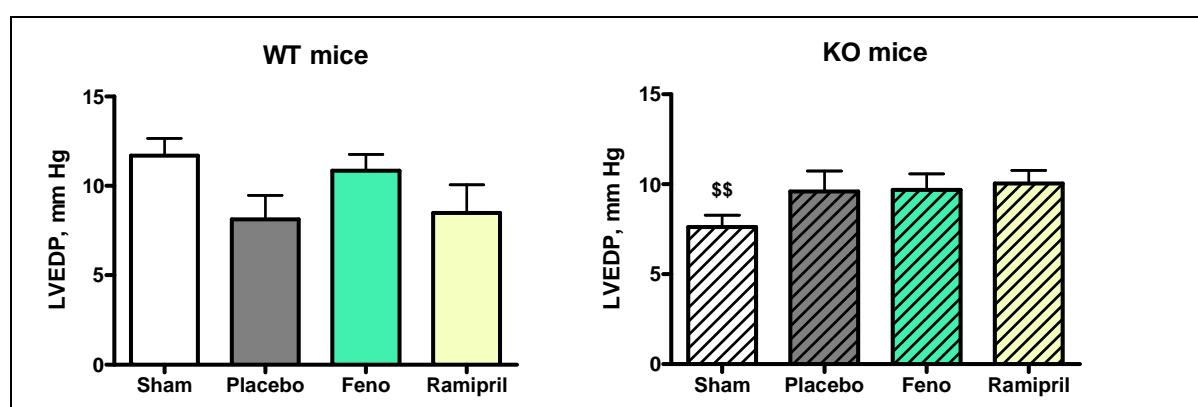


Figure 4.2.7: Left ventricular end diastolic pressure of WT and KO mice after six weeks of treatment; n= 15; mean \pm SEM; \$\$ p<0.01 vs respective WT group; unpaired t-test; Note the lower LVEDP in Sham KO mice compared to Sham WT mice.

No significant differences of LVEDP were observed between WT and KO Fenofibrate and Ramipril treated groups.

- **Contractility (left ventricular dP/dt_{max})**

Left ventricular dP/dt_{max} , as a measure of contractility was similar in Sham WT and KO mice with values of 7784 and 8054 mmHg/s (Figure 4.2.8 and Appendix table 36).

DOCA treatment of mice resulted in a significant increase of left ventricular dP/dt_{max} by 15 % in Placebo WT mice and by 11 % in Placebo KO mice compared to the respective Sham groups after six weeks ($p < 0.05$ in WT and $p < 0.01$ in KO in unpaired t-test).

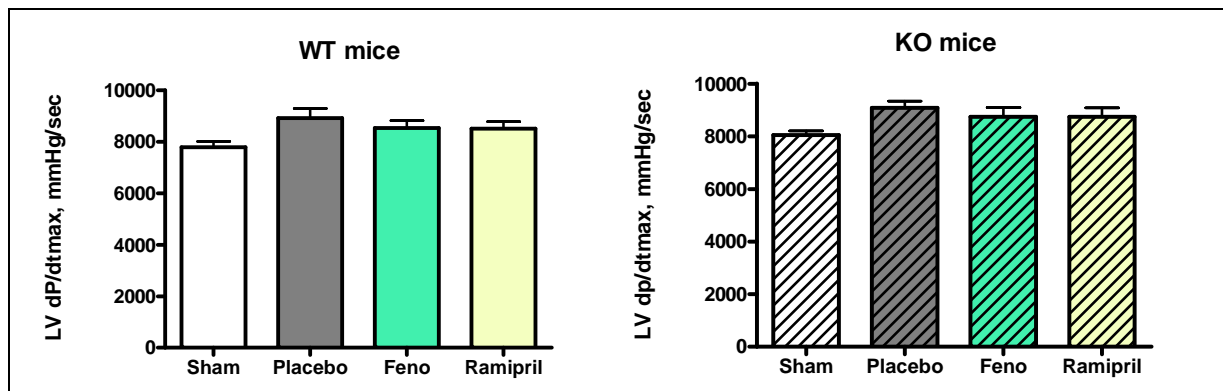


Figure 4.2.8: Left ventricular contractility (dP/dt_{max}) of WT and KO mice after six weeks of treatment; n= 15; mean \pm SEM

In WT and KO mice, left ventricular dP/dt_{max} of Fenofibrate and Ramipril treated groups were comparable to their respective Placebo groups.

- **Relaxation (left ventricular dP/dt_{min})**

Left ventricular dP/dt_{min} as a measure for relaxation was comparable in all WT and KO groups with values between -10319 and -9031 mmHg/s (Appendix table 37).

- **Left ventricular relaxation constant tau**

Left ventricular relaxation constant tau was similar in Sham and in Placebo groups of WT and KO mice, with 12.7, 11.5, 14.8 and 15.6 ms, respectively (Figure 4.2.9 and Appendix table 38).

A tendency towards increase of tau by 17 % in Placebo WT mice and by 36 % in Placebo KO mice compared to their respective Sham groups was seen after six weeks of DOCA treatment.

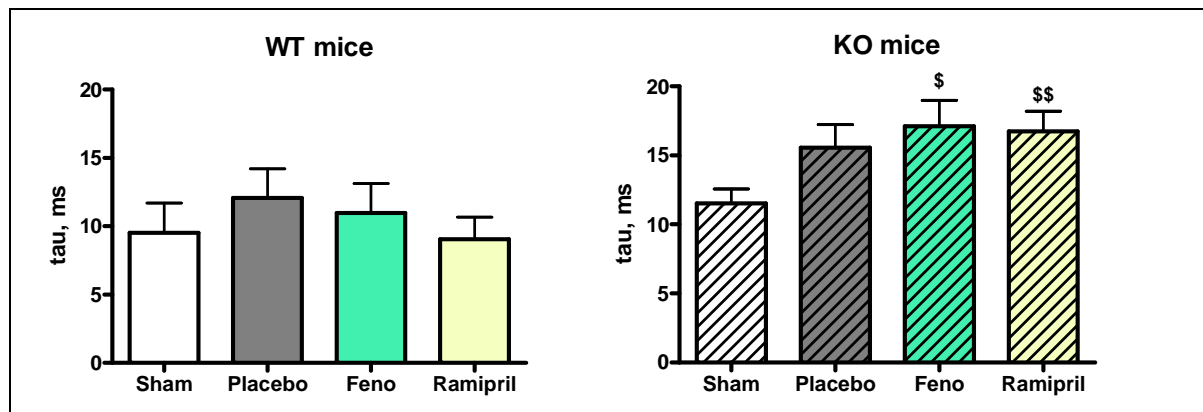


Figure 4.2.9: Left ventricular relaxation constant tau of WT and KO mice after six weeks of treatment; n= 15; mean ± SEM; \$ p<0.05, \$\$ p<0.01 vs respective WT group; unpaired t-test; Note the lacking effect of fenofibrate and Ramipril on KO mice compared to WT mice.

In both WT and KO mice Fenofibrate and Ramipril treated groups were comparable to their respective Placebo groups.

4.2.3 Diuresis in WT and KO mice

- **Baseline diuresis (0-Diuresis)**

Baseline parameters, such as urine volume, urea and Na⁺ / K⁺ quotient, from diuresis analysis were comparable in WT and KO groups (Appendix table 39). However, Protein / Creatinine quotient was significantly increased by 60 % in KO mice compared to their respective WT mice (Figure 4.2.10).

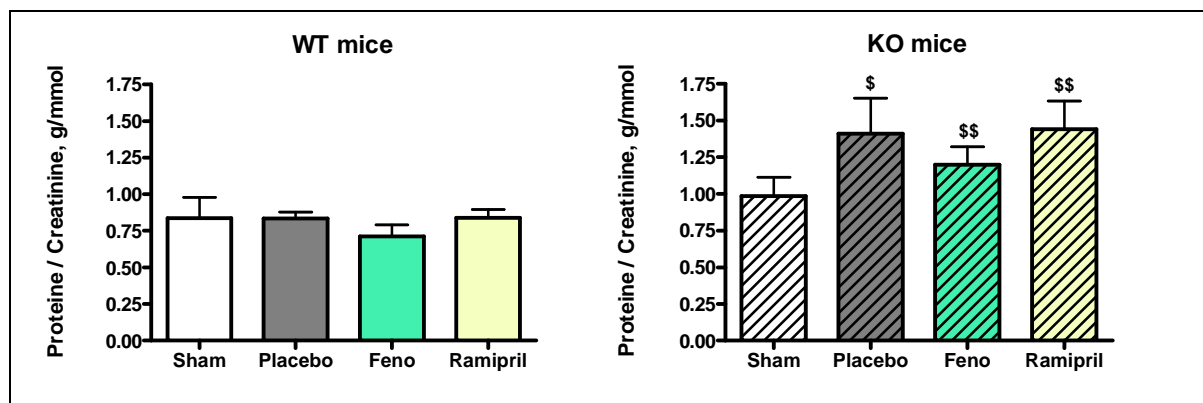


Figure 4.2.10: Proteine / Creatinine ratio of WT and KO mice before surgery; n= 15; mean \pm SEM; ANOVA, followed by Student-Newmann-Keuls post hoc analysis; \$ p<0.05, \$\$ p<0.01 vs respective WT group; unpaired t-test; Note the higher proteine / creatinine ration in KO mice compared to WT mice.

▪ Final diuresis

Urine volume tended to be increased in Placebo WT compared to Sham WT mice by 184 % and significantly increased in Placebo KO compared to Sham KO mice by 433 % (p<0.05) after six weeks of DOCA treatment (Appendix table 40). Urine volume was tendencially further increased in Placebo KO compared to Placebo WT mice (73 %, p>0.05) and significantly increased in Ramipril treated KO compared to Ramipril treated WT mice (88 %, p<0.05).

Urine urea content was significantly decreased by 62 % and by 74 % in Placebo WT and KO mice, respectively, compared to their respective Sham groups (p<0.001) and significantly further decreased in DOCA treated KO compared to DOCA treated WT mice (p<0.001 for Fenofibrate and p<0.05 for Ramipril treated groups).

Urine Na⁺ / K⁺ quotient was significantly increased by 360 % and by 475 % in Placebo WT and KO mice compared to their respective Sham groups (p<0.01) and significantly further increased in KO compared to WT mice (p<0.05 in Sham, Placebo, Fenofibrate and Ramipril treated mice).

Urine protein / creatinine quotients were significantly increased by 106 % in Placebo WT mice and by 340 % in Placebo KO mice compared to their respective Sham groups (both p<0.001) (Figure 4.2.11).

In WT mice, treatment with Fenofibrate resulted in slightly decreased protein / creatinine quotient and treatment with Ramipril in a significant decrease of the quotient (p<0.05) compared to the Placebo group.

In KO mice treatment with Fenofibrate and Ramipril did not significantly influence the protein / creatinine quotient compared to the Placebo group.

However the quotient was significantly increased by 42 % in Placebo KO compared to Placebo WT mice ($p < 0.05$).

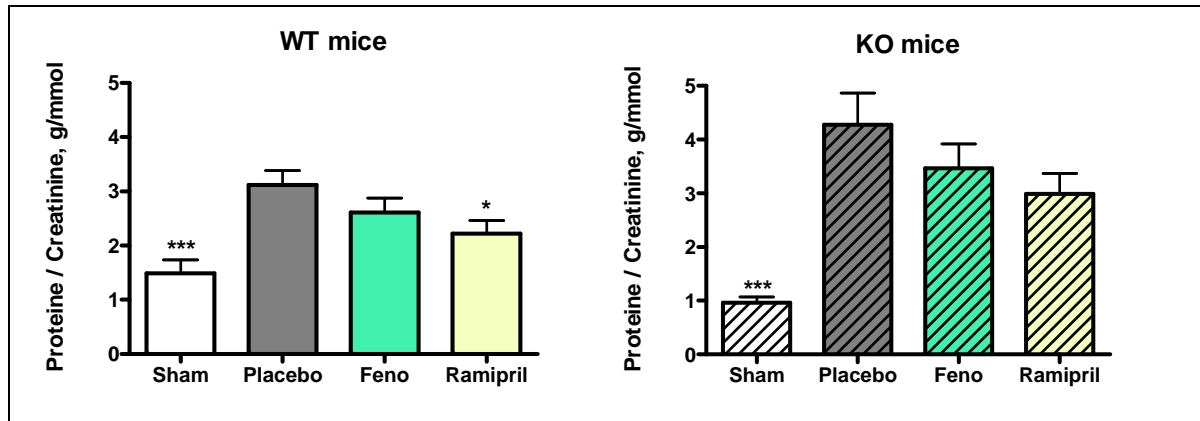


Figure 4.2.11: Proteine / Creatinine ratio of WT and KO mice after five weeks of treatment; n= 15; mean \pm SEM; * $p < 0.05$, *** $p < 0.001$ vs respective Placebo; ANOVA, followed by Student-Newmann-Keuls post hoc analysis

- **Difference between baseline and final diuresis**

Urine volume between baseline and final measurements was significantly 24 fold increased in Placebo WT and 27 fold in Placebo KO mice compared to their respective Sham mice (both $p < 0.05$) (Appendix table 41). Furthermore, this difference tended to be further increased in Placebo KO compared to Placebo WT mice and significantly increased in Ramipril KO compared to Ramipril WT mice (twice as high increase in KO compared to WT Ramipril treated mice, $p < 0.05$). In KO mice, treatment with Ramipril significantly increased this difference compared to Placebo mice ($p < 0.05$).

Urine urea content between baseline and final measurements was in the tendency decreased by 252 % in Placebo KO compared to Sham KO mice and significantly decreased by 453 % in Placebo WT compared to Sham WT mice ($p < 0.001$).

Urine Na^+ / K^+ quotient between baseline and final measurements was significantly increased in Placebo treated WT and KO mice compared to their respective Sham mice ($p < 0.05$ in WT and $p < 0.01$ in KO) and significantly further increased in Placebo

KO compared to Placebo WT mice (doubling of quotient in KO compared to WT mice, $p < 0.05$).

Urine protein / creatinine quotient between baseline and final measurements was 3.3 fold increased in Placebo WT mice and 155 fold in Placebo KO mice compared to their respective Sham (both $p < 0.01$) (Figure 4.2.12).

In WT mice, treatment with Ramipril significantly decreased this difference by 40 % compared to the Placebo group ($p < 0.05$).

In KO mice, treatment with Fenofibrate and Ramipril did not significantly influence this difference compared to the Placebo group.

However the difference was significantly decreased by 98 % in Sham KO compared to Sham WT mice ($p < 0.05$).

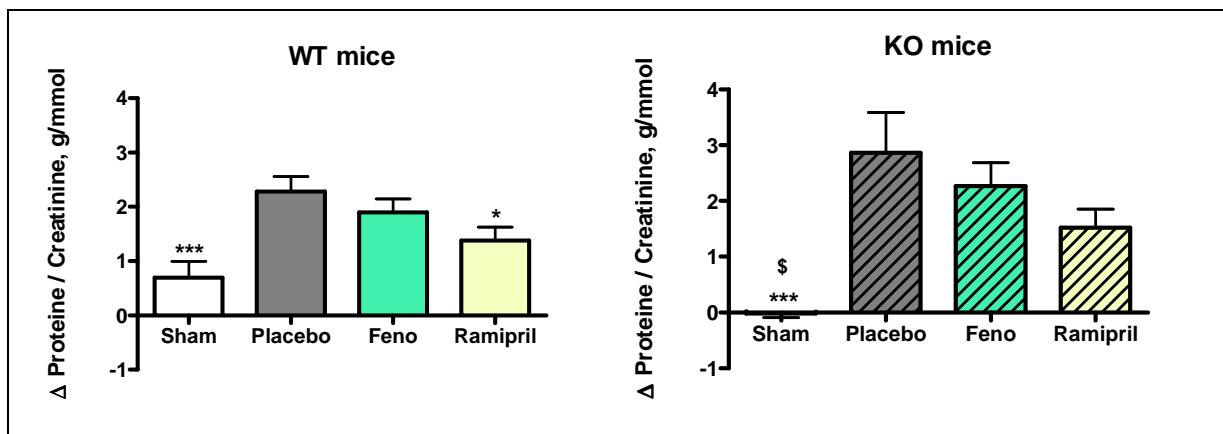


Figure 4.2.12: Delta of Protein / Creatinine ratio of WT and KO mice; $n = 15$; mean \pm SEM; * $p < 0.05$, ** $p < 0.01$, *** $p < 0.001$ vs respective Placebo; ANOVA, followed by Student-Newmann-Keuls post hoc analysis; \$ $p < 0.05$ vs respective WT group; unpaired t-test;

4.2.4 Biomarker analysis / RT-PCR analysis

- Expression of PPAR and PPAR regulated genes

- PPAR

PPAR mRNA expression was not significantly downregulated after nephrectomy and DOCA treatment (Appendix table 42).

- PPAR α regulated genes: Pyruvate dehydrogenase kinase, isozyme-4 (PDK-4)

PDK-4 mRNA expression was decreased in Placebo mice compared to their respective Sham mice ($p < 0.05$ in KO mice) (Figure 4.2.13 and Appendix table 43). However, expression of PDK-4 was lower in PPAR α KO mice compared to their respective WT mice ($p < 0.05$ in Placebo mice).

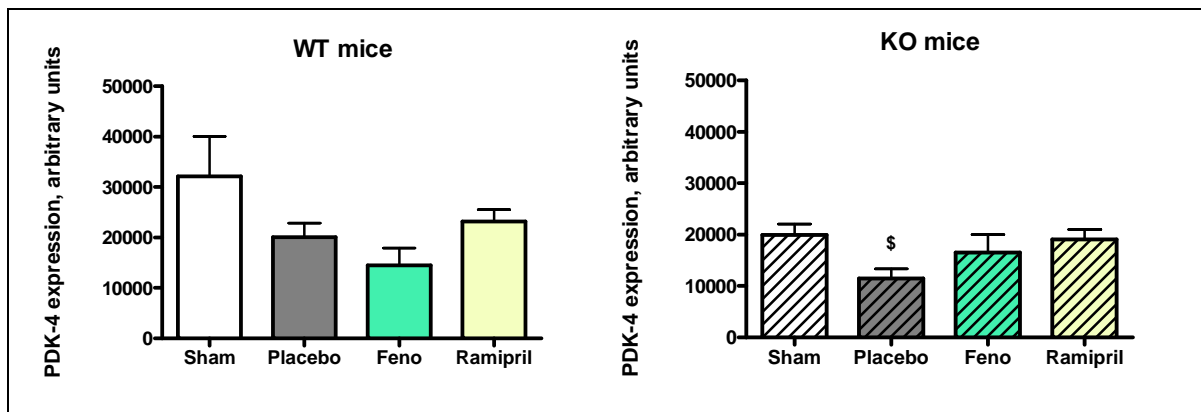


Figure 4.2.13: PDK-4 mRNA expression of WT and KO mice after six weeks of treatment; $n = 15$; mean \pm SEM; ^{\$} $p < 0.05$ vs respective WT group; unpaired t-test;

Treatment with Fenofibrate or Ramipril had no effect on the expression of PDK-4 in both WT and KO mice.

▪ Markers of hypertrophy

As markers of hypertrophy, expression of atrial natriuretic peptide (ANP) and myosin heavy chain- β (MyHC β) were analyzed.

- Atrial natriuretic peptide (ANP)

DOCA treatment of mice resulted in a significant increase of ANP mRNA expression levels in Placebo WT and KO mice compared to their respective Sham groups ($p < 0.01$ in WT and $p < 0.05$ in KO) (Figure 4.2.14 and Appendix table 44). Although ANP mRNA expression was comparable in Sham WT and KO groups, increase was

more displayed in DOCA treated KO as in WT mice (3 fold in Placebo WT and 4.3 fold in Placebo KO mice).

In WT mice, treatment with Fenofibrate and Ramipril tendentially decreased ANP mRNA expression levels by 26 and 30 % compared to Placebo mice, respectively. In KO mice, ANP mRNA expression levels were similar in Placebo and Fenofibrate treated groups, but tendentially decreased by 41 % after treatment with Ramipril compared to Placebo mice.

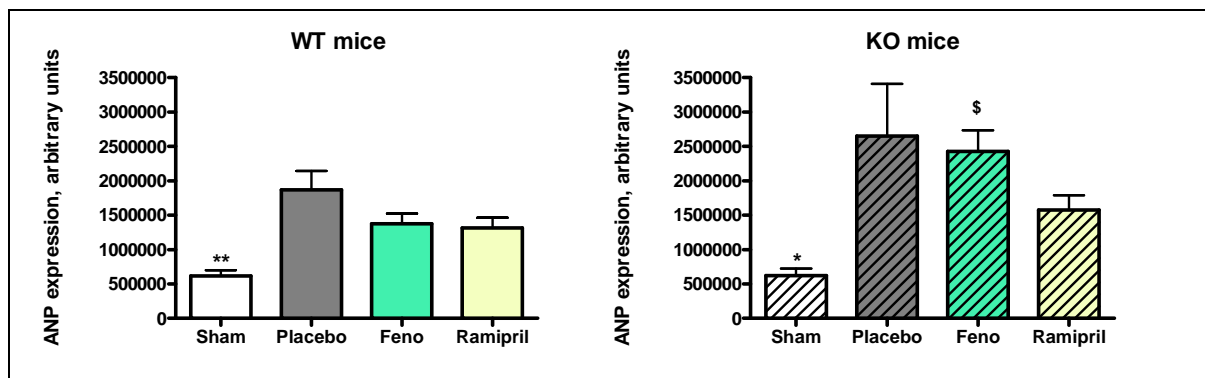


Figure 4.2.14: ANP mRNA expression of WT and KO mice after six weeks of treatment; n= 15; mean \pm SEM; * p<0.05, ** p<0.01 vs respective Placebo; ANOVA, followed by Student-Newmann-Keuls post hoc analysis; \$ p<0.05 vs respective WT group; unpaired t-test; Note the lack of effect of fenofibrate on the ANP mRNA expression in KO mice.

o Myosin heavy chain- (MyHC)

Levels of MyHC mRNA expression were almost three times as high in Sham KO as in Sham WT mice (p<0.05) and almost 1.6 times as high in Placebo KO as in Placebo WT mice (Figure 4.2.15 and Appendix table 45).

DOCA treatment of mice resulted in a significant 3.3 fold increase of MyHC mRNA expression levels in Placebo compared to Sham WT mice (p<0.05) and in a tendencial increase by 1.8 fold in Placebo KO compared to Sham KO mice.

In WT mice, treatment with Fenofibrate tendentially decreased MyHC mRNA expression levels by 30 % compared to Placebo mice.

In KO mice, no significant differences of MyHC mRNA expression levels were observed after treatment with Fenofibrate or Ramipril compared to Placebo mice.

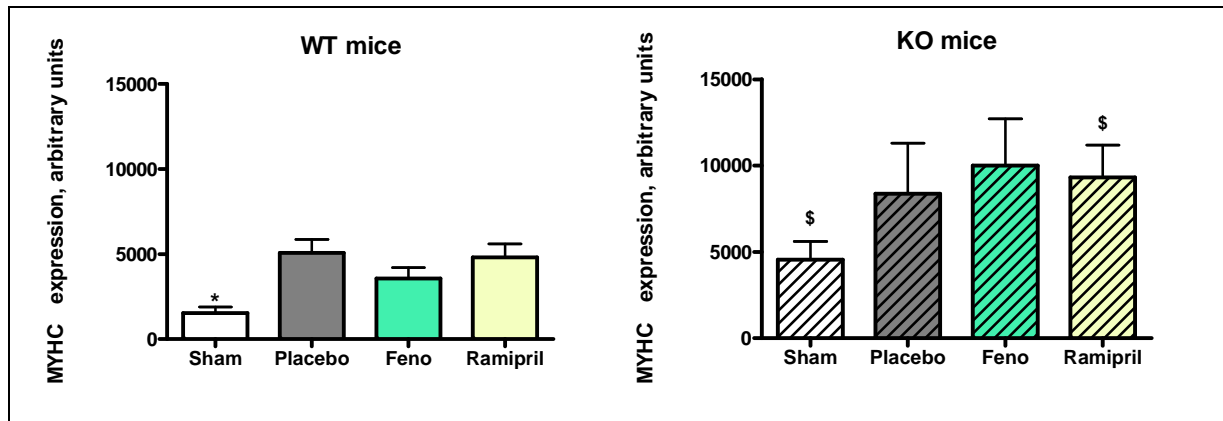


Figure 4.2.15: MyHC mRNA expression of WT and KO mice after six weeks of treatment; n= 15; mean \pm SEM; * $p < 0.05$ vs respective Placebo; ANOVA, followed by Student-Newmann-Keuls post hoc analysis; § $p < 0.05$ vs respective WT group; unpaired t-test; Note the higher expression of MyHC in KO mice compared to WT mice.

▪ Markers of fibrosis and interstitial matrix remodelling

As a marker of fibrosis, collagen 1A1 (COL1A1) was analyzed and as markers of interstitial matrix remodelling, tissue inhibitor of metalloproteinase 1 (TIMP1) and osteopontin were analyzed.

○ Collagen 1A1 (COL1A1)

No significant differences of collagen mRNA expression were seen between groups of WT and KO mice (Appendix table 46).

○ Tissue inhibitor of metalloproteinase 1 (TIMP1)

DOCA treatment of mice resulted in a 2.8 fold increase of TIMP1 mRNA expression levels in Placebo WT compared to Sham WT mice and in a 4.4 fold increase in Placebo KO compared to Sham KO mice (Figure 4.2.16 and Appendix table 47). Although TIMP1 mRNA expression was comparable in Sham WT and KO groups, increase was more displayed in Placebo and Fenofibrate treated KO as in their respective WT groups.

In WT mice, treatment with Fenofibrate and Ramipril tend to decrease TIMP1 mRNA expression levels by 18 and 33 %, respectively, compared to Placebo mice.

In KO mice, TIMP1 mRNA expression levels were similar in Placebo and Fenofibrate treated groups, but tendentially decreased by 64 % after treatment with Ramipril compared to Placebo mice.

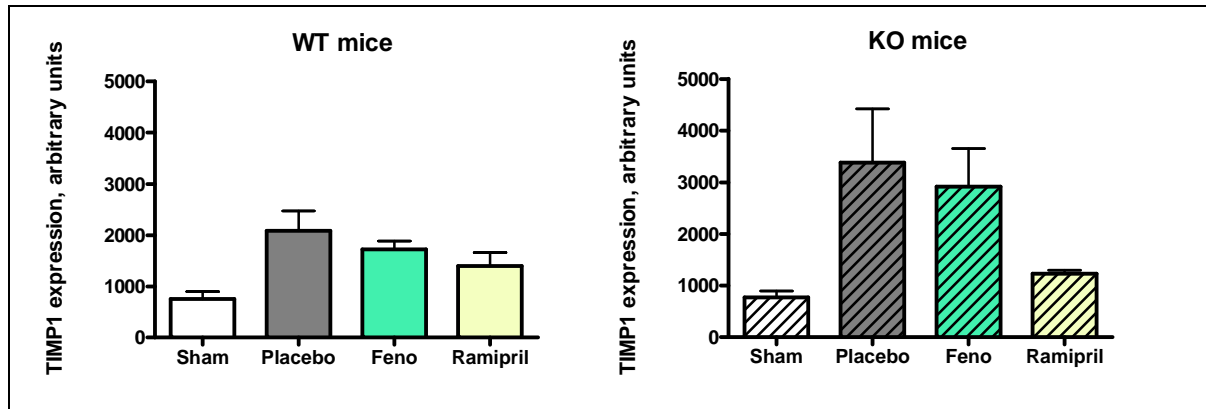


Figure 4.2.16: TIMP1 mRNA expression of WT and KO mice after six weeks of treatment; n= 15; mean \pm SEM; * $p < 0.05$ vs respective Placebo; ANOVA, followed by Student-Newmann-Keuls post hoc analysis

- Osteopontin

DOCA treatment of mice resulted in a 3 and 9 fold increase of osteopontin mRNA expression levels in Placebo compared to Sham groups in WT and KO mice, respectively (Figure 4.2.17 and Appendix table 48). Although OPN mRNA expression was comparable in Sham WT and KO groups, increase was more displayed in Placebo and Fenofibrate treated KO as in their respective WT groups.

In WT mice, treatment with Fenofibrate and Ramipril tendend to decrease OPN mRNA expression levels by 39 and 49 %, respectively, compared to Placebo mice. In KO mice, OPN mRNA expression levels were similar in Placebo and Fenofibrate treated groups, but tendend to decrease by 74 % after treatment with Ramipril compared to Placebo mice.

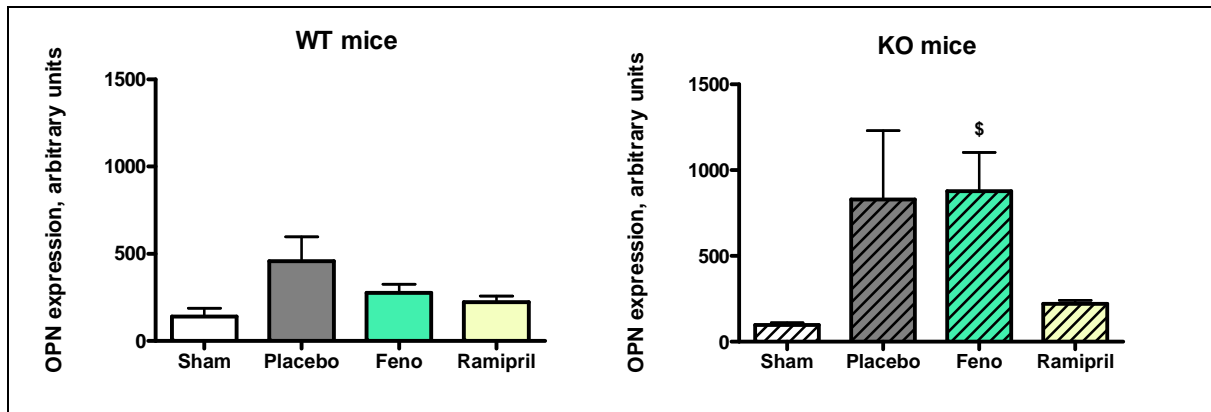


Figure 4.2.17: Osteopontin mRNA expression of WT and KO mice after six weeks of treatment; n= 15; mean \pm SEM; ^{\$} p<0.05 vs respective WT group; unpaired t-test;

4.2.5 Blood analysis

▪ Triglycerides

Triglycerides levels were comparable in Sham and Placebo groups (Figure 4.2.18 and Appendix table 49).

DOCA treatment of mice resulted in an increase by 40 and 49 % of triglyceride levels in Placebo WT and KO groups compared to their respective Sham groups.

In WT mice, Placebo and Ramipril treated groups had comparable triglyceride levels, but treatment with Fenofibrate tendentially decreased triglyceride levels by 22 % compared to Placebo mice.

In KO mice, Placebo, Fenofibrate and Ramipril treated groups had comparable triglyceride levels.

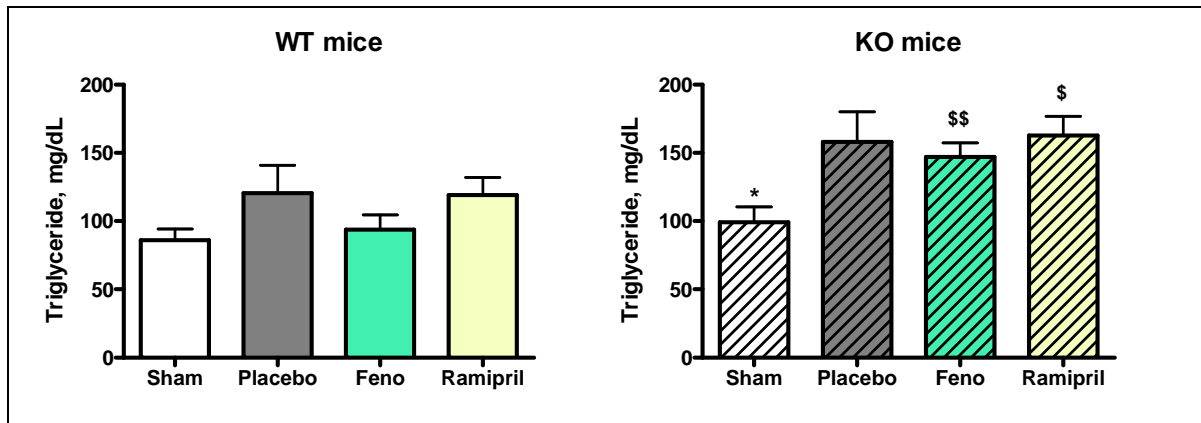


Figure 4.2.18: Plasma triglycerides levels of WT and KO mice after six weeks of treatment; n= 15; mean \pm SEM; * $p < 0.05$ vs respective Placebo; ANOVA, followed by Student-Newmann-Keuls post hoc analysis; \$ $p < 0.05$, \$\$ $p < 0.01$ vs respective WT group; unpaired t-test; Note the higher triglycerides plasma levels in KO mice compared to WT mice.

- **Total cholesterol**

Total cholesterol levels were 23 % higher in Sham KO compared to Sham WT mice ($p < 0.001$ in unpaired t-test) (Figure 4.2.19 and Appendix table 50). Similarly, Placebo KO mice had tendentially higher levels of cholesterol compared to Placebo WT mice (+ 47 %).

Furthermore, a significant increase of the total cholesterol levels by 75 % in Placebo WT mice and by 109 % in Placebo KO mice compared to their respective Sham groups was seen after six weeks of DOCA treatment ($p < 0.01$).

In WT mice, total cholesterol levels were comparable in Placebo, Fenofibrate and Ramipril treated groups.

In KO mice, no significant differences in cholesterol levels were seen in all treated groups, but cholesterol levels were about 42 % higher compared to WT mice.

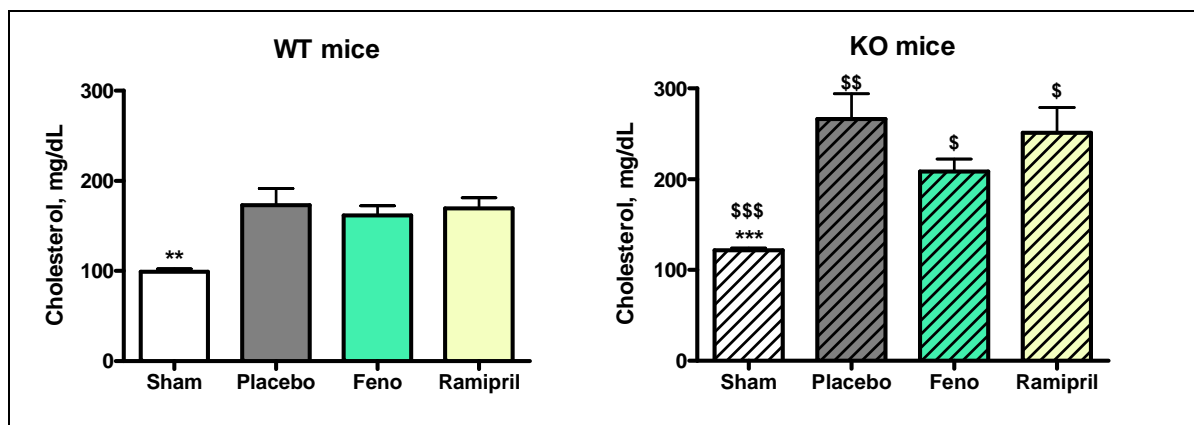


Figure 4.2.19: Plasma total cholesterol levels of WT and KO mice after six weeks of treatment; n= 15; mean \pm SEM; ** p<0.01, *** p<0.001 vs respective Placebo; ANOVA, followed by Student-Newmann-Keuls post hoc analysis; \$ p<0.05, \$\$ p<0.01, \$\$\$ p<0.001 vs respective WT group; unpaired t-test;

Note the higher cholesterol plasma levels in KO mice compared to WT mice.

▪ HDL cholesterol

High density lipoprotein cholesterol levels were significantly higher in Sham KO compared to Sham WT mice (16 %, p<0.01) and significantly increased by 28 % in Placebo KO mice compared to Placebo WT mice (Figure 4.2.20 and Appendix table 51).

DOCA treatment of mice resulted in a significant increase of HDL cholesterol levels by 78 % in Placebo WT mice and by 96 % in Placebo KO mice compared to their respective Sham groups (p<0.001 in WT and p<0.01 in KO).

In WT and KO mice, no significant differences of HDL levels were seen in DOCA treated groups after six weeks, but HDL levels were about 41 % higher in KO compared to WT groups.

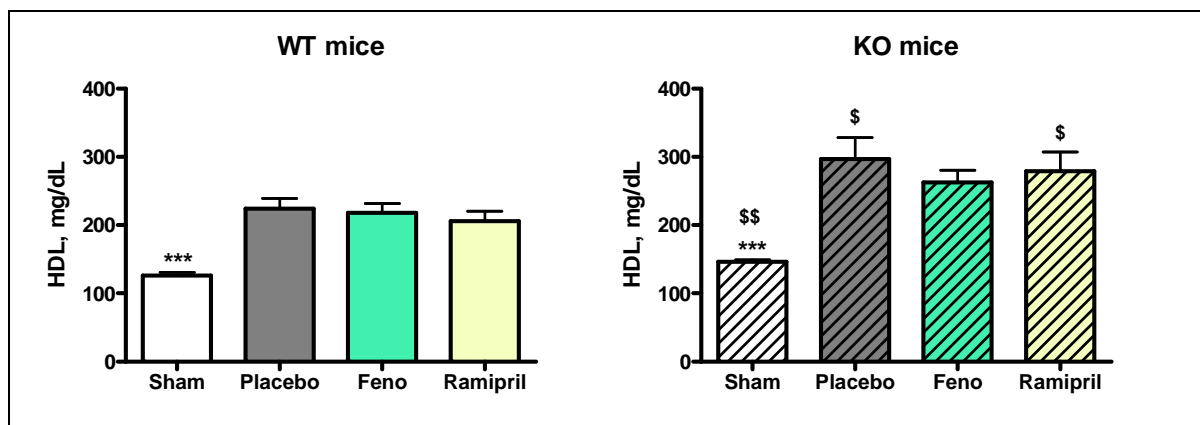


Figure 4.2.20: Plasma HDL cholesterol levels of WT and KO mice after six weeks of treatment; n= 15; mean \pm SEM; *** p<0.001 vs respective Placebo; ANOVA, followed by Student-Newmann-Keuls post hoc analysis; \$ p<0.05, \$\$ p<0.01 vs respective WT group; unpaired t-test; Note the higher HDL plasma levels in KO mice compared to WT mice.

- **LDL cholesterol**

Low density lipoprotein cholesterol levels were significantly higher in KO mice compared to WT mice (133 %, p<0.001 in Sham and 78 %, p<0.05 in Placebo) (Figure 4.2.21 and Appendix table 52).

In WT and KO mice, a significant increase of LDL cholesterol levels by 800 % in Placebo WT mice and by 586 % in Placebo KO mice compared to their respective Sham groups (p<0.001) was observed after six weeks of DOCA treatment.

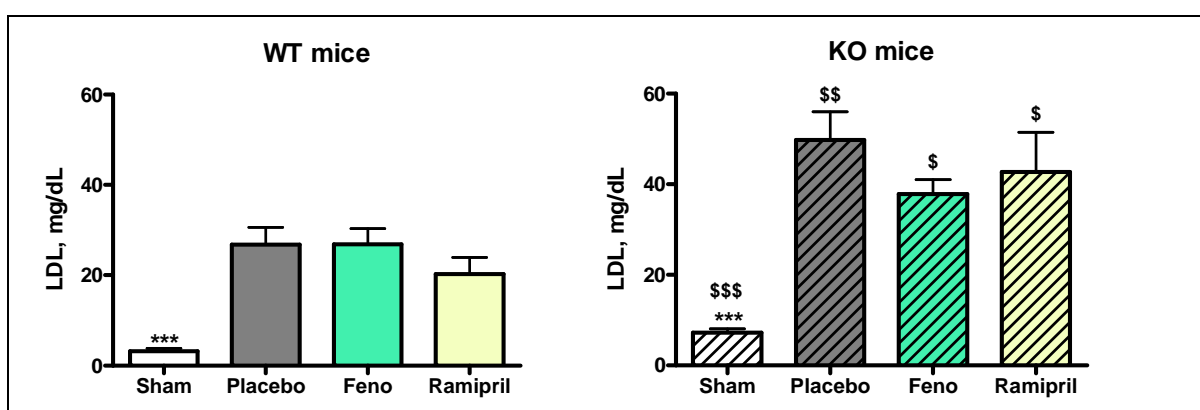


Figure 4.2.21: Plasma LDL cholesterol levels of WT and KO mice after six weeks of treatment; n= 15; mean \pm SEM; ** p<0.01, *** p<0.001 vs respective Placebo; ANOVA, followed by Student-Newmann-Keuls post hoc analysis; \$ p<0.05, \$\$ p<0.01, \$\$\$ p<0.001 vs respective WT group; unpaired t-test;

Note the higher LDL plasma levels in KO mice compared to WT mice.

In WT and KO mice, no significant differences of LDL levels were seen in DOCA treated groups after six weeks, but LDL levels in KO groups were about 86 % higher compared to WT groups.

5. Discussion

The present study demonstrates that PPAR α plays a critical role in the development of myocardial remodelling related to heart failure. Comparing PPAR α knock-out (KO) and wild type (WT) mice, the experiments show that the lack of PPAR α accelerates heart failure development and, using fenofibrate, that activation of PPAR α ameliorates heart failure through modifying morphology, haemodynamics and biomarkers. Altogether, these data suggest that a PPAR α agonist may be a new therapeutic option for the treatment or prevention of heart failure.

In the majority of cases, heart failure is triggered by an initial ischaemic event, the myocardial infarction or, in 30 % of cases, by long time hypertension. To characterize the PPAR α effects in ischaemia induced heart failure, the chronic myocardial infarction (cMI) mouse model was used. To mimic the pathophysiological changes in hypertension induced heart failure the DOCA salt mouse model was used.

The cMI rat model resembles the pathophysiological changes of remodelling and cardiac dysfunction seen in patients with ischaemia induced heart failure (Pfeffer et al. 1979, Halapas et al. 2008). The cMI rats develop myocardial hypertrophy, inflammation and fibrosis resulting in left ventricular systolic and diastolic dysfunction with reduced contractility and increased left ventricular enddiastolic pressure. Similar effects are seen in the mouse cMI model (Lutgens et al. 1999).

In the DOCA model hypertension is induced by nephrectomy of one kidney, administration of the aldosterone agonist DOCA and feeding of animals with a high salt diet (Friedman et al. 1948, Halapas et al. 2008). DOCA treated rats and mice develop pronounced heart and kidney damage with increased heart hypertrophy and fibrosis, and kidney dysfunction (Kim et al. 1997). The development of morphological changes in the heart is much more pronounced than the haemodynamic ones which are mainly limited to an increase of blood pressure. These effects are due to the stimulation of mineralocorticoid receptors by DOCA, giving rise to a hyperaldosteronism-like phenotype. This induces constriction of the peripheral vessels, Na⁺ reabsorption in the nephron and passive water retention. Those changes lead to volume increase in blood vessels followed by pressure overload in the heart and responsive hypertrophic growth of the myocytes in order to preserve

cardiac output after activation of the renin-angiotension-aldosterone system among others (Mann et al. 2005, Francis 2001, Cohn et al. 2000).

Both the cMI and the DOCA models have been used to evaluate the protective effects of PPAR expression levels and activities on ischaemia and hypertension induced heart failure.

5.1 Heart failure in PPAR WT and KO mice

The effects of physiological levels of PPAR expression and activity on the development of heart failure were investigated in WT mice by the comparison of placebo vs. sham groups.

Effects of an abolished PPAR activity in heart failure were evaluated in PPAR KO mice, which are characterized by an insertion of a nonsense mutation in the ligand binding domain of the PPAR gene, resulting in a non-functional protein (Lee et al. 1995).

Survival of WT mice was twice as high as of KO mice after cMI induction, suggesting that KO mice are more sensitive to an ischaemic event by a permanent ligation of the LAD especially during the first week after surgery. The absence of PPAR activity seems to render these mice more susceptible to tissue injury. This increased vulnerability of hearts of KO mice was also seen in the morphological and functional changes induced by heart failure. These data are in agreement with literary findings showing an increased mortality after transverse aortic constriction in PPAR KO compared to WT mice (Smeets et al. 2008).

Hypertrophy of the left ventricle, as reflected by an increase of the relative left ventricular weight, occurred in cMI and DOCA models (see 4.1.1 and 4.2.1). Pathological hypertrophy was due to the remodelling processes in the ventricle. Remodelling was accompanied by an increase of the expression of ANP and MyHC, which are markers for hypertrophy, and of Collagen 1A1 and TIMP1 which are markers for fibrosis and interstitial matrix remodelling in WT and KO placebo mice (see 4.1.3 and 4.2.4). The lack of a significant increase of collagen mRNA expression

levels, can be explained by the rapid turnover of collagen mRNA. Indeed, Chapman et al. (1990) demonstrated that mRNA expression of collagen I and III was increased three days after abdominal aortic banding (pressure overload), but that levels after eight weeks almost returned to control levels.

It is known from previous publications that myocardial infarction leads to a shift of the adult gene expression profile towards a foetal expression pattern, with increased ANP and MyHC mRNA expression levels (Ritter et al. 2003, Swynghedauw et al. 1999), as well as increased fibrosis and extra cellular matrix regulating gene expression such as collagen type I and TIMP1 (Thomas et al. 1998, Cleutjens et al. 1995). Additionally, our results, regarding hypertrophy of the left ventricle and expression of ANP, MyHC and TIMP1, are also in agreement with changes which are well known in DOCA models.

Furthermore, DOCA treatment induced hypertrophic growth of the left ventricle and an increase of relative lung weight in our study. The increase of peripheral organ weight is induced by congestion of the peripheral blood in DOCA induced hypertension. There are hints that the development of hypertrophy and remodelling might, at least partially, be due to an interaction between PPAR and the renin-angiotensin-aldosterone-system. It is well known that the renin-angiotensin-aldosterone-system is activated by pressure overload. Myocardial ACE expression is increased in hypertrophied ventricles and results in increased Angiotensin II levels (Schunkert et al. 1990). Angiotensin II induces fibrosis of the right and left ventricles after pressure overload (Sun et al. 1997, Young et al. 1995, Robert et al. 1995, Brilla et al. 1990) probably by inducing endothelin 1 (Wollert et al. 1999). The interaction between the ACE system and PPAR activity will be more fully discussed later.

Although hypertrophy and remodelling processes are seen in WT and KO mice in heart failure models, there are marked differences between the extent of remodelling occurring in these mice.

Although sham WT and KO mice showed comparable relative heart weights, mRNA expression levels of MyHC, collagen 1A1 and TIMP1 were higher in sham KO compared to sham WT mice in both models. Additionally, although the morphological

changes were similar in both placebo WT and KO mice at the end of the studies, mRNA expression levels of hypertrophy and fibrosis markers were much more pronounced in placebo KO as in WT mice (see 4.1.3 and 4.2.4). Similar findings are reported by Smeets et al. (2008) in PPAR KO mice with transverse aortic constriction. PPAR KO mice subjected to aortic constriction showed higher mRNA expression levels of e.g., ANP and collagen 1 when compared to WT mice. Additionally, osteopontin, an important marker for interstitial matrix remodelling, was noticeably increased in placebo WT and KO mice. But the increase of osteopontin mRNA expression levels between placebo and sham mice was much higher in KO compared to WT mice (18 and 8 fold in KO mice vs. 3 fold in WT mice in the cMI and DOCA studies, respectively). This suggests a more pronounced matrix remodelling in PPAR KO compared to WT mice. These data further document the higher susceptibility of PPAR KO mice towards hypertrophy, fibrosis and interstitial matrix regulation in heart failure and the importance of basal PPAR expression levels for heart protection.

In summary, basal PPAR activity seems to be protective in heart failure and abrogated PPAR activity renders mice more susceptible to heart failure.

Remodelling processes during heart failure resulted in a worsening of cardiac function, which was assessed by haemodynamic measurements in WT and KO mice. The degree of deterioration of cardiac function was tremendously higher in PPAR KO compared to WT mice in both models.

In sham KO mice, haemodynamics, except for diastolic function (LVEDP), were comparable to sham WT mice in the cMI and DOCA models. LVEDP was lower in KO compared to WT mice in both studies. Those changes in LVEDP are consistent with data reported by Loichot et al. (2006) showing that PPAR KO mice had an alteration of cardiac contractile performance (left ventricular fractional shortening measured by echocardiography) under basal conditions without change in blood pressure nor heart rate.

Haemodynamics showed a further deterioration of systolic and diastolic function in KO mice compared to WT mice. In the cMI study, systolic blood pressure and

contractility further decreased, LVEDP and the relaxation time further increased in PPAR KO compared to WT mice. In the DOCA study, haemodynamic changes were not as marked as in the cMI study. One explanation could be the shorter duration of the DOCA study and the lower strength of the stimulus used for the induction of heart failure. It is also known that haemodynamic effects, apart from increased systolic blood pressure, are not always observed after DOCA treatment in rats (Iglarz et al. 2003).

The results of our studies add to several previous publications, showing increased sensitivity to heart failure in PPAR KO compared to WT mice. It has been showed in an ischaemia / reperfusion study, that hearts from PPAR KO mice were more susceptible for myocardial dysfunctions (longer time of recovery and lower developed force) than those from WT mice and that the beneficial effects of fenofibrate treatment were lost in KO mice (Tabernero et al. 2002). Similarly, Yue et al. (2003) demonstrated greater infarct sizes in PPAR KO mice hearts after ischaemia / reperfusion than in WT mice hearts. It also seems that PPAR KO mice had reduced systolic performance in echocardiographic measurements without changes in heart rate and blood pressure (Loichot et al. 2006). Furthermore, isolated perfused hearts from these mice had reduced developed force at basal levels and after β -adrenergic stimulation compared to WT mice and these effects were associated with myocardial fibrosis. Finally, it has been reported that PPAR KO mice had reduced systolic performance without ventricular dilatation in echocardiography and significant cardiomyocyte hypertrophy in histological investigations (Guellich et al. 2007). Markers of oxidative damage were increased in PPAR KO mice hearts. These data indicate that functional PPAR seems to be required to protect and preserves contractile function in cardiac muscle.

5.2 Heart failure under treatment with a PPAR agonist in WT and KO mice

Our next step was to evaluate the effects of activation of PPAR by a PPAR agonist, fenofibrate, on heart failure.

Enhancement of PPAR activity was determined by treatment of WT and KO mice with fenofibrate. Increased PPAR activity might have beneficial effects in heart failure by amelioration of energy supply for the myocardium and / or reduction of heart remodelling and improvement of function (Finck 2007 and Schiffrin 2005).

Increase of PPAR activity levels by fenofibrate induced an almost two fold increase of the liver weight (see 4.1.1 and 4.1.2) in WT but not in KO mice. This is due to peroxisome proliferation with hepatocellular hypertrophy and hyperplasia with final hepatomegaly, a known effect of PPAR agonists in rodents, but not in humans (Kliwer et al. 2001).

Treatment with fenofibrate decreased relative left ventricular and heart weight in WT but not in KO mice in cMI and DOCA models. This decrease of the cardiac hypertrophy was closely connected to a significant decrease of expression levels of hypertrophy markers, ANP and MyHC in WT mice.

Effects of fenofibrate on pressure overload induced hypertrophy are controversial. Iglarz et al. (2003) and Ogata et al. (2004) did not report any improvement of relative left ventricular weight after fenofibrate treatment in DOCA rats, whereas Lebrasseur et al. (2007), Irukayama-Tomobe et al. (2004), Rose et al. (2007) and Li et al. (2008) showed significant improvement of relative left ventricular weight after treatment with fenofibrate in mice with aldosterone induced hypertension, rats with aortic banding or spontaneous hypertensive rats (SHR), respectively. In parallel to the prevention of heart hypertrophy by fenofibrate, Lebrasseur et al. (2007) also showed improved MyHC mRNA expression levels after treatment with a PPAR agonist.

In contrast, effects of a PPAR agonist on cardiac remodelling after ischaemia-induced heart failure has not yet been published, having first been evaluated in this study.

Fibrosis gene expression levels, such as collagen 1A1 and TIMP-1 were improved in WT mice by treatment with the PPAR agonist, although this effect was not as marked in the DOCA study as in the cMI study. This is in agreement with data from Ogata et al. (2002, 2004), who showed a decrease of fibrosis after treatment with fenofibrate in pressure overloaded rats.

Furthermore, the PPAR agonist improved mRNA expression levels of osteopontin, a marker of interstitial matrix remodelling, in cMI WT mice. It has been reported that osteopontin expression is increased in the heart during hypertrophy and heart failure in a banding study with mice (Xie et al. 2004). It has also been showed that treatment of macrophages with fibrates inhibited osteopontin expression through negative cross-talk with AP-1 dependent trans-activation of the osteopontin promoter (Nakamachi et al. 2007). Finally, the down regulation of osteopontin expression after treatment with fenofibrate in Dahl-salt sensitive rats has been reported (Ichihara et al. 2006).

Our data provide evidence that treatment with a PPAR agonist has antihypertrophic and antifibrotic effects and modulates the interstitial matrix in WT mice in ischaemia and hypertension induced heart failure.

Remodelling processes during heart failure resulted in a worsening of cardiac function, which was assessed by haemodynamic measurements in WT and KO mice. Whereas increase of PPAR activity by fenofibrate resulted in an improvement of cardiac function and amelioration of hypertrophy and fibrosis.

In the cMI study, treatment with the PPAR agonist tended to improve LVEDP and the relaxation constant tau and significantly improved contractility. No effects were observed in KO mice.

From literary sources it is known that PPAR agonists improve myocardial contractile dysfunction after ischaemia / reperfusion in WT mice, and that those effects are abolished in PPAR KO mice (Yue et al. 2003, Tabernero et al. 2002). Li et al. (2008) and Ogata et al. (2004) showed improved diastolic functions in pressure overload induced heart failure models after treatment with fenofibrate. Our data provides evidence that cardiac dysfunction can also be improved by treatment with fenofibrate in ischaemia induced heart failure.

In the DOCA study, haemodynamic parameters were not as deteriorated as seen in the cMI study and no improvement with fenofibrate was detected. As already discussed, the study duration might have been too short to show the effects of PPAR agonists on haemodynamics or the concentration of the compounds was too

low, as suggested by the lack of PDK4 gene induction in the myocardium, to have had a sufficient effect.

Furthermore, DOCA treatment induces an increase of systolic blood pressure in rats, an effect also observed in WT and KO mice. Treatment with fenofibrate did not improve blood pressure. This is in agreement with studies performed in DOCA treated rats by Iglarz et al. (2003) or Aldosterone treated mice by Lebrasseur et al. (2007). In contrast, Zhou et al. (2008) reported that treatment of WT mice with DOCA salt induced hypertension with clofibrate, a PPAR α agonist, could significantly reduce mean arterial blood pressure by increasing expression of 20-hydroxyeicostetraenoic acid (20-HETE). These data suggest that mechanistical differences between various fibrates and their in vivo activity exist.

In summary, abrogation of PPAR α activity renders mice much more susceptible towards hypertrophy, fibrosis and inflammation and boosts deterioration of heart function in hypertension and ischaemia induced heart failure. Basal PPAR α activity can attenuate heart failure and increase of PPAR α activity back to normal levels seems to further improve the protection of the heart.

5.3 Cardiorenal syndrome

Heart failure is often associated with kidney dysfunction, called the cardiorenal syndrome. The cardiorenal syndrome is associated with a high mortality (Heywood 2004). The glomerular filtration rate of heart failure patients is an important determinant of survival (Dries et al. 2000). Furthermore, an increase in serum creatinine levels is a very specific marker for poor prognosis (Smith et al. 2003, Gottlieb et al. 2002).

The causes of heart failure associated renal insufficiency are diverse. Decreased renal perfusion, as induced by hypovolemia, vasoconstriction or hypotension (low cardiac output), but also high central venous pressure are important factors for renal dysfunction (Firth et al. 1988) resulting in inflammatory and remodelling processes. The simultaneous protection of heart and kidney would, therefore, be beneficial in heart failure patients.

In the DOCA study we evaluated the effects of PPAR α expression levels on kidney protection. Urine volumes were comparable within sham WT and KO mice, showing comparable renal functions in these animals. However, the protein / creatinine ratio was increased in KO as compared to WT mice. This might be an early indication that basal PPAR α activity is needed for normal kidney function even without the challenge of heart failure induction.

Nephrectomy of one kidney in the DOCA model induced a successive hypertrophy of the remaining right kidney in WT and KO mice. This is in agreement with literary sources (Hayslett 1979). At the end of the DOCA study, diuresis of placebo WT and KO mice resulted in increased urine volumes, protein / creatinine ratios, Na⁺ / K⁺ ratios and decreased urea concentration in the urine of mice compared to their respective sham groups. These effects are in accordance with well established data in DOCA studies in rats (Newaz et al. 2005, Matsumura et al. 1999, Stumpe et al. 1970).

But, similarly to the heart failure data, KO mice showed enhanced deterioration of kidney function: urine volumes, protein / creatinine ratios and Na⁺ / K⁺ ratios were much more pronounced and urea further decreased in KO compared to WT mice. This is in agreement with a study by Newaz et al. (2005) which showed a higher increase of urine protein content in PPAR α KO compared to WT mice after DOCA treatment. Additionally, Park et al. (2006) reported that PPAR α KO mice had more severe diabetic nephropathy compared to WT mice.

In summary, PPAR α activity is not only important for the protection of the heart, but also for kidney function in ischaemia and hypertension induced heart failure.

5.4 Mechanisms for the protective effects of PPAR α activity

There are several possible explanations for the shades of protective effects by different PPAR α activity levels. One explanation is based on the protective role of PPAR α in cardiac remodelling, independently from lipid modulation and fuel utilization in the heart.

PPAR α has an important function in cardiac remodelling by direct modulation of interstitial matrix remodelling, fibrosis and hypertrophy through the activation or inhibition of different genes or signalling pathways, like Activator protein-1, Endothelin-1, ACE or the NF- κ B pathways (Newaz et al. 2005, Ogata et al. 2004 and 2002, Iglarz et al. 2003). This was also shown in our studies by the modulation of genes involved in hypertrophy, like MyHC- β or matrix remodelling, like TIMP-1 and osteopontin.

One example for the interaction of PPAR α with pathways involved in hypertrophy and fibrosis is the interplay of PPAR α with the renin-angiotensin-aldosterone system.

In the cMI and DOCA studies, treatment of WT mice with fenofibrate resulted in comparable or even better protection from hypertrophy and fibrosis as well as improvement of cardiac functions than the treatment with the ACE inhibitor ramipril. Surprisingly, ramipril could not protect the heart from hypertrophy, fibrosis and deterioration of haemodynamic function in cMI KO mice. Only the reduction of blood pressure was still observed. These data suggest that the beneficial effects of ACE inhibitors, which are recommended by the European Society of Cardiology in the standard therapy of heart failure patients (ESC guidelines 2008), depend at least partially on PPAR α activity in ischaemia induced heart failure. Restoration of PPAR α activity in heart failure patients might, therefore, even improve ACE inhibitor related protection of hearts from further deterioration in patients.

The interaction between PPAR α and ACE inhibitors has also been described in literature. It has been shown that enalapril upregulates the PPAR α expression in mice with angiotensin II induced atherosclerosis, resulting in anti-inflammatory effects (downregulation of NF- κ B, ICAM-1, VCAM-1) (Da Cunha et al. 2005).

It has also been reported that overexpression of angiotensinogen in the myocardium induces the down regulation of PPAR α activity, resulting in a reduction of the fatty acid oxidation pathway in mice (Pellieux et al. 2006). Additionally, the PPAR response element has been identified in the renin gene of spontaneous hypertensive rats (Di Nicolantonio et al. 1998).

The interaction between PPAR α and the renin-angiotensin-aldosterone pathway is only one example of several pathways which might be involved in protection from failure development by PPAR α .

A further explanation for the protective effects by PPAR is based on the energy status and the energy utilization of the heart during heart failure. The healthy myocardium obtains 60-90 % of its energy from fatty acid oxidation (FAO) (Huss et al. 2004). Inherited defects in many key enzymes of FAO are associated with cardiomyopathy and sudden death in children and young adults (Kelly et al. 1994) and cardiac hypertrophy and failure are accompanied by a switch from fatty acids to glucose utilization and PPAR down regulation (Finck 2007). PPAR is highly expressed in tissues with elevated capacity for FAO, like liver, kidney and heart, and it is an important transcriptional regulator of myocardial energy and lipid homeostasis, through modulation of key enzymes of the FAO pathway such as medium chain acetyl coenzyme A dehydrogenase (MCAD) or carnitin palmitoyl transferase-1 (CPT-1) (Finck, 2007 and Schiffrin, 2005). The absence of PPAR activity results in a complete change of the fuel utilization and energy supply in the heart.

PPAR KO mice have decreased basal levels of enzymes involved in fatty acids oxidation, like carnitine palmitoyl transferase-1 (CPT-1) or medium chain acyl-coenzyme A dehydrogenase (MCAD) (Aoyama et al. 1998). This was also confirmed in our studies. Indeed expression of pyruvate dehydrogenase kinase, isozyme 4 (PDK4) was reduced (see 4.1.3 and 4.2.4) in KO compared to WT mice in the DOCA and cMI experimental settings. Furthermore KO mice had similar plasma levels of triglycerides, but increased plasma levels of total cholesterol, HDL and LDL compared to WT mice. Those increased lipid plasma levels are due to decreased expression of fatty acids-oxidation related genes because of the lack of PPAR activity and an accumulation of lipids (Ahmed et al. 2007, Francis et al. 2002, Peters et al. 1997).

Several reports indicate that the capacity of PPAR KO mice for constitutive myocardial oxidation is markedly reduced compared to WT mice and their mRNA expression levels of fatty acid transporters are decreased (Watanabe et al. 2000). At last, myocardium of PPAR KO mice had decreased ATP concentration after exposure to stress (starvation and high temperature).

It has also been demonstrated that cardiac PPAR gene expression falls and its activity is altered at the posttranscriptional level via the extracellular signal-regulated kinase mitogen-activated protein kinase pathway during hypertrophic growth, and that the decrease in PPAR activity was followed by a decrease in muscle carnitin palmitoyl transferase-1 (mCPT-1) (Barger et al. 2000).

It seems that an energy profile with decreased fatty acid and increased glucose utilization in isolated hearts of PPAR KO mice is sufficient for sustaining normal energy metabolism and contractile function at baseline but that the metabolic reserve is depleted at high workload, which induces functional deterioration (Luptak et al. 2005). Similarly, it has been showed that glucose oxidation rates are significantly higher and FAO significantly lower in PPAR KO mice compared to WT mice during pre- and postischaemic perfusions (Sambandam et al. (2006). Additionally, Gélinas et al. (2008) demonstrated an impaired capacity to withstand a rise in preload, in isolated working hearts from PPAR KO mice, because of a restricted reserve to enhance glycolysis when the energy demand is increased.

All together these data suggest that the lack of PPAR results in decreased FAO in the heart and deteriorated heart function. Restoring PPAR activity should therefore be beneficial in cardiac energy supply and function.

However, effects of PPAR agonist on the energy supply of the heart are controversial.

On the one hand it has been reported that reactivation of PPAR in early stages of heart failure development could be deleterious by accumulating lipids in the myocardium and worsening cardiac dysfunction. Some data showed that reactivation of PPAR with a PPAR agonist, results in severe depression of cardiac power and efficiency in the hypertrophied heart because of the prevention of substrate switching in an aortic banding study in rats (Young et al. 2001). To maintain its contractile function, the hypertrophied heart decreases its reliance on fatty acids as a major substrate for ATP generation while increasing its reliance on glucose as a fuel, mainly through regulation of PPAR. However, this study only lasted one week and the long term down regulation of PPAR and FAO may contribute to energy starvation (lower ATP production through Glucose oxidation) of the myocardium and cardiac lipotoxicity (storage of lipid in the myocyte followed by apoptosis). The process which at first appears to be adaptive may turn out maladaptive in the longer term (Balakumar et al. 2007, Ogata et al. 2004). Furthermore, it has been shown that PPAR agonists prevent cardiac lipotoxicity in hypertension induced heart failure (Ogata et al. 2004).

On the other hand, PPAR agonists, such as fenofibrate, restore FAO and reduce glycolysis in heart in preclinical models, resulting in protective effects for heart failure development.

An ischaemia / reperfusion study in PPAR WT and KO mice showed that treatment with a PPAR agonist reversed the decrease of myocardial FAO enzyme activity and the increased serum levels of free fatty acids in WT mice but not KO mice and that those effects are associated with improved contractile function in those mice (Yue et al. 2003). Furthermore, it has been reported in a study of lipotoxic cardiomyopathy in mice, that treatment with fenofibrate reduced the high plasma and myocardial triglyceride levels and increased the low ATP content of the heart and that those effects were also accompanied by an improved left ventricular function and survival of mice (Asai et al. 2006).

This study shows that reactivation of PPAR by fenofibrate is beneficial in heart failure by reducing triglycerides levels and improving cardiac function. Furthermore fenofibrate had anti-hypertrophic and anti-fibrotic effects on the left ventricle, which further contribute to the improvement of cardiac function.

So far these protective effects by fibrates have not been described in patients with heart failure. In patients, fenofibrate is used as a lipid lowering drug, which decreases triglycerides and LDL cholesterol and increases HDL cholesterol (Fruchart et al. 2006, Staels et al. 1998). The protective effect on heart failure development in preclinical heart failure models has never been evaluated in clinical studies with heart failure patients. Clinical studies using PPAR agonists in patients had lipid lowering endpoints and patients with heart failure were excluded from the trials. Additionally, no hint of a protective effect have been reported from clinical studies determining lipid modulation in patients with heart diseases. This discrepancy between preclinical and clinical data might be due to the dose of fenofibrate used in animal models and patients and the tissue distribution of fenofibrate. In preclinical models (including our studies) dosages of 80 mg/kg/day of fenofibrate were used. The human daily dose is 300 mg (~4 mg/kg/day). It might well be that dosages of the weak PPAR agonist fenofibrate which are suitable for lipid modulation in patients are not sufficient for protection of the heart. Additionally, fenofibrate is tremendously enriched in liver compared to heart (Balfour et al. 1990) in animals and patients, meaning that the

concentration of fenofibrate in the heart might be too low for the induction of PPAR regulated genes involved in slowing of remodelling processes and probably not adequate for heart failure protection in patients.

The distribution of a PPAR compound, which would be comparable in liver and heart, could open up the opportunity to reach drug tissue levels which might be suitable to delay heart failure development in patients.

In summary, one important factor for the protective effects of PPAR in heart failure development might be the modulation of fuel (FAO / glucose oxidation) utilization in the heart. Reduction or abolishment of PPAR activity leads to depletion of metabolic reserves and energy allocation especially under high workload resulting in morphological and functional deterioration of the heart. Whereas restoration of PPAR activity leads to normalization of energy supply and protection of heart function. Another important factor for the protective effects of PPAR in heart failure might be the effects on cardiac remodelling with antihypertrophic and antifibrotic effects as well as regulating interstitial matrix.

Further investigations are needed to completely elucidate the complex interplay between PPAR activity, fuel utilization and direct antihypertrophic and antifibrotic effects in the heart.

5.5 Conclusion

In conclusion, this study shows that the level of PPAR expression and activity determines the susceptibility of mice towards heart failure. Remodelling and functional restriction is much more pronounced in PPAR KO compared to WT mice. PPAR expression is needed as an important protective factor to attenuate heart failure. The absence of PPAR activity renders KO mice pronouncedly more sensitive for heart failure and worsens remodelling processes and heart function. On the contrary, treatment with PPAR agonists to normalize PPAR activity, which is reduced in heart failure, ameliorates heart failure in ischaemia and pressure overload induced heart failure by mechanisms involved in energy homeostasis and/or anti matrix remodelling, antifibrotic and antihypertrophic processes.

The normalization of PPAR activity by PPAR agonists should, therefore, be beneficial in patients and merits further clinical investigations.

6. Summary

Heart failure is a progressive clinical syndrome which is characterized by the inability of the heart to pump or fill with a sufficient amount of blood through the systemic circulation. One receptor, which seems to be involved in the remodelling processes accompanying the progression of heart failure, is the peroxisome proliferator-activated receptor alpha (PPAR α). Indeed, it seems that PPAR α is downregulated in patients with heart failure and has antihypertrophic and antifibrotic effects on the myocardium. Thus, the aim of this study was to investigate the role of PPAR α in the remodelling processes related to heart failure, in models of ischaemia (chronic myocardial infarction model) and hypertension (deoxycorticosterone acetate / DOCA salt model) induced heart failure, the two most important causes of heart failure development in patients. To this end, the effects of abrogation of PPAR α activity in knock-out (KO) mice were compared to normal activity in wild-type (WT) mice and activation of PPAR α by the PPAR α agonist fenofibrate (80 mg/kg/d) in the two aforementioned models. Furthermore the treatment with fenofibrate was compared to a standard therapy with the ACE inhibitor ramipril (10 mg/kg/d).

Left ventricular function was evaluated via invasive haemodynamic measurements 9 weeks after coronary ligation and 6 weeks after beginning of DOCA treatment. Left ventricular expression profiles of hypertrophy and fibrosis genes were analyzed by real-time PCR. At last, lipid profiles in the plasma were measured. In the DOCA model, kidney function was additionally measured by diuresis.

PPAR α KO mice with ischaemia induced heart failure showed a significantly reduced survival compared to WT mice after surgery (60 % compared to 80%).

Both models resulted in hypertrophy of the left ventricle which was also reflected in the biomarker analysis. For both models markers of hypertrophy and fibrosis were enhanced compared to Sham mice. Furthermore KO mice showed higher levels of myosin heavy chain (MyHC), collagen and tissue inhibitor of metalloproteinase 1 (TIMP1) than WT mice (almost 3 fold increase). On the contrary, treatment with fenofibrate or ramipril could prevent increases of the biomarkers in WT mice but not in KO mice.

In both models, worsening of morphology was also reflected in the cardiac function. Although baseline haemodynamics were similar in sham WT and Sham KO mice,

they were significantly differing between the treated WT and KO mice. Indeed, contractility ($LVdp/dt_{max}$) and relaxation ($LVdp/dt_{min}$ and relaxation constant tau) were more impaired in KO compared to WT mice. Similarly to the morphology, KO mice showed more impaired cardiac function than WT mice and treatment with fenofibrate and ramipril partially restored ventricular function in WT but not KO mice.

In conclusion, this study shows that the level of PPAR expression and activity determines the susceptibility of mice towards heart failure development. The absence of PPAR activity renders KO mice tremendously more sensitive for heart failure development and worsens remodelling processes and heart function. On the contrary, treatment with fenofibrate to normalize PPAR activity, which is reduced in heart failure, ameliorates heart failure in ischaemia and pressure overload induced heart failure by mechanisms involved in energy homeostasis and/or anti matrix remodelling, antifibrotic and antihypertrophic processes.

The normalization of PPAR activity by PPAR agonists should, therefore, be beneficial in patients and is of value for further clinical investigations.

7. Zusammenfassung

Herzinsuffizienz ist ein progressives klinisches Syndrom, charakterisiert durch das Unvermögen des Herzens den Kreislauf mit genügend Blut zu versorgen. Ein Rezeptor, der an den Herzinsuffizienz begleitenden Remodelling Prozessen, beteiligt zu sein scheint, ist der „peroxisome proliferator-activated receptor alpha (PPAR α). In der Tat, scheint der PPAR α bei Patienten mit Herzinsuffizienz herunter reguliert zu sein und soll außerdem antihypertrophe und antifibrotische Wirkungen auf das Myokard haben. Ziel dieser Studie war es daher, die Rolle von PPAR α bei den mit Herzinsuffizienz assoziierten Remodelling Prozessen mit Hilfe einer durch Ischämie- (chronischer Myokardinfarkt Modell) und Hypertonie- (deoxycorticosterone Acetate / DOCA Salz Modell) induzierten Herzinsuffizienz, zu untersuchen. Zu diesem Zweck wurden die Effekte der Aufhebung der PPAR α Aktivität bei knock-out (KO) Mäusen mit der normalen Aktivität in Wildtyp (WT) Mäusen und Aktivierung von PPAR α durch den PPAR α Agonisten, Fenofibrate (80 mg/kg/d), in den zwei oben erwähnten Modellen, verglichen. Zusätzlich wurde die Fenofibratebehandlung mit einer Standardtherapie mit einem ACE Hemmer, Ramipril (10 mg/kg/d), verglichen.

Die linksventrikuläre Funktion wurde 9 Wochen nach Ligation der Koronararterie oder 6 Wochen nach Anfang der DOCA Behandlung mittels invasiver hämodynamischer Messungen bewertet. Genexpression für Hypertrophie und Fibrose wurde mittels real-time PCR Analyse gemessen. Schließlich wurden Plasma Lipidprofile ermittelt. Zusätzlich wurde die Nierenfunktion mittels Diurese in dem DOCA Modell bestimmt.

PPAR α KO Mäuse mit durch Ischämie induzierter Herzinsuffizienz zeigten signifikant reduzierte Überlebensraten nach der Operation im Vergleich zu den WT Mäusen (60 % im Gegensatz zu 80%).

Beide Modelle resultierten in einer Hypertrophie des linken Ventrikels, was durch eine Gewichtsermittlung und Biomarkeranalyse gezeigt werden konnte. In beiden Modellen, sowohl bei WT als auch bei KO herzinsuffizienten Mäusen verglichen zu deren respektiven scheinoperierten Tieren, konnte eine zwei- bis zehnmal erhöhte Genexpression für Hypertrophie und Fibrose nachgewiesen werden. Zusätzlich, zeigten KO Mäuse eine höhere Genexpression für myosin heavy chain (MyHC), collagen und tissue inhibitor of metalloproteinase 1 (TIMP1) als WT Mäuse (fast 3fache Erhöhung). Die Behandlung mit dem ACE Hemmer Ramipril konnte die

Erhöhung der Biomarker sowohl in der Gruppe der WT, als auch in der Gruppe der KO Mäuse verhindern, während Behandlung mit dem PPAR Agonist Fenofibrate, wie erwartet, nur einen Effekt bei den WT, nicht aber bei den KO Mäusen, zeigte.

In beiden Modellen, wurde die Verschlechterung der Morphologie ebenso in einer Verschlechterung der Herzfunktion wiedergespiegelt. Obwohl die Basalwerte der Hämodynamikmessungen vergleichbar zwischen scheinoperierten WT und KO Tieren waren, wurden große Unterschiede in den anderen Gruppen festgestellt. Kontraktilität ($LVdp/dt_{max}$) und Relaxation ($LVdp/dt_{min}$ und Relaxationskonstante τ) waren verschlechtert in der Gruppe der KO Mäuse verglichen zu der der WT Mäuse (etwa 20%). Ähnlich zu der Morphologie, zeigten KO Mäuse eine verschlechterte Herzfunktion verglichen mit der der WT Mäuse. Wiederum konnte die Behandlung mit Ramipril die Herzfunktion der WT und KO Mäuse teilweise wiederherstellen, während eine Behandlung mit Fenofibrate lediglich bei den WT Mäusen, nicht aber bei den KO Mäusen eine Verbesserung ermöglichte.

Schließlich zeigt diese Studie, dass die Expressions- und Aktivitätshöhe von PPAR die Empfindlichkeit der Mäuse gegenüber Herzinsuffizienzentwicklung bedingt. Der Mangel an PPAR Aktivität verursacht eine höhere Empfindlichkeit der KO Mäuse gegenüber einer Herzinsuffizienz und eine Verschlechterung der damit assoziierten Remodellingsprozesse und der Herzfunktion. Im Gegensatz dazu führt eine Behandlung mit Fenofibrate zur Wiederherstellung der mit einer Herzinsuffizienz einhergehenden herabgesetzten PPAR Aktivität. Im Zuge dessen verbessert Fenofibrate eine durch Ischämie und Hypertonie induzierte Herzinsuffizienz. Seine Wirkung erzielt es bei Mechanismen involviert in Energie Homöostase und / oder Matrix Remodelling, antifibrotische- und antihypertrophe Prozesse.

Zusammenfassend kann man sagen, dass eine Normalisierung der PPAR Aktivität bei PPAR Agonisten sehr nützlich bei Patienten mit Herzinsuffizienz ist und unbedingt Inhalt weiterer klinischer Untersuchungen sein sollte.

8. Reference list

Adeghate E. et al. (2005) Subchronic exposure to high-dose ACE-inhibitor moexipril induces catalase activity in rat liver. *Mol Cell Biochem* 280:159-63

Ahmed W. et al. (2007) PPARs and their metabolic modulation: new mechanisms for transcriptional regulation? *J Intern Med* 262:184-98

Aoyama T. et al. (1998) Altered constitutive expression of fatty acid-metabolizing enzymes in mice lacking the peroxisome proliferator-activated receptor alpha (PPARalpha). *J Biol Chem* 273:5678-84

Asai T. et al. (2006) Combined therapy with PPARalpha agonist and L-carnitine rescues lipotoxic cardiomyopathy due to systemic carnitine deficiency. *Cardiovasc Res* 70:566-77

Balakumar P. et al. (2007) PPAR ligands: are they potential agents for cardiovascular disorders? *Pharmacolog*; 80:1-10

Balfour J.A. et al. (1990) Fenofibrate. A review of its pharmacodynamic and pharmacokinetic properties and therapeutic use in dyslipidaemia. *Drugs*; 40:260-90

Barger P.M. et al. (2000) Deactivation of peroxisome proliferator-activated receptor-alpha during cardiac hypertrophic growth. *J Clin Invest* 105:1723-30

Braissant O. et al. (1996) Differential expression of peroxisome proliferator-activated receptors (PPARs): tissue distribution of PPAR-alpha, -beta, and -gamma in the adult rat. *Endocrinology* 137:354-66

Brilla C.G. et al. (1990) Remodeling of the rat right and left ventricles in experimental hypertension. *Circ Res* 67:1355-64

Chapman D. et al. (1990) Regulation of fibrillar collagen types I and III and basement membrane type IV collagen gene expression in pressure overloaded rat myocardium. *Circ Res* 67:787-94

Cleutjens J.P. et al. (1995) Collagen remodeling after myocardial infarction in the rat heart. *Am J Pathol* 147:325-38

Cohn J.N. et al. (2000) Cardiac remodeling--concepts and clinical implications: a consensus paper from an international forum on cardiac remodeling. Behalf of an International Forum on Cardiac Remodelling. *J Am Coll Cardiol* 35:569-82

Da Cunha V. et al. (2005) Enalapril attenuates angiotensin II-induced atherosclerosis and vascular inflammation. *Atherosclerosis* 178:9-17

Devchand P.R. et al. (1996) The PPARalpha-leukotriene B4 pathway to inflammation control. *Nature* 384:39-43

Di Nicolantonio R. et al. (1998) Nucleotide variations in intron 1 of the renin gene of the spontaneously hypertensive rat. *Clin Exp Hypertens* 20:27-40

Dreyer C. et al. (1992) Control of the peroxisomal beta-oxidation pathway by a novel family of nuclear hormone receptors. *Cell* 68:879-87

Dries D.L. et al. (2000) The prognostic implications of renal insufficiency in asymptomatic and symptomatic patients with left ventricular systolic dysfunction. *J Am Coll Cardiol* 35:681-9

Duhaney T.A. et al. (2007) Peroxisome proliferator-activated receptor alpha-independent actions of fenofibrate exacerbates left ventricular dilation and fibrosis in chronic pressure overload. *Hypertension*.; 49:1084-94

Eichhorn E.J. et al. (1996) Medical therapy can improve the biological properties of the chronically failing heart. A new era in the treatment of heart failure. *Circulation* 94:2285-96

Eisenhofer G. et al. (1996) Cardiac sympathetic nerve function in congestive heart failure. *Circulation* 93:1667-76

European Society of Cardiology (2008) Guidelines on Diagnosis and Treatment of Acute and Chronic Heart Failure 2008. *Eur Heart J* 19:2388-442

Ferré P. (2004) The biology of peroxisome proliferator-activated receptors: relationship with lipid metabolism and insulin sensitivity. *Diabetes* 53 Suppl 1:S43-50

Finck B.N. et al. (2002) The cardiac phenotype induced by PPARAlpha overexpression mimics that caused by diabetes mellitus. *J Clin Invest* 109:121-30

Finck B.N. (2007) The PPAR regulatory system in cardiac physiology and disease. *Cardiovasc Res* 73:269-77

Firth J.D. et al. (1988) Raised venous pressure: a direct cause of renal sodium retention in oedema? *Lancet* 1:1033-5

Forman B.M. et al. (1997) Hypolipidemic drugs, polyunsaturated fatty acids, and eicosanoids are ligands for peroxisome proliferator-activated receptors alpha and delta. *Proc Natl Acad Sci U S A* 94:4312-7

Francis G.A. et al. (2003) PPAR-alpha effects on the heart and other vascular tissues. *Am J Physiol Heart Circ Physiol* 285:H1-9

Francis G.S. (2001) Pathophysiology of chronic heart failure. *Am J Med* 110 Suppl 7A:37S-46S

Friedman S.M. et al. (1948) The effect of desoxycorticosterone acetate on blood pressure, renal function, and electrolyte pattern in the intact rat. *J Exp Med* 87:329-38

Frigerio M. et al. (2005) Drugs for left ventricular remodeling in heart failure. *Am J Cardiol* 96(12A):10L-18L

Fruchart J.C. et al. (2006) Mode of action of fibrates in the regulation of triglyceride and HDL-cholesterol metabolism. *Drugs Today (Barc)* 42:39-64

Gearing K.L. et al. (1994) Structure of the mouse peroxisome proliferator activated receptor alpha gene. *Biochem Biophys Res Commun* 199:255-63

Gélinas R. et al. (2008) Alterations in carbohydrate metabolism and its regulation in PPARalpha null mouse hearts. *Am J Physiol Heart Circ Physiol* 294:H1571-80

Ginsberg H.N. et al. (2007) Evolution of the lipid trial protocol of the Action to Control Cardiovascular Risk in Diabetes (ACCORD) trial. *Am J Cardiol* 99:56i-67i

Goikoetxea M.J. et al. (2006) Altered cardiac expression of peroxisome proliferator-activated receptor-isoforms in patients with hypertensive heart disease. *Cardiovasc Res* 69:899-907

Gonzalez F.J. (1997) Recent update on the PPAR alpha-null mouse. *Biochimie* 79:139-44

Gottlieb S.S. et al. (2002) The prognostic importance of different definitions of worsening renal function in congestive heart failure. *J Card Fail* 8:136-41

Guellich A. et al. (2007) Role of oxidative stress in cardiac dysfunction of PPARalpha^{-/-} mice. *Am J Physiol Heart Circ Physiol* 293:H93-H102

Halapas A. et al. (2008) In vivo models for heart failure research. *In Vivo* 22:767-80

Hasking G.J. et al. (1986) Norepinephrine spillover to plasma in patients with congestive heart failure: evidence of increased overall and cardiorenal sympathetic nervous activity. *Circulation* 73:615-21

Hayslett J.P. (1979) Functional adaptation to reduction in renal mass. *Physiol Rev* 59:137-64

Heywood J.T. (2004) The cardiorenal syndrome: lessons from the ADHERE database and treatment options. *Heart Fail Rev* 9:195-201

Hostetler H.A. et al. (2008) Glucose directly links to lipid metabolism through high affinity interaction with peroxisome proliferator-activated receptor alpha. *J Biol Chem* 283:2246-54

Howroyd P. et al. (2004) Decreased longevity and enhancement of age-dependent lesions in mice lacking the nuclear receptor peroxisome proliferator-activated receptor alpha (PPARalpha). *Toxicol Pathol* 32:591-9

Hunt S.A. et al. (2005) ACC/AHA 2005 Guideline Update for the Diagnosis and Management of Chronic Heart Failure in the Adult: a report of the American College of Cardiology/American Heart Association Task Force on Practice Guidelines (Writing Committee to Update the 2001 Guidelines for the Evaluation and Management of Heart Failure): developed in collaboration with the American College of Chest Physicians and the International Society for Heart and Lung Transplantation: endorsed by the Heart Rhythm Society. *Circulation* 112:e154-235

Huss J.M. et al. (2004) Nuclear receptor signaling and cardiac energetics. *Circ Res* 95:568-78

Ichihara S. et al. (2006) Attenuation of cardiac dysfunction by a PPAR-alpha agonist is associated with down-regulation of redox-regulated transcription factors. *J Mol Cell Cardiol* 41:318-29

Iglarz M. et al. (2003) Peroxisome proliferator-activated receptor-alpha and receptor-gamma activators prevent cardiac fibrosis in mineralocorticoid-dependent hypertension. *Hypertension* 42:737-43

Ijpenberg A. et al. (1997) Polarity and specific sequence requirements of peroxisome proliferator-activated receptor (PPAR)/retinoid X receptor heterodimer binding to DNA. A functional analysis of the malic enzyme gene PPAR response element. *J Biol Chem* 272:20108-17

Irukayama -Tomobe Y. et al. (2004) Endothelin-1-induced cardiac hypertrophy is inhibited by activation of peroxisome proliferator-activated receptor-alpha partly via blockade of c-Jun NH2-terminal kinase pathway. *Circulation* 109:904-10

Isseman I. and Green S. (1990) Activation of a member of the steroid hormone receptor superfamily by peroxisome proliferators. *Nature* 347:645-50

Kelly D.P. et al. (1994) Inherited cardiomyopathies. *N Engl J Med* 330:913-9

Kempf T. et al. (2007) Pathophysiology of heart failure. *Internist (Berl)* 48:899-908

Kersten S. (2008) Peroxisome proliferator activated receptors and lipoprotein metabolism. *PPAR Res* 2008:132960

Kim S. et al. (1997) Involvement of angiotensin II in cardiovascular and renal injury: effects of an AT1-receptor antagonist on gene expression and the cellular phenotype. *J Hypertens Suppl* 15:S3-7

Kliwer S.A. et al. (1995) A prostaglandin J2 metabolite binds peroxisome proliferator-activated receptor gamma and promotes adipocyte differentiation. *Cell* 83:813-9

Kliwer S.A. et al. (1997) Fatty acids and eicosanoids regulate gene expression through direct interactions with peroxisome proliferator-activated receptors alpha and gamma. *Proc Natl Acad Sci U S A* 94:4318-23

Kliwer S.A. et al. (2001) Peroxisome proliferator-activated receptors: from genes to physiology. *Recent Prog Horm Res* 56:239-63

Kramer F. et al. (2008) Plasma concentrations of matrix metalloproteinase-2, tissue inhibitor of metalloproteinase-1 and osteopontin reflect severity of heart failure in DOCA-salt hypertensive rat. *Biomarkers* 13:270-81

Kudzma D.J. (2002) Effects of thiazolidinediones for early treatment of type 2 diabetes mellitus. *Am J Manag Care* 8(16 Suppl):S472-82

Lazarow P.B. et al. (1976) A fatty acyl-CoA oxidizing system in rat liver peroxisomes; enhancement by clofibrate, a hypolipidemic drug. *Proc Natl Acad Sci U S A* 73:2043-6

Lebrasseur N.K. et al. (2007) Effects of fenofibrate on cardiac remodeling in aldosterone-induced hypertension. *Hypertension* 50:489-96

Lee S.S. et al. (1995) Targeted disruption of the peroxisome proliferator-activated receptor gene in mice results in abolishment of the pleiotropic effects of peroxisome proliferators. *Mol Cell Biol* 15:3012-22

Li C.B. et al. (2008) Effects and mechanisms of PPARalpha activator fenofibrate on myocardial remodeling in hypertension. *J Cell Mol Med.* 2008 Aug 27.]

Llopis J. et al. (2000) Ligand-dependent interactions of coactivators steroid receptor coactivator-1 and peroxisome proliferator-activated receptor binding protein with nuclear hormone receptors can be imaged in live cells and are required for transcription. *Proc Natl Acad Sci U S A* 97:4363-8

Lloyd-Jones D.M. et al. (2002) Lifetime risk for developing congestive heart failure: the Framingham Heart Study. *Circulation* 106:3068-72

Loichot C. et al. (2006) Deletion of peroxisome proliferator-activated receptor-alpha induces an alteration of cardiac functions. *Am J Physiol Heart Circ Physiol* 291:H161-6

Luptak I. et al. (2005) Decreased contractile and metabolic reserve in peroxisome proliferator-activated receptor-alpha-null hearts can be rescued by increasing glucose transport and utilization. *Circulation* 112:2339-46

Lutgens E. et al. (1999) Chronic myocardial infarction in the mouse: cardiac structural and functional changes. *Cardiovasc Res* 41:586-93

Mann D.L. et al. (2005) Mechanisms and models in heart failure: the biomechanical model and beyond. *Circulation* 111:2837-49

Matsumura Y. et al. (1999) Different contributions of endothelin-A and endothelin-B receptors in the pathogenesis of deoxycorticosterone acetate-salt-induced hypertension in rats. *Hypertension* 33:759-65

McMurray J.J. et al. (2000) Epidemiology, aetiology, and prognosis of heart failure. *Heart* 83:596-602

Morgan E.E. et al. (2006) Dissociation between gene and protein expression of metabolic enzymes in a rodent model of heart failure. *Eur J Heart Fail* 8:687-93

Motojima K. (1993) Peroxisome proliferator-activated receptor (PPAR): structure, mechanisms of activation and diverse functions. *Cell Struct Funct* 18:267-77

Mukherjee R. et al. (1997) Identification, characterization, and tissue distribution of human peroxisome proliferator-activated receptor (PPAR) isoforms PPARgamma2 versus PPARgamma1 and activation with retinoid X receptor agonists and antagonists. *J Biol Chem* 272:8071-6

Nakamachi T. et al. (2007) PPARalpha agonists suppress osteopontin expression in macrophages and decrease plasma levels in patients with type 2 diabetes. *Diabetes* 56:1662-70

Nesto R.W. et al. (2003) Thiazolidinedione use, fluid retention, and congestive heart failure: a consensus statement from the American Heart Association and American Diabetes Association. October 7, 2003. *Circulation* 108:2941-8

Newaz M. et al. (2005) NAD(P)H oxidase/nitric oxide interactions in peroxisome proliferator activated receptor (PPAR)alpha-mediated cardiovascular effects. *Mutat Res* 579:163-71

Ogata T. et al. (2004) Myocardial fibrosis and diastolic dysfunction in deoxycorticosterone acetate-salt hypertensive rats is ameliorated by the peroxisome proliferator-activated receptor-alpha activator fenofibrate, partly by suppressing inflammatory responses associated with the nuclear factor-kappa-B pathway. *J Am Coll Cardiol* 43:1481-8

Ogata T. et al. (2002) Stimulation of peroxisome-proliferator-activated receptor alpha (PPAR alpha) attenuates cardiac fibrosis and endothelin-1 production in pressure-overloaded rat hearts. *Clin Sci (Lond)* 103 Suppl 48:284S-288S

Omura T. et al. (2000) Differences in time course of myocardial mRNA expression in non-infarcted myocardium after myocardial infarction. *Basic Res Cardiol* 95:316-23

Panagia M. et al. (2005) PPAR-alpha activation required for decreased glucose uptake and increased susceptibility to injury during ischemia. *Am J Physiol Heart Circ Physiol* 288:H2677-83

Park C.W. et al. (2006) PPARalpha agonist fenofibrate improves diabetic nephropathy in db/db mice. *Kidney Int* 69:1511-7

Patten R.D. et al. (1998) Ventricular remodeling and its prevention in the treatment of heart failure. *Curr Opin Cardiol* 13:162-7

Pellieux C. et al. (2006) Overexpression of angiotensinogen in the myocardium induces downregulation of the fatty acid oxidation pathway. *J Mol Cell Cardiol* 41:459-66

Peters J.M. et al. (1997) Alterations in lipoprotein metabolism in peroxisome proliferator-activated receptor alpha-deficient mice. *J Biol Chem* 272:27307-12

Pfeffer M.A. et al. (1979) Myocardial infarct size and ventricular function in rats. *Circ Res* 44:503-12

Pruimboom-Brees I. et al. (2006) A critical role for peroxisomal proliferator-activated receptor-alpha nuclear receptors in the development of cardiomyocyte degeneration and necrosis. *Am J Pathol* 169:750-60

Raji A. et al. (2002) Insulin resistance, diabetes, and atherosclerosis: thiazolidinediones as therapeutic interventions. *Curr Cardiol Rep* 4:514-21

Razeghi P. et al. (2002) Downregulation of myocardial myocyte enhancer factor 2C and myocyte enhancer factor 2C-regulated gene expression in diabetic patients with nonischemic heart failure. *Circulation* 106:407-11

Ritter O. et al. (2003) The molecular basis of myocardial hypertrophy and heart failure. *Trends Mol Med* 9:313-21

Robert V. et al. (1995) Biological determinants of aldosterone-induced cardiac fibrosis in rats. *Hypertension* 26(6 Pt 1):971-8

Rose M. et al. (2007) Ameliorative effect of combination of fenofibrate and rosiglitazone in pressure overload-induced cardiac hypertrophy in rats. *Pharmacology* 80:177-84

Sack M.N. et al. (1997) A role for Sp and nuclear receptor transcription factors in a cardiac hypertrophic growth program. *Proc Natl Acad Sci U S A* 94:6438-43

Sambandam N. et al. (2006) Chronic activation of PPARalpha is detrimental to cardiac recovery after ischemia. *Am J Physiol Heart Circ Physiol* 290:H87-95

Schiffrin E.L. (2005) Peroxisome proliferator-activated receptors and cardiovascular remodeling. *Am J Physiol Heart Circ Physiol* 288:H1037-43

Schunkert H. et al. (1990) Increased rat cardiac angiotensin converting enzyme activity and mRNA expression in pressure overload left ventricular hypertrophy. Effects on coronary resistance, contractility, and relaxation. *J Clin Invest* 86:1913-20

Schupp M. et al. (2006) Cardiac PPARalpha expression in patients with dilated cardiomyopathy. *Eur J Heart Fail* 8:290-4

Shimizu N. et al. (1998) Doppler echocardiographic assessment and cardiac gene expression analysis of the left ventricle in myocardial infarcted rats. *Jpn Circ J* 62:436-42

Smeets P.J. et al. (2008) Cardiac hypertrophy is enhanced in PPAR alpha^{-/-} mice in response to chronic pressure overload. *Cardiovasc Res* 78:79-89

Smith G.L. et al. (2003) Worsening renal function: what is a clinically meaningful change in creatinine during hospitalization with heart failure? *J Card Fail* 9:13-25

Staels B. et al. (1998) Mechanism of action of fibrates on lipid and lipoprotein metabolism. *Circulation* 98:2088-93

Stumpe K.O. et al. (1970) Fluid reabsorption in Henle's loop and urinary excretion of sodium and water in normal rats and rats with chronic hypertension. *J Clin Invest* 49:1200-12

Sun Y. et al. (1997) Fibrosis of atria and great vessels in response to angiotensin II or aldosterone infusion. *Cardiovasc Res* 35:138-47

Swynghedauw B. (1999) Molecular mechanisms of myocardial remodeling. *Physiol Rev* 79:215-62

Taberner A. et al. (2002) Activation of the peroxisome proliferator-activated receptor alpha protects against myocardial ischaemic injury and improves endothelial vasodilatation. *BMC Pharmacol* 2:10

The criteria committee of the New York Heart Association. Nomenclature and Criteria for Diagnosis of Diseases of the Heart and Great Vessels. 9th Ed. Boston. Mass: Little, Brown & Co; 1994:253-256

Thomas C.V. et al. (1998) Increased matrix metalloproteinase activity and selective upregulation in LV myocardium from patients with end-stage dilated cardiomyopathy. *Circulation* 97:1708-15

Tugwood J.D. et al. (1992) The mouse peroxisome proliferator activated receptor recognizes a response element in the 5' flanking sequence of the rat acyl CoA oxidase gene. *EMBO J* 11:433-9

Uckert S. et al. (2007) Expression of messenger ribonucleic acid encoding for phosphodiesterase isoenzymes in human female genital tissues. *J Sex Med* 4:1604-9

van Raalte D.H. et al. (2004) Peroxisome proliferator-activated receptor (PPAR)-alpha: a pharmacological target with a promising future. *Pharm Res* 21:1531-8

Wan Y.J. et al. (2000) Peroxisome proliferator-activated receptor alpha-mediated pathways are altered in hepatocyte-specific retinoid X receptor alpha-deficient mice. *J Biol Chem* 275:28285-90

Watanabe K. et al. (2000) Constitutive regulation of cardiac fatty acid metabolism through peroxisome proliferator-activated receptor alpha associated with age-dependent cardiac toxicity. *J Biol Chem* 275:22293-9

Wollert K.C. et al. (1999) The renin-angiotensin system and experimental heart failure. *Cardiovasc Res* 43:838-49

Xie Z. et al. (2004) Osteopontin modulates myocardial hypertrophy in response to chronic pressure overload in mice. *Hypertension* 44:826-31

Young M. et al. (1995) Determinants of cardiac fibrosis in experimental hypermineralocorticoid states. *Am J Physiol* 269(4 Pt 1):E657-62

Young M.E. et al. (2001) Reactivation of peroxisome proliferator-activated receptor alpha is associated with contractile dysfunction in hypertrophied rat heart. *J Biol Chem* 276:44390-5

Young M.E. et al. (2001) Uncoupling protein 3 transcription is regulated by peroxisome proliferator-activated receptor (alpha) in the adult rodent heart. *FASEB J* 15:833-45

Yue T.L. et al. (2003) Activation of peroxisome proliferator-activated receptor-alpha protects the heart from ischemia/reperfusion injury. *Circulation* 108:2393-9

Zhou Y. et al. (2008) Clofibrate attenuates blood pressure and sodium retention in DOCA-salt hypertension. *Kidney Int* 74:1040-8

Zoete V. et al. (2007) Peroxisome proliferator-activated receptor structures: ligand specificity, molecular switch and interactions with regulators. *Biochim Biophys Acta* 1771:915-25

9. Own abstracts

Kienlen E., Albrecht B., Schäfer S. (2008) Development of heart failure post myocardial infarction in peroxisome proliferator-activated receptor alpha knock-out mice. *Abstract number 290, congress of the German society of cardiology in Mannheim, Germany (27-29.03.2008).*

Kienlen E., Albrecht B., Ellinghaus P., Schäfer S. (2008) Effects of peroxisome proliferator-activated receptor alpha (PPAR α) activation levels on heart failure post myocardial infarction in wild-type and PPAR α knock-out mice. *European Heart Journal 29 (Abstract Supplement), 129 (Abstract number 834)*

Abstract selected for an oral presentation for the “young investigator award in basic science”, congress of the European society of cardiology in Munich, Germany (31.08.2008).

10. Declaration

“I declare that I have completed this dissertation single-handedly without the unauthorized help of a second party and only with the assistance acknowledged therein. I have appropriately acknowledged and referenced all text passages that are derived literally from or are based on the content of published or unpublished work of others, and all information that relates to verbal communications. I have abided by the principles of good scientific conduct laid down in the charter of the Justus Liebig University of Giessen in carrying out the investigations described in the dissertation.”

Elodie Kienlen

Erklärung

„Ich erkläre: ich habe die vorgelegte Dissertation selbständig und ohne unerlaubte fremde Hilfe und nur mit den Hilfen angefertigt, die ich in der Dissertation angegeben habe. Alle Textstellen, die wörtlich oder sinngemäß aus veröffentlichten oder nicht veröffentlichten Schriften entnommen sind, und alle Angaben, die auf mündlichen Auskünften beruhen, sind als solche kenntlich gemacht. Bei den von mir durchgeführten und in der Dissertation erwähnten Untersuchungen habe ich die Grundsätze guter wissenschaftlicher Praxis, wie sie in der „Satzung der Justus-Liebig-Universität Gießen zur Sicherung guter wissenschaftlicher Praxis“ niedergelegt sind, eingehalten.“

Elodie Kienlen

11. Acknowledgments

This project was financially supported by Bayer HealthCare AG, Wuppertal, Germany, to which I sincerely express my gratitude.

This thesis would not have come to realization without the generous help and unlimited support from a number of people to whom I sincerely thank.

Thus, I would first like to express my gratitude to my mentors, Dr. habil Stefan Schäfer and Dr. Barbara Albrecht (Department of Cardiology, Bayer HealthCare AG, Wuppertal) for guiding me through the exciting field of this thesis and for always having time for a wise advice.

I also would like to thank Prof. Dr. Ernst Petzinger (Department of pharmacology and toxicology, JLU Gießen) for accepting being my tutor for this project.

I owe special thank to Ms. Manuela Weldert for introducing me and helping me in the field of animal experiments, especially of haemodynamic measurements as central issues of this project.

I thank too Dr. Peter Ellinghaus and Ms. Ina Flocke (Department of target discovery in Bayer HealthCare, Wuppertal) for their help in the field of molecular biology and for their useful advices.

I would like to thank all my colleagues at Bayer HealthCare AG, Vera Hett, Anke Reimann, Alexander vom Stein and all other employees who helped me with this work and to get along this time in the pharmaceutical industry.

At last, for their help, support and understanding in the life outside the lab I endlessly thank my family and friends, Béatrice, Dominique, Noémie, Michaël, Florian, Sabrina, Julia and Janina.

12. Appendix

12.1 Appendix to “Material”

12.1.1 Chemicals

- **Chemicals used for the surgery and necropsy**

Bepanthen® (Panthenol)	Bayer Vital, Leverkusen, Germany
Cutasept F skin disinfectant	Bode Chemie, Hamburg, Germany
Ethanol	Merck, Darmstadt, Germany
Isoflurane CP	CP Pharma, Burgdorf, Germany
Isotonic NaCl solution 0.9	Fresenius Kabi, Bad Homburg, Germany
Nebacetin Powder Spray	Astellas Pharma GmbH, Munich, Germany
Phosphate Buffered Saline (PBS)	Sigma Aldrich Chemie GmbH. Steinheim, Germany
Sodium chloride (NaCl) for analysis	Merck, Darmstadt, Germany
Solutol	BASF, Ludwigshafen, Germany

12.1.2 Equipment

Animal scale Mettler PM 2000	Mettler Instrumente GmbH, Gießen, Germany
Cold light lamp KL 1500 LCD	Schott, Mainz, Germany
Electronic digital caliper 0-150mm	Promat, Lübeck, Germany
Eppendorf tubes 1.5 ml	Eppendorf, Wesseling-Berzdorf, Germany
Heating panel	In house production
Isoflurane Vapor 19.3	Drägerwerk AG, Lübeck, Germany
Leukosilk® adhesive tape, 1.25 and 2.5 cm width	BSN medical GmbH, Hamburg, Germany
Metabolic cages	Tecniplast, Buguggiate, Italy
Narcosis box	In house production

Narcosis mask	In house production
Neolus® Needle 23G and 27G	Terumo® Europe N.V., Lewen, Belgium
Pipettes and furnitures	Eppendorf, Wesseling-Berzdorf, Germany
Precision scale Mettler PM 400	Mettler Instrumente GmbH, Gießen, Germany
Semperguard disposable latex gloves	Semperit technische Produkte GmbH & Co KG, Vienna, Austria
Shaver contura	Wella AG, Darmstadt, Germany
S-Monovette® - Needle 20G 11/2, 85.1160	Sarstedt, Nümbrecht, Germany
S-Monovette® 1.2ml LH (Lithium-Heparin), 06.1666.001	Sarstedt, Nümbrecht, Germany
Stereo Lupe Leica M651	Leica, Wetzlar, Germany
Table vacuum cleaner "Wet 7 & Dry"	SEVERIN Elektro GmbH, Sundern, Germany
Tuberculin syringe 1ml	Codan Vertrieb GmbH & Co KG, Lensahn, Germany
Tubus for intubation	In house production
Ventilation pump minivent type 585	Hugo Sachs electronics, March, Germany

12.1.3 Surgical instruments and threads

Curved anatomical forceps: 12-503-10	Aesculap by B. Braun, Tuttlingen, Germany
Curved dissecting forceps: BD 257	Aesculap by B. Braun, Tuttlingen, Germany
Dissecting forceps: BD 23	Aesculap by B. Braun, Tuttlingen, Germany
Eye scissors: OC 500	Aesculap by B. Braun, Tuttlingen, Germany
Eyelid spreader: 17003-03	FST, Bad Oeynhausen, Germany
Metzenbaum scissors: 11-248-11	Martin GmbH, Tuttlingen, Germany
Micro suture tying forceps: FD 281	Aesculap by B. Braun, Tuttlingen, Germany
Mosquito clamp: BH 104	Aesculap by B. Braun, Tuttlingen, Germany
Needle holder Barraquer – Troutmann: 20-299-11	Martin GmbH, Tuttlingen, Germany
Needle holder Castroviejo: 20-311-14	Martin GmbH, Tuttlingen, Germany
Ethibone 5/0 thread (1 metric, V-18,	Ethicon by Johnson and Johnson, St.-

6913H).	Stevens-Woluwe, Belgium
Prolene 6/0 thread (0.7 metric, TF-6, EH7814H)	Ethicon by Johnson and Johnson, St.-Stevens-Woluwe, Belgium
Vicryl 6/0 thread (0.7 metric, TF1, V234H)	Ethicon by Johnson and Johnson, St.-Stevens-Woluwe, Belgium

12.2 Appendix to “Methods”

12.2.1 Diagnostic kits used for the urine analysis

CREA	Creatinine: Jaffé, kinetic- test, the centrifuged urine is diluted. Test kit Messrs. Roche Diagnostics GmbH using Hitachi 717 or 704
K	Potassium: flame photometric assay with lithium reference line, using flame photometer EFUX 5057, distribution Messrs. Eppendorf- Netheler- Hinz GmbH
Na	Sodium: flame photometric assay with lithium reference line, using flame photometer EFUX 5057, distribution Messrs. Eppendorf- Netheler- Hinz GmbH
PROT	Total Protein: modified according to Richterich, R., "Urin - Protein: Biuret - Methode", in: Richterich, R., Klinische Chemie, 2nd Edition, p.533 - 535, Akademische Verlagsgesellschaft, Frankfurt (1968)
UREA	Urea: enzymatic UV test, the centrifuged urine is diluted. Test kit Messrs. Roche Diagnostics GmbH using Hitachi 717 or 704

12.2.2 Diagnostic kits used for the lipid analysis

Cholesterol:	enzymatic colour test of 100µl plasma. Cartridge COBAS INTEGRA Cholesterol Gen.2 (Roche Diagnostics)
Triglyceride:	enzymatic colour test of 100µl plasma. Cartridge COBAS INTEGRA Triglycerides (Roche Diagnostics)
LDL:	enzymatic colour test of 100µl plasma. Cartridge COBAS INTEGRA LDL-Cholesterol plus 2nd generation (Roche Diagnostics)

HDL: enzymatic colour test of 100µl plasma.
 Cartridge COBAS INTEGRA HDL-Cholesterol plus 3rd generation
 (Roche Diagnostics)

12.3 Appendix to “Results”

12.3.1 cMI model

Table 1: Infarct scores of WT and KO cMI mice after eight weeks of treatment

	WT mice	KO mice
Sham	0.0 ± 0.0 AU	0.0 ± 0.0 AU
Placebo	3.2 ± 1.3 AU	3.6 ± 1.2 AU
Fenofibrate	3.4 ± 1.1 AU	3.1 ± 1.2 AU
Ramipril	3.0 ± 1.0 AU	4.0 ± 1.1 AU *

AU: arbitrary units; n= 16 (WT), 8 (KO); mean ± SEM; * p<0.05 vs respective WT group; unpaired t-test

Table 2: Body weight of WT and KO cMI mice after eight weeks of treatment

	WT mice	KO mice
Sham	30.0 ± 0.8 g	26.1 ± 0.5 g
Placebo	29.3 ± 0.6 g	25.3 ± 0.9 g
Fenofibrate	29.8 ± 0.9 g	24.7 ± 0.6 g
Ramipril	30.3 ± 0.8 g	24.4 ± 0.7 g

n= 16 (WT), 8 (KO); mean ± SEM

Table 3: Relative heart weight of WT and KO cMI mice after eight weeks of treatment

	WT mice	KO mice
Sham	4.3 ± 0.0 mg/g ***	4.2 ± 0.0 mg/g
Placebo	4.9 ± 0.1 mg/g	4.7 ± 0.0 mg/g
Fenofibrate	4.8 ± 0.1 mg/g	4.7 ± 0.1 mg/g
Ramipril	4.1 ± 0.0 mg/g ***	4.6 ± 0.2 mg/g

n= 16 (WT), 8 (KO); mean ± SEM; *** p<0.001 vs respective Placebo; ANOVA, followed by Student-Newmann-Keuls post hoc analysis

Table 4: Relative left ventricular weight of WT and KO cMI mice after eight weeks of treatment

	WT mice	KO mice
Sham	3.5 ± 0.0 mg/g ***	3.4 ± 0.0 mg/g
Placebo	4.1 ± 0.1 mg/g	3.9 ± 0.1 mg/g
Fenofibrate	3.9 ± 0.1 mg/g	3.9 ± 0.1 mg/g
Ramipril	3.2 ± 0.1 mg/g ***	3.7 ± 0.2 mg/g

n= 16 (WT), 8 (KO); mean ± SEM; *** p<0.001 vs respective Placebo; ANOVA, followed by Student-Newmann-Keuls post hoc analysis

Table 5: Relative right ventricular weight of WT and KO cMI mice after eight weeks of treatment

	WT mice	KO mice
Sham	0.83 ± 0.02 mg/g	0.85 ± 0.02 mg/g
Placebo	0.83 ± 0.02 mg/g	0.86 ± 0.02 mg/g
Fenofibrate	0.84 ± 0.02 mg/g	0.84 ± 0.02 mg/g
Ramipril	0.81 ± 0.02 mg/g	0.83 ± 0.04 mg/g

n= 16 (WT), 8 (KO); mean ± SEM

Table 6: Relative lung weight of WT and KO mice after nine weeks

	WT mice	KO mice
Sham	5.0 ± 0.1 mg/g	5.4 ± 0.1 mg/g
Placebo	5.0 ± 0.1 mg/g	5.3 ± 0.1 mg/g
Fenofibrate	4.9 ± 0.1 mg/g	5.5 ± 0.1 mg/g
Ramipril	4.9 ± 0.1 mg/g	5.5 ± 0.1 mg/g

n= 16 (WT), 8 (KO); mean ± SEM

Table 7: Relative liver weight of WT and KO cMI mice after eight weeks of treatment

	WT mice	KO mice
Sham	42.2 ± 0.7 mg/g	45.9 ± 2.1 mg/g
Placebo	42.3 ± 0.8 mg/g	45.8 ± 1.5 mg/g
Fenofibrate	70.9 ± 0.9 mg/g ***	49.2 ± 1.6 mg/g
Ramipril	45.8 ± 0.1 mg/g **	45.2 ± 1.3 mg/g

n= 16 (WT), 8 (KO); mean ± SEM; ** p<0.01, *** p<0.001 vs respective Placebo; ANOVA, followed by Student-Newmann-Keuls post hoc analysis

Table 8: Relative right kidney weight of WT and KO cMI mice after eight weeks of treatment

	WT mice	KO mice
Sham	7.0 ± 0.1 mg/g	6.8 ± 0.2 mg/g
Placebo	7.0 ± 0.1 mg/g	6.7 ± 0.1 mg/g
Fenofibrate	7.6 ± 0.1 mg/g ***	6.7 ± 0.1 mg/g
Ramipril	7.1 ± 0.1 mg/g	7.0 ± 0.2 mg/g

n= 16 (WT), 8 (KO); mean ± SEM; *** p<0.001 vs respective Placebo; ANOVA, followed by Student-Newmann-Keuls post hoc analysis

Table 9: Heart rate of WT and KO cMI mice after eight weeks of treatment

	WT mice	KO mice
Sham	443 ± 11 bpm	382 ± 15 bpm
Placebo	437 ± 10 bpm	343 ± 13 bpm
Fenofibrate	454 ± 9 bpm	339 ± 12 bpm
Ramipril	453 ± 12 bpm	337 ± 16 bpm

n= 16 (WT), 8 (KO); mean ± SEM

Table 10: Left ventricular systolic pressure of WT and KO cMI mice after eight weeks of treatment

	WT mice	KO mice
Sham	117 ± 1 mmHg	113 ± 3 mmHg **
Placebo	111 ± 3 mmHg	92 ± 2 mmHg
Fenofibrate	110 ± 2 mmHg	90 ± 3 mmHg
Ramipril	91 ± 2 mmHg ***	76 ± 3 mmHg **

n= 16 (WT), 8 (KO); mean ± SEM; ** p<0.01, *** p<0.001 vs respective Placebo; ANOVA, followed by Student-Newmann-Keuls post hoc analysis

Table 11: Left ventricular end-diastolic pressure of WT and KO cMI mice after eight weeks of treatment

	WT mice	KO mice
Sham	10.2 ± 1.0 mmHg *	6.0 ± 0.9 mmHg
Placebo	13.5 ± 0.7 mmHg	10.8 ± 1.7 mmHg
Fenofibrate	12.0 ± 0.7 mmHg	12.1 ± 2.6 mmHg
Ramipril	10.2 ± 0.7 mmHg *	9.5 ± 0.7 mmHg

n= 16 (WT), 8 (KO); mean ± SEM; * p<0.05 vs respective Placebo; ANOVA, followed by Student-Newmann-Keuls post hoc analysis

Table 12: Contractility of WT and KO cMI mice after eight weeks of treatment

	WT mice	KO mice
Sham	7685 ± 146 mmHg/s ***	7613 ± 426 mmHg/s **
Placebo	6574 ± 152 mmHg/s	4630 ± 198 mmHg/s
Fenofibrate	7273 ± 203 mmHg/s *	4679 ± 230 mmHg/s
Ramipril	6792 ± 126 mmHg/s	4050 ± 424 mmHg/s

n= 16 (WT), 8 (KO); mean ± SEM; * p<0.05, ** p<0.01, *** p<0.001 vs respective Placebo; ANOVA, followed by Student-Newmann-Keuls post hoc analysis

Table 13: Relaxation of WT and KO cMI mice after eight weeks of treatment

	WT mice	KO mice
Sham	-8986 ± 409 mmHg/s ***	-7714 ± 480 mmHg/s **
Placebo	-6482 ± 226 mmHg/s	-4244 ± 240 mmHg/s
Fenofibrate	-7184 ± 237 mmHg/s	-4028 ± 154 mmHg/s
Ramipril	-7436 ± 164 mmHg/s	-3440 ± 314 mmHg/s

n= 16 (WT), 8 (KO); mean ± SEM; ** p<0.01, *** p<0.001 vs respective Placebo; ANOVA, followed by Student-Newmann-Keuls post hoc analysis

Table 14: Relaxation constant tau of WT and KO cMI mice after eight weeks of treatment

	WT mice	KO mice
Sham	12.4 ± 0.6 ms ***	14.0 ± 1.0 ms **
Placebo	19.4 ± 1.1 ms	33.3 ± 3.4 ms
Fenofibrate	16.6 ± 1.0 ms	32.7 ± 3.9 ms
Ramipril	13.8 ± 1.0 ms ***	30.4 ± 2.7 ms

n= 16 (WT), 8 (KO); mean ± SEM; ** p<0.01, *** p<0.001 vs respective Placebo ; ANOVA, followed by Student-Newmann-Keuls post hoc analysis

Table 15: PPAR mRNA expression of WT and KO cMI mice after eight weeks of treatment

	WT mice	KO mice
Sham	1724 ± 1230 AU ***	1808 ± 261 AU
Placebo	799 ± 399 AU	1336 ± 348 AU
Fenofibrate	755 ± 335 AU	1485 ± 249 AU
Ramipril	611 ± 282 AU	1340 ± 321 AU

AU: arbitrary units; n= 16 (WT), 8 (KO); mean ± SEM; *** p<0.001 vs respective Placebo; ANOVA, followed by Student-Newmann-Keuls post hoc analysis

Table 16: PDK-4 mRNA expression of WT and KO cMI mice after eight weeks of treatment

	WT mice	KO mice
Sham	5041 ± 3345 AU	3426 ± 1433 AU
Placebo	4083 ± 2325 AU	1785 ± 836 AU
Fenofibrate	2930 ± 885 AU	2161 ± 513 AU
Ramipril	2411 ± 850 AU	2805 ± 1702 AU

AU: arbitrary units; n= 16 (WT), 8 (KO); mean ± SEM

Table 17: ANP mRNA expression of WT and KO cMI mice after eight weeks of treatment

	WT mice	KO mice
Sham	103962 ± 63242 AU ***	45774 ± 11672 AU *
Placebo	289958 ± 179822 AU	141053 ± 38669 AU
Fenofibrate	205835 ± 108855 AU *	127032 ± 38479 AU
Ramipril	152525 ± 63870 AU **	181239 ± 64050 AU

AU: arbitrary units; n= 16 (WT), 8 (KO); mean ± SEM; * p<0.05, ** p<0.01, *** p<0.001 vs respective Placebo ; ANOVA, followed by Student-Newmann-Keuls post hoc analysis

Table 18: MyHC mRNA expression of WT and KO cMI mice after eight weeks of treatment

	WT mice	KO mice
Sham	941 ± 651 AU **	6453 ± 1314 AU
Placebo	2525 ± 1919 AU	24503 ± 7753 AU
Fenofibrate	1298 ± 833 AU **	21906 ± 17562 AU
Ramipril	756 ± 605 AU ***	20766 ± 9843 AU

AU: arbitrary units; n= 16 (WT), 8 (KO); mean ± SEM; ** p<0.01, *** p<0.001 vs respective Placebo; ANOVA, followed by Student-Newmann-Keuls post hoc analysis

Table 19: Collagen 1A1 mRNA expression of WT and KO cMI mice after eight weeks of treatment

	WT mice	KO mice
Sham	3959 ± 2501 AU	7143 ± 1443 AU *
Placebo	4718 ± 2453 AU	17706 ± 4294 AU
Fenofibrate	3784 ± 1418 AU	17476 ± 5113 AU
Ramipril	3586 ± 1308 AU	17914 ± 6343 AU

AU: arbitrary units; n= 16 (WT), 8 (KO); mean ± SEM; * p<0.05 vs respective Placebo; ANOVA, followed by Student-Newmann-Keuls post hoc analysis

Table 20: TIMP1 mRNA expression of WT and KO cMI mice after eight weeks of treatment

	WT mice	KO mice
Sham	134 ± 74 AU **	509 ± 182 AU *
Placebo	428 ± 316 AU	2491 ± 497 AU
Fenofibrate	350 ± 171 AU	2184 ± 757 AU
Ramipril	263 ± 119 AU	4218 ± 1699 AU *

AU: arbitrary units; n= 16 (WT), 8 (KO); mean ± SEM; * p<0.05, ** p<0.01 vs respective Placebo; ANOVA, followed by Student-Newmann-Keuls post hoc analysis

Table 21: OPN mRNA expression of WT and KO cMI mice after eight weeks of treatment

	WT mice	KO mice
Sham	1073 ± 2824 AU	15 ± 4 AU *
Placebo	2908 ± 3999 AU	273 ± 42 AU
Fenofibrate	1949 ± 1359 AU	351 ± 293 AU
Ramipril	1261 ± 1309 AU	613 ± 233 AU *

AU: arbitrary units; n= 16 (WT), 8 (KO); mean ± SEM; * p<0.05 vs respective Placebo; ANOVA, followed by Student-Newmann-Keuls post hoc analysis

Table 22: Plasma triglycerides of WT and KO cMI mice after eight weeks of treatment

	WT mice	KO mice
Sham	125 ± 41 mg/dL	113 ± 27 mg/dL
Placebo	108 ± 29 mg/dL	140 ± 54 mg/dL
Fenofibrate	99 ± 37 mg/dL	146 ± 71 mg/dL
Ramipril	104 ± 28 mg/dL	123 ± 25 mg/dL

n= 16 (WT), 8 (KO); mean ± SEM

Table 23: Plasma total cholesterol of WT and KO cMI mice after eight weeks of treatment

	WT mice	KO mice
Sham	105 ± 10 mg/dL	128 ± 6 mg/dL
Placebo	113 ± 15 mg/dL	120 ± 9 mg/dL
Fenofibrate	160 ± 17 mg/dL ***	136 ± 14 mg/dL *
Ramipril	122 ± 12 mg/dL	132 ± 9 mg/dL

n= 16 (WT), 8 (KO); mean ± SEM; * p<0.05, *** p<0.001 vs respective Placebo; ANOVA, followed by Student-Newmann-Keuls post hoc analysis

Table 24: Plasma HDL of WT and KO cMI mice after eight weeks of treatment

	WT mice	KO mice
Sham	95 ± 7 mg/dL	126 ± 12 mg/dL
Placebo	102 ± 16 mg/dL	119 ± 11 mg/dL
Fenofibrate	151 ± 22 mg/dL ***	136 ± 15 mg/dL
Ramipril	108 ± 12 mg/dL	132 ± 18 mg/dL

n= 16 (WT), 8 (KO); mean ± SEM; *** p<0.001 vs respective Placebo; ANOVA, followed by Student-Newmann-Keuls post hoc analysis

Table 25: Plasma LDL of WT and KO cMI mice after eight weeks of treatment

	WT mice	KO mice
Sham	3 ± 2 mg/dL	7 ± 2 mg/dL
Placebo	5 ± 3 mg/dL	6 ± 3 mg/dL
Fenofibrate	16 ± 6 mg/dL ***	7 ± 2 mg/dL
Ramipril	5 ± 2 mg/dL	8 ± 2 mg/dL

n= 16 (WT), 8 (KO); mean ± SEM; *** p<0.001 vs respective Placebo; ANOVA, followed by Student-Newmann-Keuls post hoc analysis

12.3.2 DOCA model

Table 26: Body weight of WT and KO mice after six weeks of treatment

	WT mice	KO mice
Sham	30.2 ± 0.8 g **	25.1 ± 1.0 g
Placebo	26.8 ± 0.5 g	25.4 ± 0.5 g
Fenofibrate	28.8 ± 0.6 g *	25.5 ± 0.6 g
Ramipril	27.0 ± 0.6 g	26.4 ± 0.4 g

n= 15; mean ± SEM; * p<0.05, ** p<0.01 vs respective Placebo; ANOVA, followed by Student-Newmann-Keuls post hoc analysis

Table 27: Relative heart weight of WT and KO mice after six weeks of treatment

	WT mice	KO mice
Sham	4.4 ± 0.1 mg/g ***	4.3 ± 0.0 mg/g ***
Placebo	5.1 ± 0.1 mg/g	5.6 ± 0.3 mg/g
Fenofibrate	4.9 ± 0.1 mg/g *	5.2 ± 0.2 mg/g
Ramipril	4.8 ± 0.1 mg/g *	4.7 ± 0.1 mg/g **

n= 15; mean ± SEM; * p<0.05, ** p<0.01, *** p<0.001 vs respective Placebo; ANOVA, followed by Student-Newmann-Keuls post hoc analysis

Table 28: Relative left ventricular weight of WT and KO mice after six weeks of treatment

	WT mice	KO mice
Sham	3.5 ± 0.1 mg/g ***	3.5 ± 0.0 mg/g ***
Placebo	4.3 ± 0.1 mg/g	4.7 ± 0.2 mg/g
Fenofibrate	4.0 ± 0.1 mg/g **	4.4 ± 0.1 mg/g
Ramipril	4.0 ± 0.1 mg/g *	3.9 ± 0.1 mg/g **

n= 15; mean ± SEM; * p<0.05, ** p<0.01, *** p<0.001 vs respective Placebo; ANOVA, followed by Student-Newmann-Keuls post hoc analysis

Table 29: Relative right ventricular weight of WT and KO mice after six weeks of treatment

	WT mice	KO mice
Sham	0.87 ± 0.02 mg/g	0.86 ± 0.02 mg/g
Placebo	0.84 ± 0.02 mg/g	0.92 ± 0.09 mg/g
Fenofibrate	0.83 ± 0.03 mg/g	0.87 ± 0.03 mg/g
Ramipril	0.81 ± 0.02 mg/g	0.76 ± 0.02 mg/g

n= 15; mean ± SEM

Table 30: Relative lung weight of WT and KO mice after six weeks of treatment

	WT mice	KO mice
Sham	5.1 ± 0.1 mg/g	5.3 ± 0.1 mg/g
Placebo	5.4 ± 0.1 mg/g	5.8 ± 0.1 mg/g
Fenofibrate	5.2 ± 0.1 mg/g	5.9 ± 0.3 mg/g
Ramipril	5.3 ± 0.1 mg/g	5.5 ± 0.1 mg/g

n= 15; mean ± SEM

Table 31: Relative liver weight of WT and KO mice after six weeks of treatment

	WT mice	KO mice
Sham	44.1 ± 1.3 mg/g ***	43.4 ± 1 mg/g ***
Placebo	57.8 ± 1.4 mg/g	66.4 ± 1.8 mg/g
Fenofibrate	98.9 ± 3.1 mg/g ***	69.8 ± 2.0 mg/g
Ramipril	58.1 ± 1.6 mg/g	61.8 ± 1.3 mg/g

n= 15; mean ± SEM; *** p<0.001 vs respective Placebo; ANOVA, followed by Student-Newmann-Keuls post hoc analysis

Table 32: Relative right kidney weight of WT and KO mice after six weeks of treatment

	WT mice	KO mice
Sham	6.9 ± 0.2 mg/g ***	7.2 ± 0.1 mg/g ***
Placebo	12.5 ± 0.2 mg/g	14.9 ± 0.3 mg/g
Fenofibrate	13.5 ± 0.3 mg/g **	13.6 ± 0.4 mg/g *
Ramipril	13.6 ± 0.3 mg/g *	14.3 ± 0.4 mg/g

n= 15; mean ± SEM; * p<0.05, ** p<0.01, *** p<0.001 vs respective Placebo; ANOVA, followed by Student-Newmann-Keuls post hoc analysis

Table 33: Heart rate of WT and KO mice after six weeks of treatment

	WT mice	KO mice
Sham	442 ± 9 bpm	474 ± 10 bpm
Placebo	425 ± 13 bpm	504 ± 13 bpm
Fenofibrate	444 ± 8 bpm	498 ± 12 bpm
Ramipril	440 ± 11 bpm	508 ± 19 bpm

n= 15; mean ± SEM; * p<0.05 vs respective Placebo; ANOVA, followed by Student-Newmann-Keuls post hoc analysis

Table 34: Left ventricular systolic pressure of WT and KO mice after six weeks of treatment

	WT mice	KO mice
Sham	120 ± 2 mmHg ***	115 ± 2 mmHg **
Placebo	143 ± 3 mmHg	133 ± 5 mmHg
Fenofibrate	143 ± 3 mmHg	135 ± 4 mmHg
Ramipril	132 ± 3 mmHg	132 ± 4 mmHg

n= 15; mean ± SEM; ** p<0.01, *** p<0.001 vs respective Placebo; ANOVA, followed by Student-Newmann-Keuls post hoc analysis

Table 35: LVEDP of WT and KO mice after six weeks of treatment

	WT mice	KO mice
Sham	11.7 ± 1.0 mmHg	7.6 ± 0.7 mmHg
Placebo	8.1 ± 1.3 mmHg	9.6 ± 1.0 mmHg
Fenofibrate	10.8 ± 0.9 mmHg	9.7 ± 0.9 mmHg
Ramipril	8.5 ± 1.6 mmHg	10.0 ± 0.7 mmHg

n= 15; mean ± SEM

Table 36: Contractility of WT and KO mice after six weeks of treatment

	WT mice	KO mice
Sham	7784 ± 219 mmHg/s	8054 ± 146 mmHg/s
Placebo	8924 ± 366 mmHg/s	8948 ± 269 mmHg/s
Fenofibrate	8536 ± 278 mmHg/s	8749 ± 346 mmHg/s
Ramipril	8513 ± 278 mmHg/s	8737 ± 350 mmHg/s

n= 15; mean ± SEM

Table 37: Relaxation of WT and KO mice after six weeks of treatment

	WT mice	KO mice
Sham	-9251 ± 390 mmHg/s	-10066 ± 360 mmHg/s
Placebo	-9952 ± 777 mmHg/s	-9237 ± 398 mmHg/s
Fenofibrate	-9628 ± 593 mmHg/s	-9031 ± 578 mmHg/s
Ramipril	-10313 ± 673 mmHg/s	-9289 ± 490 mmHg/s

n= 15; mean ± SEM

Table 38: Relaxation constant tau of WT and KO mice after six weeks of treatment

	WT mice	KO mice
Sham	12.7 ± 0.8 ms	11.5 ± 1.1 ms
Placebo	14.8 ± 1.2 ms	15.6 ± 1.7 ms
Fenofibrate	14.4 ± 1.0 ms	16.7 ± 2.0 ms
Ramipril	12.4 ± 1.0 ms	16.8 ± 1.5 ms

n= 15; mean ± SEM

Table 39: Baseline urine parameters of WT and KO mice

	Volume (mL)	Protein/Creatinine (g/mmol)	Urea (mmol/L)	Na+/K+ (mmol/L)
Sham WT	1.4 ± 0.2	0.8 ± 0.1	796 ± 70	0.5 ± 0.1
Placebo WT	1.3 ± 0.1	0.8 ± 0.0	823 ± 87	0.6 ± 0.1
Feno WT	1.3 ± 0.2	0.7 ± 0.1	1006 ± 95	0.4 ± 0.1
Ramipril WT	1.4 ± 0.2	0.8 ± 0.1	1049 ± 130	0.5 ± 0.0
Sham KO	1.0 ± 0.2	1.0 ± 0.1	998 ± 134	0.5 ± 0.0
Placebo KO	1.2 ± 0.1	1.4 ± 0.3 ^{\$}	836 ± 102	0.5 ± 0.0
Feno KO	1.2 ± 0.2	1.2 ± 0.1 ^{\$\$}	980 ± 156	0.5 ± 0.1
Ramipril KO	1.0 ± 0.1	1.4 ± 0.2 ^{\$\$\$}	935 ± 102	0.4 ± 0.0

n= 15; mean ± SEM; ^{\$} p<0.05, ^{\$\$\$} p<0.01 vs respective WT group; unpaired t-test

Table 40: Urine parameters of WT and KO mice after five weeks of treatment

	Volume (mL)	Protein/Creatinine (g/mmol)	Urea (mmol/L)	Na+/K+ (mmol/L)
Sham WT	1.3 ± 0.2	1.5 ± 0.2 ^{***}	877 ± 125 ^{***}	0.5 ± 0.1 ^{**}
Placebo WT	3.7 ± 0.9	3.1 ± 0.3	335 ± 37	2.3 ± 0.3
Feno WT	4.1 ± 0.5	2.6 ± 0.3	346 ± 19	2.4 ± 0.3
Ramipril WT	4.8 ± 0.9	2.2 ± 0.2 [*]	290 ± 42	3.0 ± 0.6
Sham KO	1.2 ± 0.2 [*]	1.0 ± 0.1 ^{***}	823 ± 89 ^{***}	0.8 ± 0.1 ^{** \$}
Placebo KO	6.4 ± 1.0	4.4 ± 0.6 ^{\$}	216 ± 47	4.6 ± 0.9 ^{\$}
Feno KO	5.1 ± 1.0	3.5 ± 0.5	234 ± 21 ^{\$\$\$}	3.2 ± 0.5 ^{\$}
Ramipril KO	9.0 ± 1.6 ^{\$}	3.0 ± 0.4	156 ± 31 ^{\$}	5.7 ± 0.8 ^{\$}

n= 15; mean ± SEM; * p<0.05, *** p<0.001 vs respective Placebo; ANOVA, followed by Student-Newmann-Keuls post hoc analysis; ^{\$} p<0.05, ^{\$\$\$} p<0.001 vs respective WT group; unpaired t-test

Table 41: Differences between baseline and final urine parameters of WT and KO mice

	Δ Volume (mL)	Δ Protein/Creatinine (g/mmol)	Δ Urea (mmol/L)	Δ Na ⁺ /K ⁺ (mmol/L)
Sham WT	0.1 ± 0.3 *	0.7 ± 0.3 ***	88 ± 109 *	0.0 ± 0.1 *
Placebo WT	2.4 ± 0.9	2.3 ± 0.3	-487 ± 104	1.7 ± 0.4
Feno WT	2.9 ± 0.6	1.9 ± 0.3	-659 ± 101	1.9 ± 0.3
Ramipril WT	3.6 ± 0.8	1.4 ± 0.2 *	-760 ± 146	2.5 ± 0.6
Sham KO	0.2 ± 0.2 *	-0.0 ± 0.1 ** \$	-175 ± 100	0.3 ± 0.1 **
Placebo KO	5.3 ± 1.2	3.1 ± 0.8	-616 ± 134	4.1 ± 0.9 \$
Feno KO	4.1 ± 1.1	2.3 ± 0.4	-755 ± 165	2.7 ± 0.5
Ramipril KO	7.5 ± 1.7 * \$	1.5 ± 0.3	-755 ± 127	4.9 ± 0.8 \$

n= 15; mean ± SEM; * p<0.05, ** p<0.01, *** p<0.001 vs respective Placebo; ANOVA, followed by Student-Newmann-Keuls post hoc analysis; \$ p<0.05, respective WT group; unpaired t-test

Table 42: PPAR mRNA expression of WT and KO mice after six weeks of treatment

	WT mice	KO mice
Sham	1426 ± 51 AU	868 ± 260 AU **
Placebo	1548 ± 273 AU	428 ± 167 AU
Fenofibrate	1072 ± 188 AU **	527 ± 267 AU
Ramipril	1356 ± 245 AU	462 ± 92 AU

AU: arbitrary units; n=15; mean ± SEM; * p<0.05, ** p<0.01 vs respective Placebo; ANOVA, followed by Student-Newmann-Keuls post hoc analysis

Table 43: PDK-4 mRNA expression of WT and KO mice after six weeks of treatment

	WT mice	KO mice
Sham	32130 ± 13752 AU	19954 ± 4178 AU
Placebo	20098 ± 7779 AU	11424 ± 5111 AU
Fenofibrate	14485 ± 7611 AU	16510 ± 9302 AU
Ramipril	23170 ± 5751 AU	19073 ± 4295 AU

AU: arbitrary units; n= 16 (WT), 8 (KO); mean ± SEM

Table 44: ANP mRNA expression of WT and KO mice after six weeks of treatment

	WT mice	KO mice
Sham	618157 ± 142706 AU **	621687 ± 208450 AU *
Placebo	1868295 ± 729347 AU	2650689 ± 1698254 AU
Fenofibrate	1377982 ± 331739 AU	2429437 ± 807745 AU
Ramipril	1313209 ± 368028 AU	1576410 ± 474767 AU

AU: arbitrary units ; n= 15; mean ± SEM; * p<0.05, ** p<0.01 vs respective Placebo; ANOVA, followed by Student-Newmann-Keuls post hoc analysis

Table 45: MyHC mRNA expression of WT and KO mice after six weeks of treatment

	WT mice	KO mice
Sham	1531 ± 630 AU *	4550 ± 2101 AU §
Placebo	5074 ± 2085 AU	8368 ± 6582 AU
Fenofibrate	3560 ± 1447 AU	10009 ± 7148 AU
Ramipril	4798 ± 1943 AU	9304 ± 4206 AU

AU: arbitrary units ; n= 15; mean ± SEM; * p<0.05 vs respective Placebo; ANOVA, followed by Student-Newmann-Keuls post hoc analysis; § p<0.05 vs Sham WT; unpaired t-test

Table 46: Collagen 1A1 mRNA expression of WT and KO mice after six weeks of treatment

	WT mice	KO mice
Sham	28942 ± 8562 AU	21873 ± 8853 AU
Placebo	33564 ± 13290 AU	46467 ± 34332 AU
Fenofibrate	34869 ± 5540 AU	50824 ± 31685 AU
Ramipril	28339 ± 3309 AU	32936 ± 10483 AU

AU: arbitrary units; n= 15; mean ± SEM

Table 47: TIMP1 mRNA expression of WT and KO mice after six weeks of treatment

	WT mice	KO mice
Sham	753 ± 247 AU *	767 ± 257 AU
Placebo	2087 ± 1080 AU	3380 ± 2331 AU
Fenofibrate	1718 ± 379 AU	2915 ± 1951 AU
Ramipril	1395 ± 635 AU	1226 ± 161 AU

AU: arbitrary units ; n= 15; mean ± SEM; * p<0.05 vs respective Placebo; ANOVA, followed by Student-Newmann-Keuls post hoc analysis

Table 48: OPN mRNA expression of WT and KO mice after six weeks of treatment

	WT mice	KO mice
Sham	139 ± 84 AU	98 ± 27 AU
Placebo	456 ± 400 AU	828 ± 899 AU
Fenofibrate	276 ± 111 AU	877 ± 552 AU
Ramipril	223 ± 75 AU	221 ± 47 AU

AU: arbitrary units; n= 16 (WT), 8 (KO); mean ± SEM

Table 49: Plasma triglycerides of WT and KO mice after six weeks of treatment

	WT mice	KO mice
Sham	86 ± 25 mg/dL	99 ± 34 mg/dL *
Placebo	120 ± 74 mg/dL	148 ± 65 mg/dL
Fenofibrate	94 ± 38 mg/dL	145 ± 39 mg/dL
Ramipril	119 ± 44 mg/dL	163 ± 49 mg/dL

n= 15; mean ± SEM; * p<0.05 vs respective Placebo; ANOVA, followed by Student-Newmann-Keuls post hoc analysis

Table 50: Plasma total cholesterol of WT and KO mice after six weeks of treatment

	WT mice	KO mice
Sham	99 ± 10 mg/dL **	122 ± 8 mg/dL ***
Placebo	173 ± 66 mg/dL	255 ± 84 mg/dL
Fenofibrate	162 ± 38 mg/dL	208 ± 54 mg/dL
Ramipril	169 ± 40 mg/dL	251 ± 96 mg/dL

n= 15; mean ± SEM; ** p<0.01, *** p<0.001 vs respective Placebo; ANOVA, followed by Student-Newmann-Keuls post hoc analysis

Table 51: Plasma HDL cholesterol of WT and KO mice after six weeks of treatment

	WT mice	KO mice
Sham	126 ± 14 mg/dL ***	146 ± 9 mg/dL ***
Placebo	224 ± 55 mg/dL	286 ± 98 mg/dL
Fenofibrate	218 ± 44 mg/dL	261 ± 70 mg/dL
Ramipril	206 ± 50 mg/dL	279 ± 98 mg/dL

n= 15; mean ± SEM; *** p<0.001 vs respective Placebo; ANOVA, followed by Student-Newmann-Keuls post hoc analysis

Table 52: Plasma LDL cholesterol of WT and KO mice after six weeks of treatment

	WT mice	KO mice
Sham	3 ± 2 mg/dL ***	7 ± 2 mg/dL **
Placebo	27 ± 14 mg/dL	48 ± 20 mg/dL
Fenofibrate	27 ± 12 mg/dL	38 ± 12 mg/dL
Ramipril	20 ± 12 mg/dL	43 ± 30 mg/dL

n= 15; mean ± SEM; ** p<0.01, *** p<0.001 vs respective Placebo; ANOVA, followed by Student-Newmann-Keuls post hoc analysis



edition scientifique

VVB LAUFERSWEILER VERLAG

VVB LAUFERSWEILER VERLAG
STAUFBENBERGRING 15
D-35396 GIESSEN

Tel: 0641-5599898 Fax: -5599890
redaktion@doktorverlag.de
www.doktorverlag.de

ISBN 3-8359-5454-7



Coverbilder: © DIGITALstock.de